SOUTHERN AND SOUTH-WESTERN FLATLANDS

CLUSTER REPORT

CLIMATE CHANGE IN AUSTRALIA

PROJECTIONS

FOR AUSTRALIA'S NRM REGIONS

CSIRO

Australian Government
Department of the Environment
Bureau of Meteorology


−20°
−10°
0°
10°
20°
30°
40°
50°

SOUTHERN AND SOUTH-WESTERN FLATLANDS

CLUSTER REPORT

PROJECTIONS

FOR AUSTRALIA´S NRM REGIONS

CLIMATE CHANGE IN AUSTRALIA PROJECTIONS CLUSTER REPORT – SOUTHERN AND SOUTH-WESTERN FLATLANDS

ISBN

Print: 978-1-4863-0428-8
Online: 978-1-4863-0429-5

CITATION

Hope, P. *et al.* 2015, *Southern and South-Western Flatlands Cluster Report*, Climate Change in Australia Projections for Australia's Natural Resource Management Regions: Cluster Reports, eds. Ekström, M. *et al.*, CSIRO and Bureau of Meteorology, Australia.

CONTACTS

E: enquiries@csiro.au

T: 1300 363 400

ACKNOWLEDGEMENTS

Lead Author – Pandora Hope.

Contributing Authors – Debbie Abbs, Jonas Bhend, Francis Chiew, John Church, Marie Ekström, Dewi Kirono, Andrew Lenton, Chris Lucas, Kathleen McInnes, Aurel Moise, Didier Monselesan, Freddie Mpelasoka, Bertrand Timbal, Leanne Webb and Penny Whetton.

Editors – Marie Ekström, Penny Whetton, Chris Gerbing, Michael Grose, Leanne Webb and James Risbey.

Additional acknowledgements – Janice Bathols, Tim Bedin, John Clarke, Clement Davis, Tim Erwin, Craig Heady, Peter Hoffman, Jack Katzfey, Julian O'Grady, Tony Rafter, Surendra Rauniyar, Rob Smalley, Bertrand Timbal, Yang Wang, Ian Watterson, and Louise Wilson.

Project coordinators – Kevin Hennessy, Paul Holper and Mandy Hopkins.

Design and editorial support – Alicia Annable, Siobhan Duffy, Liz Butler, and Peter Van Der Merwe.

We gratefully acknowledge the assistance of Andrew Tait, Michael Hutchinson and David Karoly.

We acknowledge the World Climate Research Programme's Working Group on Coupled Modelling, which is responsible for CMIP, and we thank the climate modelling groups for producing and making available their model output. For CMIP the U.S. Department of Energy's Program for Climate Model Diagnosis and Intercomparison provides coordinating support and led development of software infrastructure in partnership with the Global Organization for Earth System Science Portals.

This report has been printed on ecoStar, a recycled paper made from 100% post-consumer waste.

TABLE OF CONTENTS

PREFACE

Australia's changing climate represents a significant challenge to individuals, communities, governments, businesses and the environment. Australia has already experienced increasing temperatures, shifting rainfall patterns and rising oceans.

The Intergovernmental Panel on Climate Change (IPCC) *Fifth Assessment Report* (IPCC, 2013) rigorously assessed the current state and future of the global climate system. The report concluded that:

- greenhouse gas emissions have markedly increased as a result of human activities
- human influence has been detected in warming of the atmosphere and the ocean, in changes in the global water cycle, in reductions in snow and ice, in global mean sea level rise, and in changes in some climate extremes
- it is extremely likely that human influence has been the dominant cause of the observed warming since the mid-20th century
- continued emissions of greenhouse gases will cause further warming and changes in all components of the climate system.

In recognition of the impact of climate change on the management of Australia's natural resources, the Australian Government developed the Regional Natural Resource Management Planning for Climate Change Fund. This fund has enabled significant research into the impact of the future climate on Australia's natural resources, as well as adaptation opportunities for protecting and managing our land, soil, water, plants and animals.

Australia has 54 natural resource management (NRM) regions, which are defined by catchments and bioregions. Many activities of organisations and ecosystem services within the NRM regions are vulnerable to impacts of climate change.

For this report, these NRM regions are grouped into 'clusters', which largely correspond to the broad-scale climate and biophysical regions of Australia (Figure A). The clusters are diverse in their history, population, resource base, geography and climate. Therefore, each cluster has a unique set of priorities for responding to climate change.

CSIRO and the Australian Bureau of Meteorology have prepared tailored climate change projection reports for each NRM cluster. These projections provide guidance on the changes in climate that need to be considered in planning.

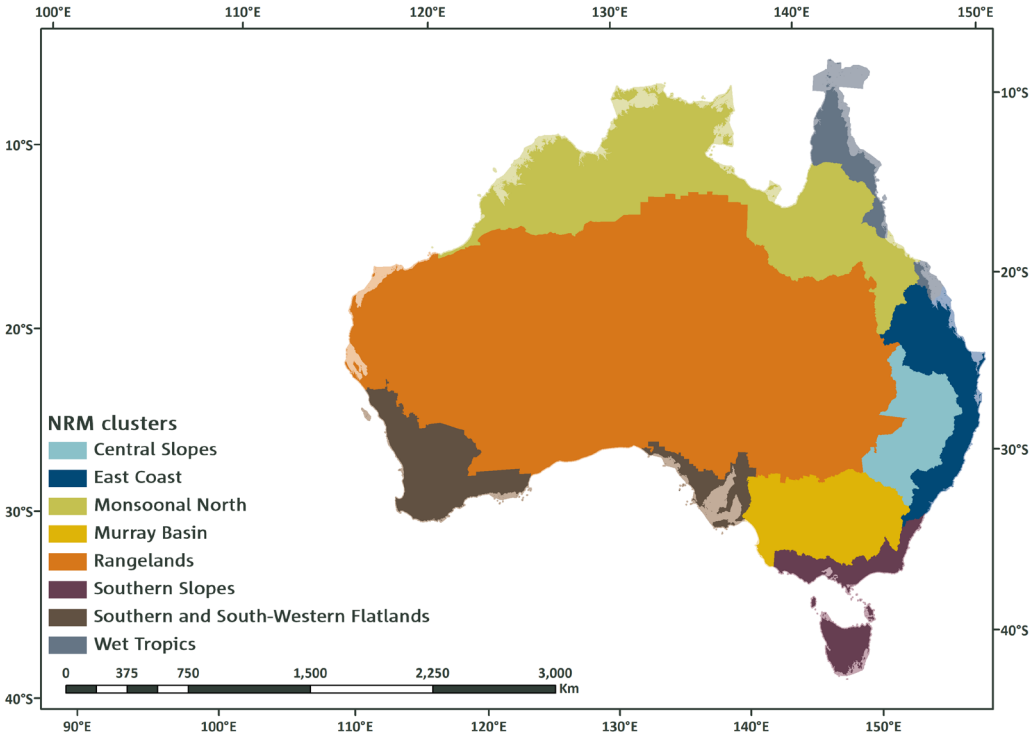

FIGURE A: THE EIGHT NATURAL RESOURCE MANAGEMENT (NRM) CLUSTERS

This is the regional projections report for the Southern and South-Western Flatlands cluster. This document provides projections in a straightforward and concise format with information about the cluster as a whole, as well as additional information at finer scales where appropriate.

This cluster report is part of a suite of products. These include a brochure for each cluster that provides the key projection statements in a brief format. There is also the Australian climate change projections Technical Report, which describes the underlying scientific basis for the climate change projections. Box 1 describes all supporting products.

This report provides the most up to date, comprehensive and robust information available for this part of Australia, and draws on both international and national data resources and published peer-reviewed literature.

The projections in this report are based on the outputs of sophisticated global climate models (GCMs). GCMs are based on the laws of physics, and have been developed over many years in numerous centres around the world. These models are rigorously tested for their ability to reproduce past climate. The projections in this report primarily use output from the ensemble of model simulations brought together for the Coupled Model Inter-comparison Project phase 5 (CMIP5) (Taylor *et al.,* 2012), where phase 5 is the most recent comparison of model simulations addressing, amongst other things, projections of future climates. In this report, outputs from GCMs in the CMIP5 archive are complemented by regional climate modelling and statistical downscaling.

BOX 1: CLIMATE CHANGE IN AUSTRALIA – PRODUCTS

This report is part of a suite of Climate Change in Australia (CCIA) products prepared with support from the Australian Government's Regional Natural Resource Management Planning for Climate Change Fund. These products provide information on climate change projections and their application.

CLUSTER BROCHURES

Purpose: key regional messages for everyone

A set of brochures that summarise key climate change projections for each of the eight clusters. The brochures are a useful tool for community engagement.

CLUSTER REPORTS

Purpose: regional detail for planners and decision-makers

The cluster reports are to assist regional decision-makers in understanding the important messages deduced from climate change projection modelling. The cluster reports present a range of emissions scenarios across multiple variables and years. They also include relevant sub-cluster level information in cases where distinct messages are evident in the projections.

TECHNICAL REPORT

Purpose: technical information for researchers and decision-makers

A comprehensive report outlining the key climate change projection messages for Australia across a range of variables. The report underpins all information found in other products. It contains an extensive set of figures and descriptions on recent Australian climate trends, global climate change science, climate model evaluation processes, modelling methodologies and downscaling approaches. The report includes a chapter describing how to use climate change data in risk assessment and adaptation planning.

WEB PORTAL

URL: www.climatechangeinaustralia.gov.au

Purpose: one stop shop for products, data and learning

The CCIA website is for Australians to find comprehensive information about the future climate. This includes some information on the impacts of climate change that communities, including the natural resource management sector, can use as a basis for future adaptation planning. Users can interactively explore a range of variables and their changes to the end of the 21st century. A 'Climate Campus' educational section is also available. This explains the science of climate change and how climate change projections are created.

Information about climate observations can be found on the Bureau of Meteorology website (www.bom.gov.au/climate). Observations of past climate are used as a baseline for climate projections, and also in evaluating model performance.

EXECUTIVE SUMMARY

INTRODUCTION

This report presents projections of future climate for the Southern and South-Western Flatlands (SSWF) based on our current understanding of the climate system, historical trends and model simulations of the climate response to changing greenhouse gas and aerosol emissions. This cluster has two geographically distinct sub-clusters, which are often referred to separately in this report. The southern Western Australia sub-cluster is termed SSWFW while the southern South Australian sub-cluster is SSWFE. The simulated climate response is that of the CMIP5 climate model archive, which also underpins the science of the *Fifth Assessment Report* of the Intergovernmental Panel on Climate Change (IPCC, 2013).

The global climate model (GCM) simulations presented here represent the full range of emission scenarios, as defined by the Representative Concentration Pathways (RCPs) used by the IPCC, with a particular focus on RCP4.5 and RCP8.5. The former represents a pathway consistent with low-level emissions, which stabilise the carbon dioxide concentration at about 540 ppm by the end of the 21st century. The latter is representative of a high-emission scenario, for which the carbon dioxide concentration reaches about 940 ppm by the end of the 21st century.

Projections are generally given for two 20-year time periods: the near future 2020–2039 (herein referred to as 2030) and late in the century 2080–2099 (herein referred to as 2090). The spread of model results are presented as the range between the 10th and 90th percentile in the CMIP5 ensemble output. For each time period, the model spread can be attributed to three sources of uncertainty: the range of future emissions, the climate response of the models, and natural variability. Climate projections do not make a forecast of the exact sequence of natural variability, so they are not 'predictions'. They do however show a plausible range of climate system responses to a given emission scenario and also show the range of natural variability for a given climate. Greenhouse gas concentrations are similar amongst different RCPs for the near future, and for some variables, such as rainfall, the largest range in that period stems from natural variability. Later in the century, the differences between RCPs are more pronounced, and climate responses may be larger than natural variability.

For each variable, the projected change is accompanied by a confidence rating. This rating follows the method used by the IPCC in the *Fifth Assessment Report*, whereby the confidence in a projected change is assessed based on the type, amount, quality and consistency of evidence (which can be process understanding, theory, model output, or expert judgment) and the degree of agreement amongst the different lines of evidence (IPCC, 2013). The confidence ratings used here are set as *low, medium, high* or *very high*.

HIGHER TEMPERATURES

Temperatures in the cluster have increased since national records began in 1910, especially since 1960. Mean surface air temperatures have increased by 1.1 °C in SSWFW and 0.7 °C in SSWFE between 1910 and 2013 using a linear trend.

Continued increases for the SSWF cluster for mean, maximum and minimum temperature are projected with *very high confidence*. There is *high confidence* in these projections as there is robust understanding of the driving mechanisms of warming and strong agreement on direction and magnitude of change amongst GCMs and downscaling results.

For the near future (2030), the mean annual warming is around 0.5 to 1.1 °C above the climate of 1986–2005, with only minor differences between RCPs. For late in the 21st century (2090) the mean annual warming is 1.2 to 2.0 °C for RCP4.5 and 2.6 to 4.0 °C for RCP8.5. Each individual season is projected to warm by about the same amount as the annual mean.

HOTTER AND MORE FREQUENT HOT DAYS, LESS FROST

Substantial increases in the maximum temperature on the hottest days, the frequency of hot days and the duration of warm spells are projected with *very high confidence* based on model results and physical understanding. Correspondingly, a decrease in the frequency of frost days is projected with *high confidence*.

For example, in Perth, the numbers of days above 35 °C and above 40 °C are 150 % greater by 2090 under RCP4.5 and median warming. The number of days above 35 °C in Adelaide also increases by around 150 % by 2090, while the number of days above 40 °C nearly doubles. There is also a decrease in the number of days with frost risk at these sites. Under RCP8.5, Adelaide is projected to be frost free on average by 2090.

LESS RAINFALL IN WINTER AND SPRING, CHANGES IN OTHER SEASONS UNCLEAR

The cluster has a predominantly Mediterranean climate, with high winter rainfall and little summer rainfall in both the sub-clusters. There has been a prolonged period of extensive drying from the 1970s in SSWFW and from the 1990s to the present in both sub-clusters, particularly in autumn and early winter .

Decreases in winter and spring (and annual) rainfall are projected with *high confidence*. There is strong model agreement and good understanding of the contributing underlying physical mechanisms driving this change (relating to the southward shift of winter storm systems and greater prevalence of high pressure systems). By 2030 winter rainfall may change by -15 to +5 %. By 2090, these ranges are around -30 to -5 % under RCP4.5 for SSWFW, and -45 to -15 % under RCP8.5. For SSWFE, under RCP4.5 by 2090 the changes are -25 to 0 % while under RCP8.5 the range is -45 to -5 %. For the whole cluster (SSWF), under RCP4.5 by 2090 the range is -25 to -5 % while under RCP8.5 the range is -45 to -15 %.

Changes in autumn and summer are unclear.

INCREASED INTENSITY OF HEAVY RAINFALL EVENTS, DROUGHT DURATION TO INCREASE

Understanding of physical processes and high model agreement provide *high confidence* that the intensity of heavy rainfall events will increase in SSWFE and *medium confidence* that intensity will increase in SSWFW. This increase in rainfall intensity is projected despite projected decreases in mean rainfall. Projections of the magnitude of change have *low confidence* and therefore the time when any change may be evident against natural variability cannot be reliably projected.

Under all RCPs, and at all time periods into the future, the time spent in meteorological drought is projected to increase compared to the present climate. These increases become quite marked by 2090 under RCP8.5. The projected changes are strongly driven by the projected decline in annual rainfall and are of *high confidence*.

DECREASE IN WINTER MEAN WIND SPEED

Small changes in mean surface wind speeds are projected with *high confidence* under all RCPs by 2030. Decreases in winter mean surface winds are projected for 2090 under RCP4.5 and RCP8.5 with *high confidence* based on model results and physical understanding (relating to decreased storminess).

Decreases are also suggested for extreme wind speeds, particularly for the rarer extremes under both RCP4.5 and RCP8.5. Medium model agreement and limitations to the method suggest *medium confidence* in this projection.

INCREASED SOLAR RADIATION AND REDUCED RELATIVE HUMIDITY IN WINTER AND SPRING

Little change to solar radiation by 2030 is projected with *high confidence*. By 2090, under RCP4.5 and RCP8.5 there is *high confidence* in increased winter radiation and *medium confidence* in an increase in spring and in little change in summer and autumn. The magnitude of the increases are up to 5 % and 10 % respectively for RCP4.5 and RCP8.5 in winter and about half that in spring.

Little change in relative humidity by 2030 is projected with *high confidence*, but for 2090 for winter and spring, across both sub-clusters, there is *high confidence* for a decrease (up to about 5 % under RCP8.5).

INCREASED EVAPORATION RATES, AND REDUCED SOIL MOISTURE AND RUNOFF

Projections for potential evapotranspiration indicate increases in all seasons with the largest absolute rates projected in summer by 2090 with *high confidence*. However, despite high model agreement there is *medium confidence* in the magnitude of these projections due to shortcomings in the simulations of observed historical changes.

Decreases in rainfall and increases in potential evapotranspiration are projected to lead to a decrease in soil moisture and runoff by 2090 under both RCP4.5 and RCP8.5 with *high confidence*. Decreases in soil moisture and runoff are strongly influenced by those in rainfall, but tend to be enhanced due to the increase in potential evapotranspiration. More detailed hydrological modelling is needed to assess changes to runoff, including the magnitude of the projected decreases.

HARSHER FIRE–WEATHER CLIMATE IN THE FUTURE

There is *high confidence* that climate change will result in a harsher fire-weather climate in the future. However, there is *low confidence* in the magnitude of the change as this is strongly dependent on the summer rainfall projection.

HIGHER SEA LEVELS AND MORE FREQUENT SEA LEVEL EXTREMES

Relative sea level has risen around Australia at an average rate of 1.4 mm/year between 1966 and 2009 and 1.6 mm/year after the influence of the El Niño Southern Oscillation (ENSO) on sea level is removed.

There is *very high confidence* that sea level will continue to rise during the 21st century. By 2030, the projected range of sea level rise at Fremantle and Port Adelaide is 0.07 to 0.17 m above the 1986–2005 level, with only minor differences between emission scenarios. As the century progresses, projections are sensitive to emissions pathways. By 2090, RCP4.5 gives a rise of 0.28 to 0.65 m and RCP8.5 gives a rise of 0.39 to 0.84 m. These ranges of sea level rise are considered *likely* (at least 66 % probability). However, if a collapse in the marine based sectors of the Antarctic ice sheet were initiated, these projections could be several tenths of a metre higher by late in the century.

Taking into account the nature of extreme sea levels along the SSWF coastlines and the uncertainty in the sea level rise projections, an indicative extreme sea level 'allowance' is provided. The allowance being the minimum distance required to raise an asset to maintain current frequency of breaches under projected sea level rise. In 2030, the vertical allowances along the cluster coastline are in the range of 11 to 13 cm for all RCPs, and by 2090, 48 to 56 cm for RCP4.5 and 66 to 76 cm for RCP8.5.

WARMER AND MORE ACIDIC OCEANS IN THE FUTURE

Sea surface temperature (SST) has increased significantly across the globe over recent decades and warming is projected to continue with *very high confidence*. Across the coastal waters of the SSWF cluster region in 2090, warming is projected in the range of 1.5 to 3.9 °C for RCP8.5.

About 30 % of the anthropogenic carbon dioxide emitted into the atmosphere over the past 200 years has been absorbed by the oceans. This has led to a 0.1 pH fall in the ocean's surface water pH (a 26 % rise in acidity). Continued acidification will compromise the ability of calcifying marine organisms such as corals, oysters and some plankton to form their shells or skeletons. There is *very high confidence* that around Australia the ocean will become more acidic and also *high confidence* that the rate of ocean acidification will be proportional to carbon dioxide emissions. By 2030, pH is projected to fall by up to additional 0.08 units in the coastal waters of the cluster. By 2090, pH is projected to fall by up to 0.15 under RCP4.5 and up to 0.33 under RCP8.5. These values would represent an additional 40 % and 110 % in acidity respectively.

MAKING USE OF THESE PROJECTIONS FOR CLIMATE ADAPTATION PLANNING

These regional projections provide the best available science to support impact assessment and adaptation planning in the Southern and South-Western Flatlands cluster. This report provides some guidance on how to use these projections, including the Australian Climate Futures web tool, available from the Climate Change in Australia website. The web tool allows users to investigate the range of climate model outcomes for their region across timescales and RCPs of interest, and to select and use data from models that represents a particular change of interest (*e.g.* warmer and drier conditions).

1 THE SOUTHERN AND SOUTH-WESTERN FLATLANDS CLUSTER

This report describes climate change projections for the Southern and South-Western Flatlands (SSWF) cluster (Figure 1.1). The cluster comprises NRM regions of Western Australia (Wheatbelt (Avon), Perth (Swan), South West, South Coast and Northern Agricultural) and South Australia (Eyre Peninsula, Northern and Yorke, Kangaroo Island, Adelaide and Mt Lofty Ranges). South Australia's Spencer Gulf, Gulf St Vincent and Investigator Strait, as well as some coastal zones in Western Australia are considered part of the cluster. Projections are presented for the whole cluster and also individually for the western sub-cluster (termed Southern and South-Western Flatlands West (SSWFW)) and the eastern sub-cluster (termed Southern and South-Western Flatlands East (SSWFE)) (Figure 1.1).

All but one of these NRM regions are on the coast. Although termed 'Flatlands', there are orographic features, such as the Darling Scarp, the Stirling Ranges and Mt Lofty Ranges that all influence local rainfall and temperature gradients. Landscapes in the cluster range from forest to desert. Dryland agriculture is a major industry. Other industries include sheep, mixed livestock, grapes and forestry.

Fisheries such as rock lobster are also important. Water supply and management is an issue for all regions and the question of how climate change will impact on the primary production, biodiversity and land-use is a major focus for NRM managers in this cluster.

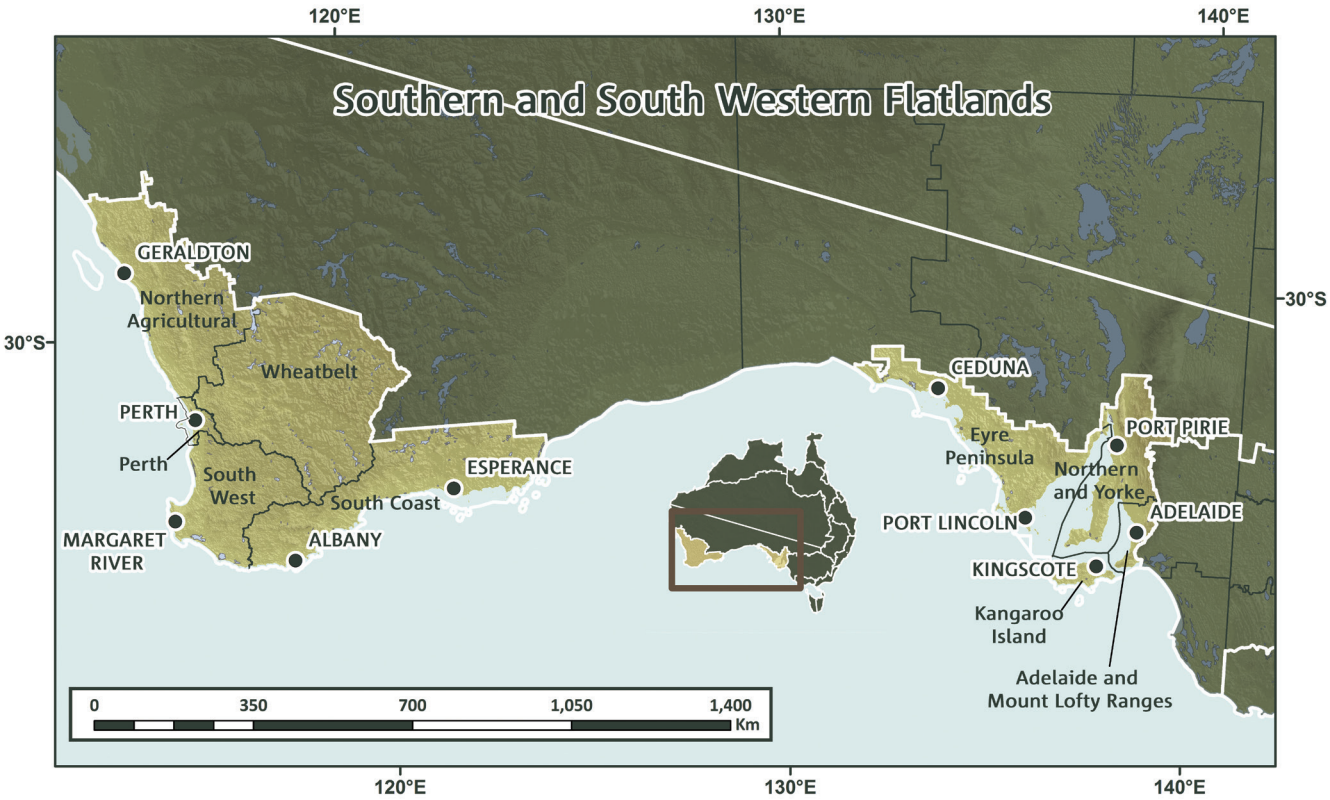

FIGURE 1.1: THE SOUTHERN AND SOUTH-WESTERN FLATLANDS (SSWF) NRM CLUSTER AND MAIN LOCALITIES WITH RESPECT TO THE AUSTRALIAN CONTINENT. THE SUB-CLUSTERS EAST (SSWFE) AND WEST (SSWFW) ARE SEPARATED BY COASTLINE OF THE GREAT AUSTRALIAN BIGHT.

2 CLIMATE OF SOUTHERN AND SOUTH–WESTERN FLATLANDS

The climate of the SSWF cluster is dominated by the seasonal north-south transition of the sub-tropical ridge (STR). The STR is the climatological mean band of high pressure that extends west to east across the Australian continent in winter and shifts south of the continent in summer[1]. In winter, rain bearing storms and fronts associated with the westerlies south of Australia impact upon this cluster. In summer, conditions are generally dry. In the sections below, the current climate of SSWF is presented for the period 1986–2005 (Box 3.1 presents the observational data sets used in this report).

There are two geographically distinct regions that make up the cluster. Both the SSWFW and SSWFE sub-clusters have west and south-facing coasts exposed to fronts and troughs through the cool season. Both sub-clusters have strong gradients in rainfall and temperature. In summer, rainfall deriving from tropical systems can be important to this cluster.

Maps of daily mean temperature show the largest spatial variability in summer, with a strong gradient from south to north (Figure 2.1). Mean summer maximum temperatures range from 24 °C in the south up to more than 33 °C at the northern extent of the SSWFW sub-cluster. In winter, there are slightly warmer mean temperatures along the coast, but a small range across the cluster (Figure 2.1b).

The warmest days on average occur in January, while the coolest nights occur in July (Figure 2.2). Like the summer mean, there is a strong gradient from south to north in January maximum temperatures, ranging from about 24 °C in the south to up to 39 °C along the north-east edge of the Northern Agricultural NRM region (Figure 2.1c). Day to day temperatures, particularly in summer, are cooled by onshore afternoon sea breezes at many locations throughout the cluster. Winter nights can, on average, get as cool as 3 °C in the inland areas of the cluster and up to 12 °C on the west coast (Figure 2.1d). The annual average temperature for SSWFW is 17.7 °C and somewhat lower (16.7 °C) for SSWFE (Figure 2.2).

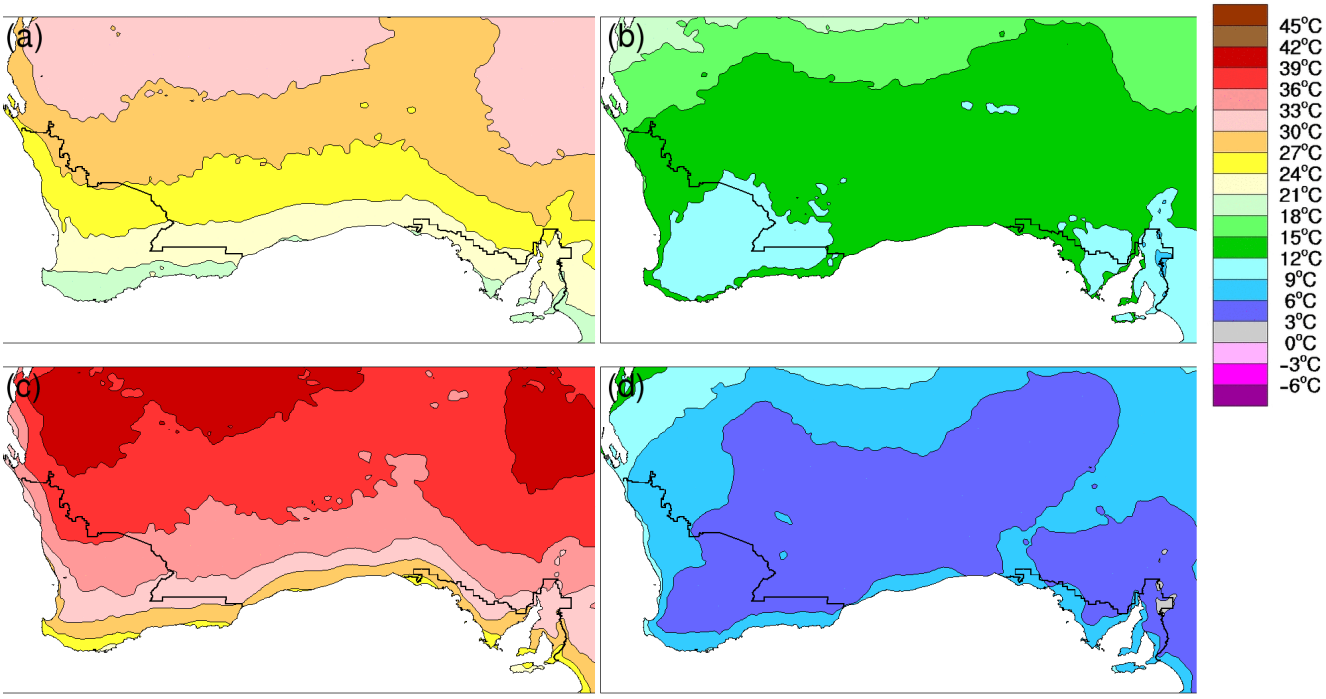

FIGURE 2.1: MAPS OF (A) AVERAGE SUMMER DAILY MEAN TEMPERATURE, (B) AVERAGE WINTER DAILY MEAN TEMPERATURE, (C) AVERAGE JANUARY MAXIMUM DAILY TEMPERATURE AND (D) AVERAGE JULY MINIMUM DAILY TEMPERATURE THE PERIOD 1986–2005.

1 http://www.bom.gov.au/watl/about-weather-and-climate/australian-climate-influences.shtml

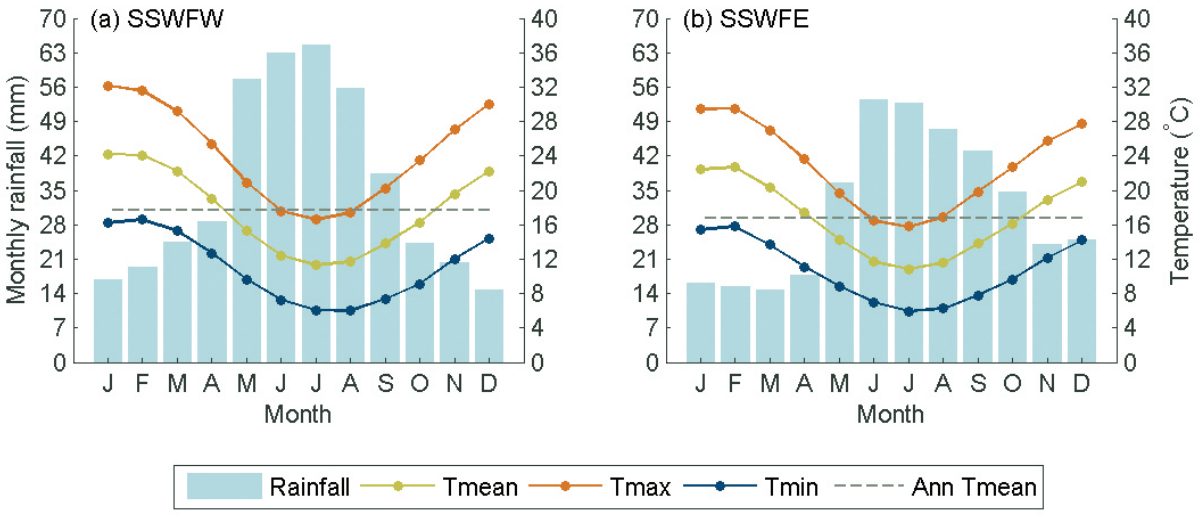

FIGURE 2.2: MONTHLY RAINFALL (BLUE BARS) AND TEMPERATURE CHARACTERISTICS FOR THE SSWF CLUSTER WEST (A) AND EAST (B) (1986–2005). *TMEAN* IS MONTHLY MEAN TEMPERATURE (GREEN LINE), *TMAX* IS MONTHLY MEAN MAXIMUM TEMPERATURE (ORANGE LINE), *TMIN* IS MONTHLY MEAN MINIMUM TEMPERATURE (BLUE LINE), AND *ANN TMEAN* IS THE ANNUAL AVERAGE OF MEAN TEMPERATURE (GREY LINE) (17.7 °C FOR SSWFW AND 16.9 °C FOR SSWFE). TEMPERATURE AND RAINFALL DATA ARE FROM AWAP.

Geographically, there are strong gradients in mean rainfall across both sub-clusters. The far south-west of SSWFW receives annual rainfall totals of 1200 mm while only 300 mm falls further inland. SSWFE is drier, but still shows a strong gradient. The east of the sub-cluster can receive 600 mm near the coast, but regions further inland and along the top of the Great Australian Bight receive totals closer to 200 mm. In the regions with higher rainfall totals, the seasonal cycle of rainfall across the Southern and South-Western Flatlands cluster is Mediterranean, with low rainfall in summer and higher rainfall in winter. This is reflected in the sub-cluster averages (Figure 2.2).

Spatially, for the period 1986–2005, the winter (June to August) rainfall pattern (Figure 2.3b) reflects the annual totals. The pattern of mean rainfall in summer (December to February) for SSWFW reflects some contribution from winter-type storms in late spring, which carry rain to the south-western corner (Figure 2.3a). A north-west to south-east band of slightly higher totals on the eastern edge of SSWFW is associated with easterly troughs (Raut *et al.,* 2014) and the breakdown of tropical cyclones. There is slightly more rainfall in this band in the warmer half of the year than in the cooler half of the year. Warm season rainfall also contributes to the annual total over inland areas of SSWFE.

Seasonal rainfall characteristics in the Southern and South-Western Flatlands cluster are determined by complex interactions of several rainfall drivers that influence this region. Rainfall has been relatively consistent from year to year across the cluster in winter in the recent period, but sporadic storms from either the tropics or mid-latitudes in summer mean there has been greater variability and lower totals. The term 'driver' is used to signify a system's role in the generation of rainfall and includes a range of synoptic weather features and large-scale modes of variability. The major driver of the seasonal average differences in rainfall totals is the sub-tropical ridge shifting south in summer and north in winter. When the sub-tropical ridge is in its summer position, fronts, troughs and lows rarely extend north from the 'Roaring Forties' to impact on these regions directly. Winter rainfall is associated with troughs and frontal systems (Hope *et al.,* 2014), cut-off lows and other low pressure systems linked to the westerlies. The different systems can produce a different pattern of rainfall across south-west Australia, where cut-off lows provide more inland rainfall and frontal systems bring more rainfall to the west coast (Pook *et al.,* 2012).

FIGURE 2.3: FOR THE 1986–2005 PERIOD, AVERAGE RAINFALL FOR (A) SUMMER (DECEMBER TO FEBRUARY) AND (B) WINTER (JUNE TO AUGUST).

Year to year variability in the intensity and position of the sub-tropical ridge can influence the amount of rainfall that falls over the SSWF cluster (see Box 2.1). The extent of the Hadley Cell and influences from the tropics can also affect fronts that bring rainfall to southern Australia. An index of the north-south variability of the westerlies and the resulting changes in mean sea level pressure is called the 'Southern Annular Mode' (SAM). When the index of SAM is positive, there are higher pressures over Australia and the west facing coasts of the SSWF cluster receive less rainfall in winter (Hendon *et al.,* 2007). This was the case in 2010, which saw the longest stretch of the SAM index in a positive state on record (Lovitt, 2011, Indian Ocean Climate Initiative, 2012), along with the lowest rainfall totals in south-west Australia. Tropical influences such as El Niño and La Niña and the Indian Ocean Dipole (IOD) also impact on rainfall variability across the SSWF, especially in southern South Australia. For further details on SAM, El Niño and La Niña, or the Indian Ocean Dipole, please see Chapter 4 in the Technical Report.

BOX 2.1: OBSERVED CHANGES IN MERIDIONAL CIRCULATION AND THEIR RELEVANCE TO THE SOUTHERN AND SOUTH-WESTERN FLATLANDS CLUSTER

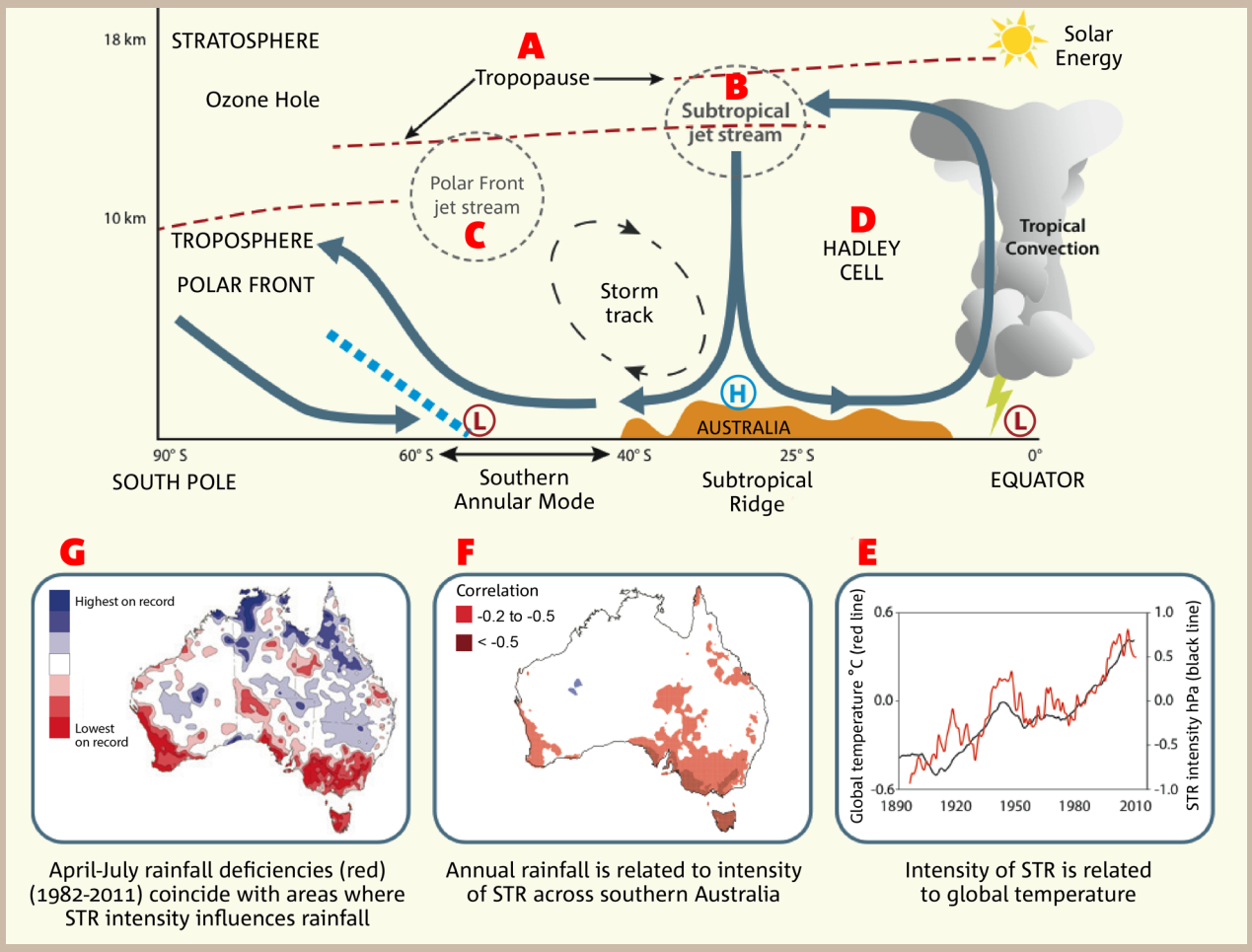

April-July rainfall deficiencies (red) (1982-2011) coincide with areas where STR intensity influences rainfall

Annual rainfall is related to intensity of STR across southern Australia

Intensity of STR is related to global temperature

The figure above uses a north-south cross-section through the atmosphere in eastern Australian longitudes to illustrate the atmospheric circulation in this plane ('the meridional circulation') and how changes in this may affect regional climate. The mean meridional circulation transfers excess energy received at the Equator toward the Pole. The following changes have been observed in key components of this process:

The tropics have expanded in recent decades. The edge of the tropical tropopause (A) has trended poleward during the last 30 years (Lucas *et al.,* 2014). The sub-tropical jet (B) has been observed to decrease in intensity while the polar front jet (C) has increased in intensity (Frederiksen and Frederiksen, 2011). The descending arm of the Hadley Cells (D) has trended poleward during the last 30 years (Nguyen *et al.,* 2013).

All these large-scale changes indicate a poleward extension of the Mean Meridional Circulation (Lucas *et al.,* 2014). This extension affects the climate observed across southern Australia, including intensification of the sub-tropical ridge during the last 120 years, in conjunction with global warming (E) (Timbal and Drosdowsky, 2013). Annual rainfall in much of southern Australia has a significant negative relationship with the intensity of the sub-tropical ridge (F), in particular for April to July rainfall (Timbal and Drosdowsky, 2013). The spatial extent of the negative rainfall anomalies for the early part of the cool season (April to July) during the last 30 years (G) coincide with the areas where the sub-tropical ridge (STR) influences the rainfall.

3 SIMULATING REGIONAL CLIMATE

Researchers use climate models to examine future global and regional climate change. These models have a foundation in well-established physical principles and are closely related to the models used successfully in weather forecasting. Climate modelling groups from around the world produce their own simulations of the future climate, which may be analysed and compared to assess climate change in any region. For this report, projections are based on historical and future climate simulations from the CMIP5 model archive that holds the most recent simulations, as submitted by approximately 20 modelling groups (Taylor *et al.,* 2012). The number of models used in these projections varies by RCP and variable depending on availability, *e.g.* for monthly temperature and rainfall, data are available for 39 models for RCP8.5 but only 28 models for RCP2.6 (see Chapter 3 in the Technical Report).

The skill of a climate model is assessed by comparing model simulations of the current climate with observational data sets (see Box 3.1 for details on the observed data used for model evaluation for the SWWF cluster). Accurate simulation of key aspects of the regional climate provides a basis for placing some confidence in the model's projections. However, models are not perfect representations of the real world. Some differences in model output relative to the observations are to be expected. The measure of model skill can also vary depending on the scoring measure used and regions being assessed.

BOX 3.1: COMPARING MODELS AND OBSERVATIONS: EVALUATION PERIOD, DATA SETS, AND SPATIAL RESOLUTION

Model skill is assessed by running simulations over historical time periods and comparing simulations with observed climate data. Projections presented here are assessed using the 1986–2005 baseline period, which conforms to the *Fifth Assessment Report* (IPCC, 2013). The period is also the baseline for projected changes, as presented in bar plots and tabled values in the Appendix. An exception is the time series projection plots, which use a baseline of 1950–2005, as explained in Section 6.2.2 of the Technical Report.

Several data sets are used to evaluate model simulations of the current climate. For assessment of rainfall and temperature, the observed data are derived from the Australian Water Availability Project (AWAP) (Jones *et al.,* 2009) and from the Australian Climate Observations Reference Network – Surface Air Temperature (ACORN-SAT), a data set developed for the study of long-term changes in monthly and seasonal climate (Fawcett *et al.,* 2012). For mean sea level pressure derived indices the HadSLP2 dataset is used (Allan and Ansell, 2006).

The spatial resolution of climate model data (around 200 km between the edges of grid cells) is much coarser than observations, and while for the SSWFW sub-cluster most CMIP5 models provide coverage by full grid cells, only a handful of models provide full grid cell coverage for the SSWFE sub-cluster. This means that simulation of past and future climates should be interpreted as representative of a region including adjacent areas of neighbouring cluster regions.

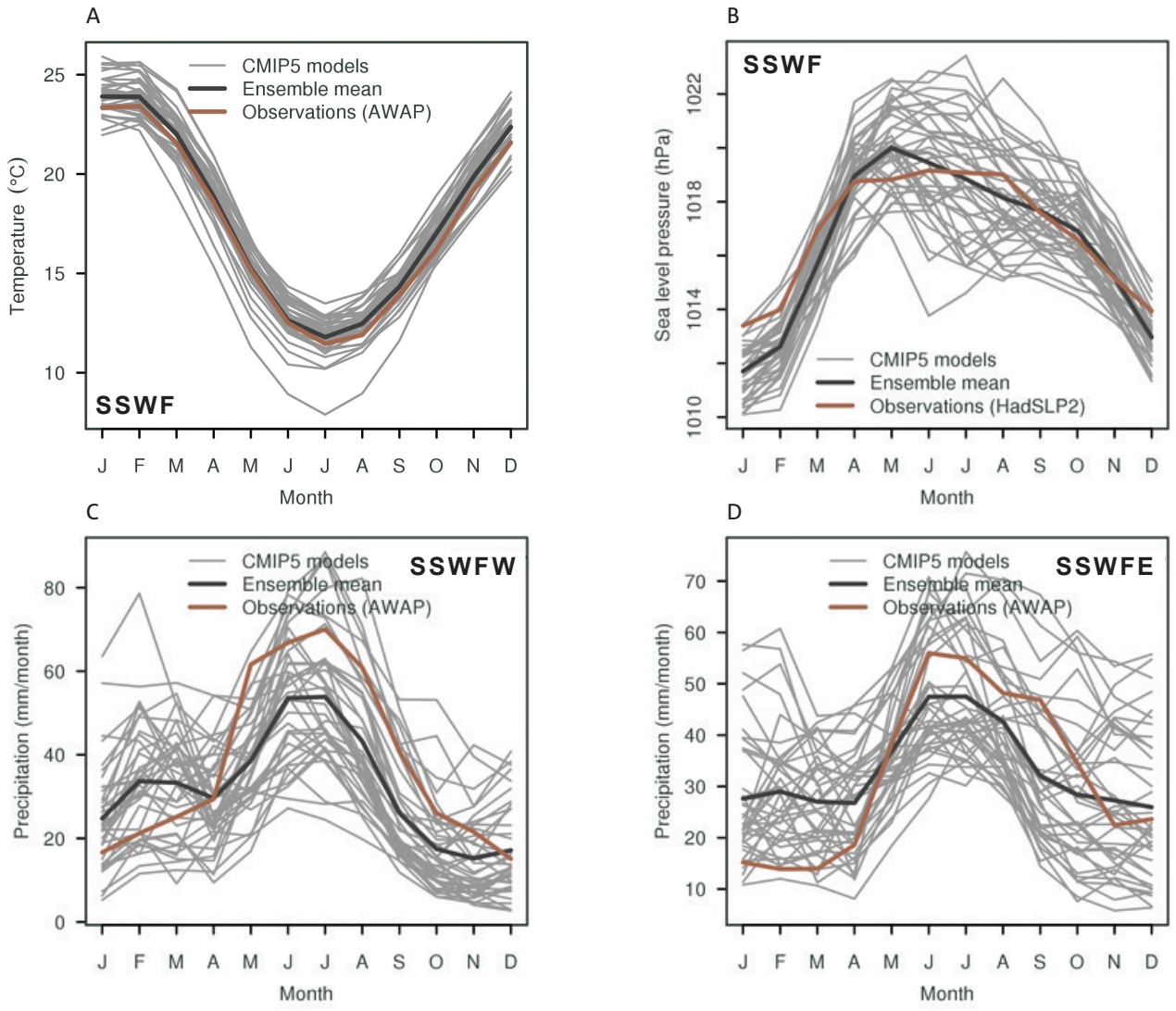

FIGURE 3.1: THE ANNUAL CYCLE OF TEMPERATURE (A), AND SEA LEVEL PRESSURE (B) IN THE SSWF CLUSTER, AND THE ANNUAL CYCLE OF RAINFALL FOR SSWFW (C) AND SSWFE (D) SIMULATED BY CMIP5 MODELS (GREY LINES) WITH MODEL ENSEMBLE MEAN (BLACK LINE) AND OBSERVED CLIMATOLOGY (TEMPERATURE AND RAINFALL BASED ON AWAP AND SEA LEVEL PRESSURE ON HADSLP2) FOR THE BASELINE PERIOD 1986–2005 (BROWN LINE).

All GCMs considered for this report competently reproduced the cluster annual cycle of temperature (Figure 3.1a), although one model simulated temperatures that were too cold in winter. There was more spread in the simulation of the correct mean magnitude of mean sea level pressure in each month (Figure 3.1b), possibly because the location of the sub-tropical ridge differs a little in some models. However, the timing of the annual cycle is generally correct across all models. The similarities in seasonal patterns between models and observed data, and the knowledge that regional pressure and temperatures are strongly related to the general circulation of the atmosphere, together indicate that the models do a reasonable job of simulating the current atmosphere and are likely to simulate reasonable future projections.

It is important that these models simulate the seasonal timing of the shifts in pressure as this relates closely to the seasonal shift in the sub-tropical ridge, one of the major drivers of rainfall variability for this cluster (see Box 2.1). The climate models simulate the high rainfall peak in winter for both sub-clusters (Figures 3.1c and 3.1d); however, many also simulate a secondary peak in late summer, particularly in south-western Australia. This is due to summer rainfall extending further south from the tropics in these models than what is observed. This means that the drivers of change in summer may show a stronger tropical influence than observed.

The recent observed trends were also evaluated by season. Most simulations showed a decline in rainfall from 1960–2005 in the cooler seasons, but the magnitude was generally less than observed. For many models the decline is later in the year than observed (late autumn and early winter).

Evaluation of CMIP5 models also extends to some of the drivers for rainfall variability in the SSWF cluster. For example, earlier versions of the CMIP5 models were able to produce a clear Southern Annular Mode (Raphael and Holland, 2006), but the shape and orientation of the pattern varies among the models.

Tropical influences such as ENSO are also important for climate variability, particularly in SSWFE. While capturing the pattern of ENSO is still a challenge, the CMIP5 models, as a whole, are improved compared to the previous generation of climate models (CMIP3), as demonstrated by the fact that the 10 best performing models in capturing the ENSO-rainfall relationship across Australia (for 1980–1999) are CMIP5 models (see Figure 5.9 in the Technical Report).

In addition to the CMIP5 model results, downscaling can be used to derive finer spatial information in the regional projections, thus potentially capturing processes occurring on a finer scale. While downscaling can provide added value on finer scale processes, it increases the uncertainty in the projections since there is no single best downscaling method, but a range of methods that are more or less appropriate depending on the application. It is advisable to consider more than one technique, as different downscaling techniques have different strengths and weaknesses.

For the regional projections we consider downscaled projections from two techniques: outputs from a dynamical downscaling model, the Conformal Cubic Atmospheric Model (CCAM) (McGregor and Dix, 2008) using six CMIP5 GCMs as input; and the Bureau of Meteorology analogue-based statistical downscaling model with 22 CMIP5 GCMs as input for rainfall and 21 CMIP5 GCMs as input for temperature (Timbal and McAvaney, 2001). Where relevant, projections from these methods are compared to those from GCMs (the primary source of climate change projections in this report). The downscaled results are only emphasised if there are strong reasons for giving the downscaled data more credibility than the GCM data (see Section 6.3 in the Technical Report for further details on downscaling).

4 THE CHANGING CLIMATE OF THE SOUTHERN AND SOUTH-WESTERN FLATLANDS

This Section presents projections of climate change to the end of the 21st century for a range of climate variables, including average and extreme conditions, of relevance to the SSWF cluster. Where there are relevant observational data available, the report shows historical trends.

As outlined in the *Fifth Assessment Report* (IPCC, 2013), greenhouse gases, such as carbon dioxide, have a warming effect on global climate. These gases absorb heat that would otherwise be lost to space, and re-radiate it back into the atmosphere and to the Earth's surface. The IPCC concluded that it was *extremely likely* that more than half of the observed increase in global average surface air temperature from 1951–2010 has been caused by the anthropogenic increase in greenhouse gas emissions and other anthropogenic forcings. Further increases in greenhouse gas concentrations resulting primarily from burning fossil fuel will lead to further warming, as well as other physical and chemical changes in the atmosphere, ocean and land surface.

The CMIP5 simulations give the climate response to a set of greenhouse gas, aerosol and land-use scenarios that are consistent with socio-economic assumptions of how the future may evolve. These scenarios are known as the Representative Concentration Pathways (RCPs) (Moss *et al.*, 2010; van Vuuren *et al.*, 2011). Box 4.1 presents a brief introduction to the RCPs.

In its *Fifth Assessment Report* (IPCC, 2013), the IPCC concluded that global mean surface air temperatures for 2081–2100 relative to 1986–2005 are likely to be in the following ranges: 0.3 to 1.7 °C warmer for RCP2.6 (representing low emissions); 1.1 to 2.6 °C and 1.4 to 3.1 °C warmer for RCP4.5 and RCP6.0 respectively (representing intermediate emissions); and 2.6 to 4.8 °C warmer for RCP8.5 (representing high emissions).

The projections for the climate of the SSWF cluster consider model ranges of change, as simulated by the CMIP5 ensemble. However, the projections should be viewed in the context of the confidence ratings that are provided, which consider a broader range of evidence than just the model outputs. The

BOX 4.1: REPRESENTATIVE CONCENTRATION PATHWAYS (RCPs)

The climate projections presented in this report are based on climate model simulations following a set of greenhouse gas, aerosol and land-use scenarios that are consistent with socio-economic assumptions of how the future may evolve. The well mixed concentrations of greenhouse gases and aerosols in the atmosphere are affected by emissions as well as absorption through land and ocean sinks.

There are four Representative Concentration Pathways (RCPs) underpinned by different emissions. They represent a plausible range of radiative forcing (in W/m^2) during the 21st century relative to pre-industrial levels. Radiative forcing is a measure of the energy absorbed and retained in the lower atmosphere. The RCPs are:

- RCP8.5: high radiative forcing (high emissions)
- RCP4.5 and 6.0: intermediate radiative forcing (intermediate emissions)
- RCP2.6: low radiative forcing (low emissions).

RCP8.5, represents a future with little curbing of emissions, with carbon dioxide concentrations reaching 940 ppm by 2100. The higher of the two intermediate concentration pathways (RCP6.0) assumes implementation of some mitigation strategies, with carbon dioxide reaching 670 ppm by 2100. RCP4.5 describes somewhat higher emissions than RCP6.0 in the early part of the century, with emissions peaking earlier then declining, and stabilisation of the carbon dioxide concentration at about 540 ppm by 2100. RCP2.6 describes emissions that peak around 2020 and then rapidly decline, with the carbon dioxide concentration at about 420 ppm by 2100. It is likely that later in the century active removal of carbon dioxide from the atmosphere would be required for this scenario to be achieved. For further details on all RCPs refer to Section 3.2 and Figure 3.2.2 in the Technical Report.

The previous generation of climate model experiments that underpins the science of the IPCC's *Fourth Assessment Report* used a different set of scenarios. These are described in the IPCC's Special Report on Emissions Scenarios (SRES) (Nakićenović and Swart, 2000). The RCPs and SRES scenarios do not correspond directly to each other, though carbon dioxide concentrations under RCP4.5 and RCP8.5 are similar to those of SRES scenarios B1 and A1FI respectively.

In the Technical and Cluster Reports, RCP6.0 is not included due to a smaller sample of model simulations available compared to the other RCPs. Remaining RCPs are included in most graphical and tabulated material of the Cluster Reports, with the text focusing foremost on results following RCP4.5 and RCP8.5.

projected change is assessed for two 20-year periods: a near future 2020–2039 (herein referred to as 2030) and a period late in the 21st century, 2080–2099 (herein referred to as 2090) following RCPs 2.6, 4.5 and 8.5 (Box 4.1)[2].

The spread of model results is presented in graphical form (Box 4.2) and provided as tabulated percentiles in Table 1 (10th, 50th and 90th) and Table 3 (5th, 50th and 95th, for sea level rise) in the Appendix. CMIP5 results for additional time periods between 2030 and 2090 are provided through the Climate Change in Australia website (Box 1).

Unless otherwise stated, users of these projections should consider the projected change, as indicated by the different plots and tabulated values, applicable to each location within the cluster.

4.1 RANGES OF PROJECTED CLIMATE CHANGE AND CONFIDENCE IN PROJECTIONS

Quantitative projections of future climate change for the SSWF cluster are presented as ranges. This allows for differences in how future climate may evolve due to three factors – greenhouse gas and aerosol emissions, the climate response and natural variability – that are not known precisely:

- Future emissions cannot be known precisely and are dealt with here by examining several different RCPs described in Box 4.1. There is no 'correct' scenario, so the choice of how many and which scenarios to examine is dependent on the decision-making context.
- The response of the climate system to emissions is well known in some respects, but less well known in others. The thermodynamic response (direct warming) of the atmosphere to greenhouse gases is well understood, although the global climate sensitivity varies. However, changes to atmospheric circulation in a warmer climate are one of the biggest uncertainties regarding the climate response. The range between different climate models (and downscaled models) gives some indication of the possible responses. However, the range of model results is not a systematic or quantitative assessment of the full range of possibilities, and models have some known regional biases that affect confidence.
- Natural variability (or natural 'internal variability' within the climate system) can dominate over the 'forced' climate change in some instances, particularly over shorter time frames and smaller geographic areas. The precise evolution of climate due to natural variability (*e.g.* the sequence of wet years and dry years) cannot be predicted (IPCC, 2013, see Chapter 11). However, the projections presented here allow for a range of outcomes due to natural variability, based on the different evolutions of natural climatic variability contained within each of the climate model simulations.

The relative importance of each of these factors differs for each variable, different timeframes and spatial scale.

For some variables with large natural variability, such as rainfall, the predominant reason for differing projections in the early period is likely to be natural variability rather than differences in emission scenarios (the influence of which becomes relatively more important as greenhouse gas concentrations increase).

In addition, unpredictable events, such as large volcanic eruptions, and processes not included in models, could influence climate over the century. See the *Fifth Assessment Report* (IPCC, 2013) Chapter 11 for further discussion of these issues.

The projections presented are accompanied by a confidence rating that follows the system used by the IPCC in the *Fifth Assessment Report* (Mastrandrea *et al.,* 2010), whereby the confidence in a projected change is assessed based on the type, amount, quality and consistency of evidence (which can be process understanding, theory, model output, or expert judgment) and the extent of agreement amongst the different lines of evidence. Hence, this confidence rating does not equate precisely to probabilistic confidence. The levels of confidence used here are set as *low, medium, high* or *very high*. Note that although confidence may be high in the direction of change, in some cases confidence in magnitude of change may be medium or low (*e.g.* due to some known model deficiency). When confidence is low only qualitative assessments are given. More information on the method used to assess confidence in the projections is provided in Section 6.4 of the Technical Report.

4.2 TEMPERATURE

Surface air temperatures in the cluster have warmed since national records began in 1910, especially since 1960 (Figure 4.2.1, Figure 4.2.2). From 1910–2013, mean temperature has risen by 1.1 °C in SSWFW and 0.7 °C in SSWFE using a linear trend. In the same period, daytime maximum temperatures rose by 1.1 °C in SSWFW and 0.8 °C in SSWFE, and overnight minimum temperatures increased by 1.1 °C in SSWFW and by 0.6 °C in SSWFE using a linear trend.

Marked decadal variability can be seen when comparing long-term trends in minimum and maximum temperature for the 20th century (Figure 4.2.3). Both records show increases since the mid 20th century, but at varying rates. From the 1960s the values of the anomalies in minimum temperature were generally of higher magnitude than the anomalies of maximum temperature, but in recent years and at times earlier in the century, the anomalies of the maximum temperature were greater than for those for the minimum. The recent shift to higher maximum temperature anomalies may be linked to drier conditions in recent years. Drier conditions are likely associated with less cloud which then allows greater solar input during the day, but also allows more heat to be released through the atmosphere at night, leading to relatively cooler minimum anomalies.

2 For sea level rise and sea allowance, the future averaging periods are 2020–2040 and 2080–2100. In the report, these are referred to as 2030 and 2090 respectively.

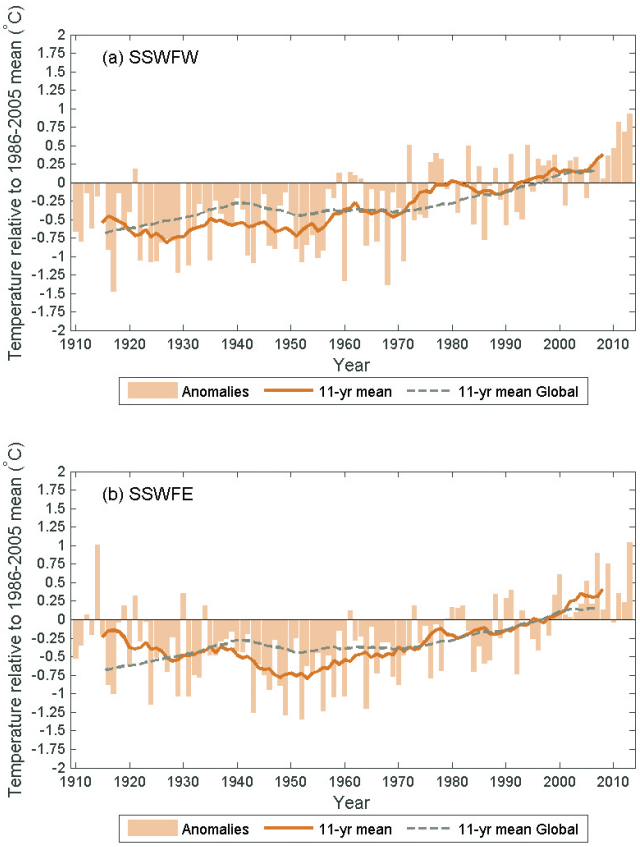

Projected annual warming for the Southern and South-Western Flatlands cluster throughout the 21st century is shown in Figure 4.2.4 for RCP2.6, RCP4.5 and RCP8.5 for SSWFW and SSWFE separately. Model simulations of future warming show inter-annual variability of similar magnitude to that of observed data (*e.g.* the overlaid observational time series stays largely within the lightly shadowed band representing the 10th and 90th year to year variability of the model ensemble) and overall there is good agreement between model and observed data on decadal scales.

FIGURE 4.2.1: OBSERVED ANNUAL MEAN TEMPERATURE ANOMALIES (°C) FOR 1910–2013 COMPARED TO THE BASELINE 1986–2005 FOR (A) SSWFW AND (B) SSWFE. CLUSTER AVERAGE DATA ARE FROM ACORN-SAT AND GLOBAL DATA ARE FROM HADCRUT3V (BROHAN *ET AL.*, 2006).

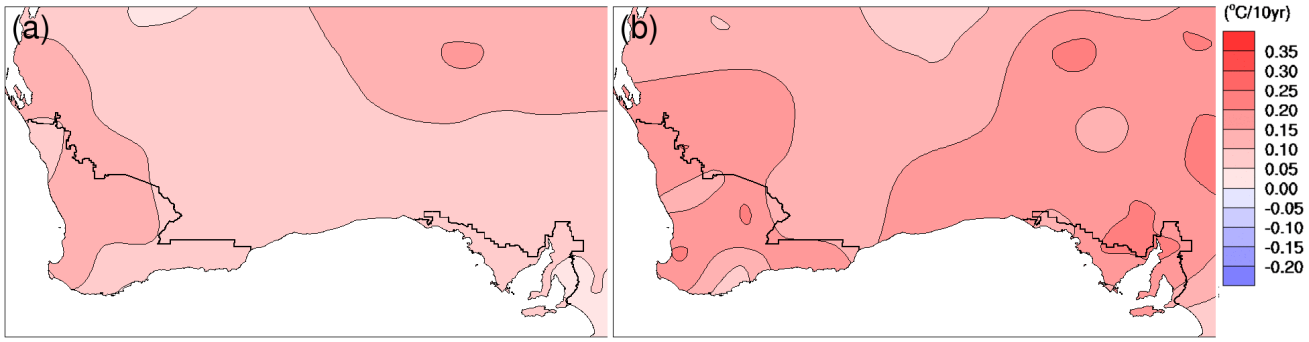

FIGURE 4.2.2: MAPS OF TREND IN MEAN TEMPERATURE (°C/10YEARS) FOR (A) 1910–2013 AND (B) 1960–2013 (ACORN-SAT).

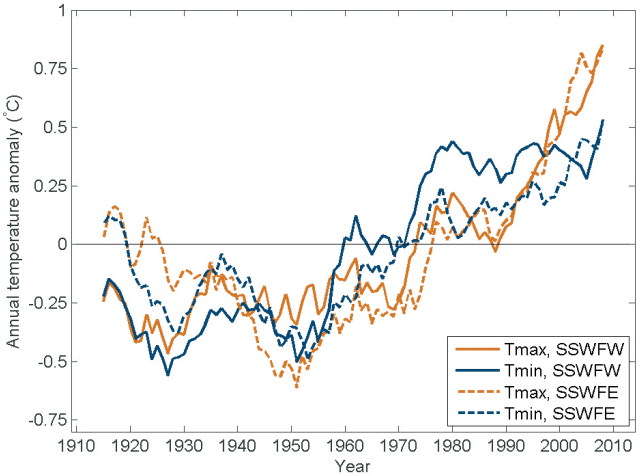

FIGURE 4.2.3: OBSERVED ANNUAL MEAN OF DAILY MAXIMUM (ORANGE LINE) AND MINIMUM (BLUE LINE) TEMPERATURE (°C, 11-YEAR RUNNING MEAN), PRESENTED AS ANOMALIES RELATIVE TO THEIR RESPECTIVE 1910–2013 MEAN VALUE (ACORN-SAT); SSWFW IS IN SOLID LINES AND SSWFE IN DASHED LINES.

BOX 4.2: UNDERSTANDING PROJECTION PLOTS

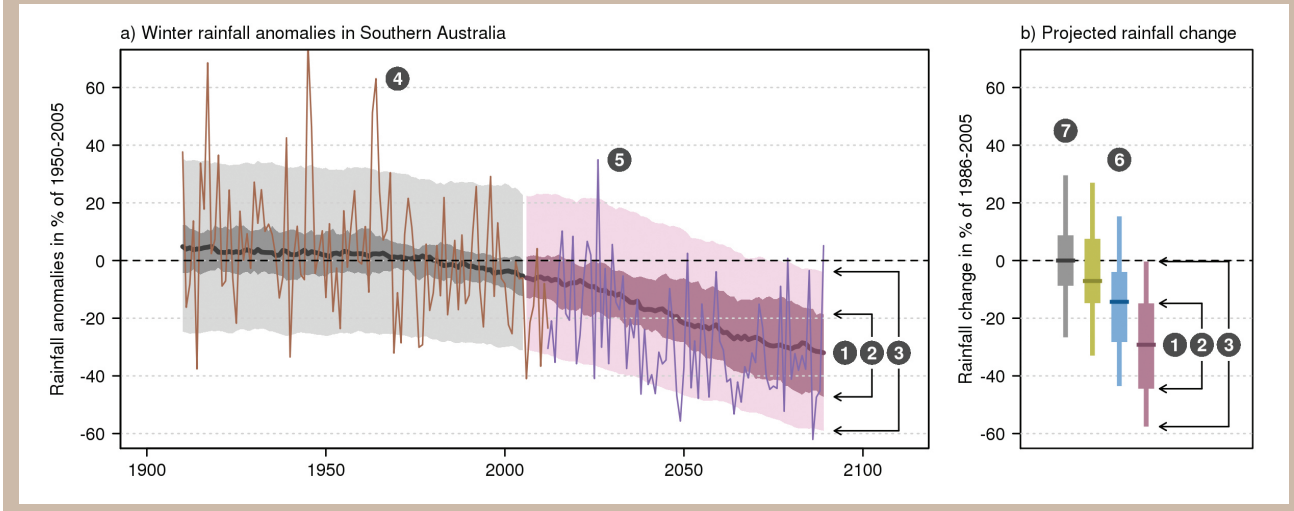

Projections based on climate model results are illustrated using time series (a) and bar plots (b). The model data are expressed as anomalies from a reference climate. For the time series (a), anomalies are calculated as relative to 1950–2005, and for the bar plots (b) anomalies are calculated as the change between 1986–2005 and 2080–2099 (referred to elsewhere as '2090'). The graphs can be summarised as follows:

1. The middle (bold) line in both (a) and (b) is the median value of the model simulations (20-year moving average); half the model results fall above and half below this line.
2. The bars in (b) and dark shaded areas in (a) show the range (10th to 90th percentile) of model simulations of 20-year average climate.
3. Line segments in (b) and light shaded areas in (a) represent the projected range (10th to 90th percentile) of individual years taking into account year to year variability in addition to the long-term response (20-year moving average).

In the time series (a), where available, an observed time series (4) is overlaid to enable comparison between observed variability and simulated model spread. A time series of the future climate from one model is shown to illustrate what a possible future may look like (5). ACCESS1-0 was used for RCP4.5 and 8.5, and BCC-CSM-1 was used for RCP2.6, as ACCESS1-0 was not available.

In both (a) and (b), different RCPs are shown in different colours (6). Throughout this document, green is used for RCP2.6, blue for RCP4.5 and purple for RCP8.5, with grey bars used in bar plots (b) to illustrate the expected range of change due to natural internal climate variability alone (7).

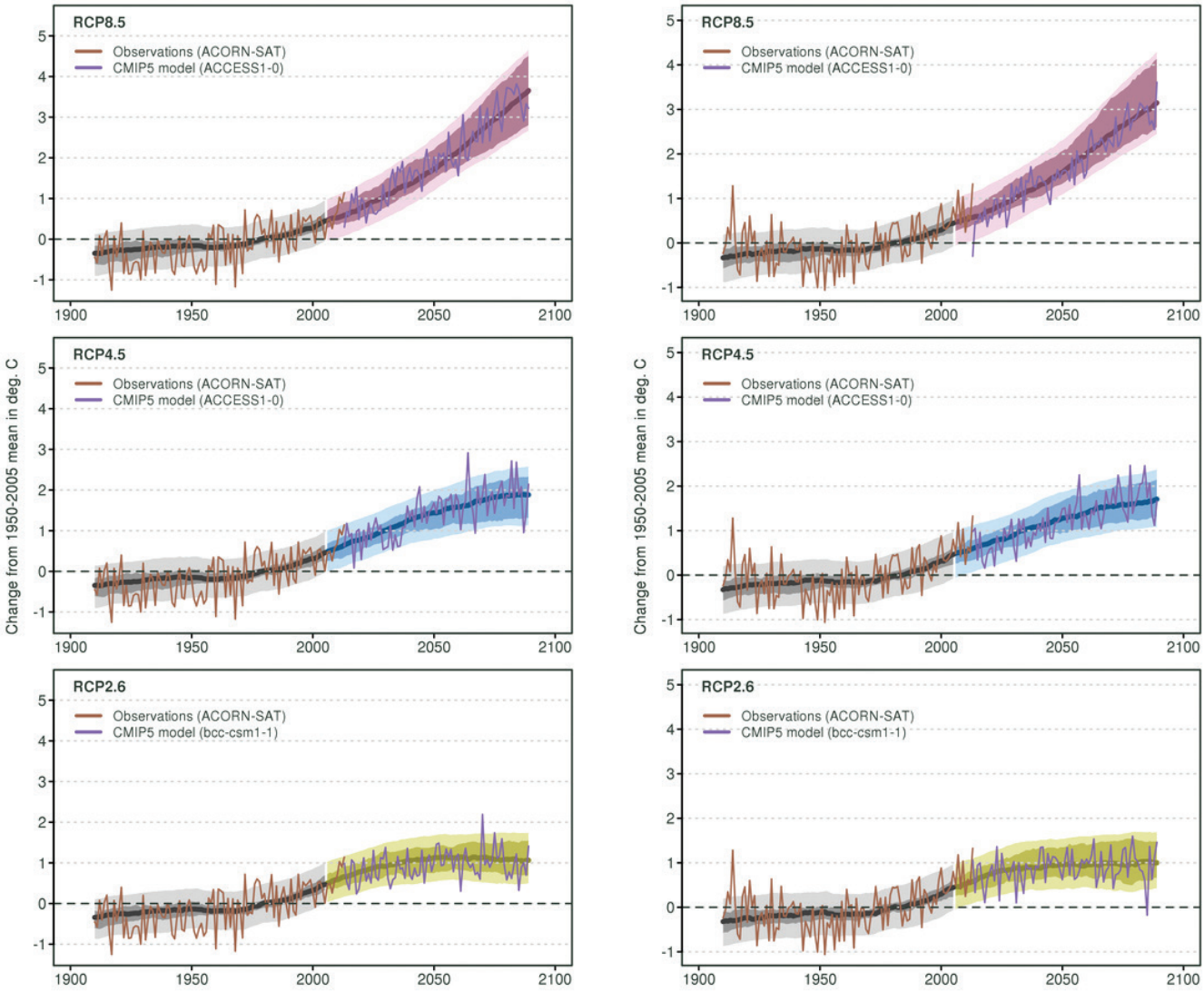

FIGURE 4.2.4: TIME SERIES FOR ANNUAL AVERAGE SURFACE AIR TEMPERATURE (°C) FOR 1910–2090, AS SIMULATED IN CMIP5 RELATIVE TO THE 1950–2005 MEAN. PANELS ON THE LEFT ARE SSWFW AND PANELS ON RIGHT SSWFE. THE CENTRAL LINE IS THE MEDIAN VALUE, AND THE SHADING IS THE 10TH AND 90TH PERCENTILE RANGE OF 20-YEAR MEANS (INNER) AND SINGLE YEAR VALUES (OUTER). THE GREY SHADING INDICATES THE PERIOD OF THE HISTORICAL SIMULATION, WHILE THREE FUTURE SCENARIOS ARE SHOWN WITH COLOUR-CODED SHADING: RCP8.5 (PURPLE), RCP4.5 (BLUE) AND RCP2.6 (GREEN). ACORN-SAT OBSERVATIONS AND PROJECTED VALUES FROM A TYPICAL MODEL ARE SHOWN. TIME SERIES PLOTS ARE EXPLAINED IN BOX 4.2.

The projected increase in temperature reflects the emission scenario, since high concentrations of greenhouse gases in the atmosphere are strongly related to near surface temperature. Table 1 in the Appendix lists the 10th and 90th percentiles for the near future time period (2030) and late in the century (2090). With regard to the near future, projections fall in the range of 0.5 to 1.2 °C for SSWFW, 0.4 to 1.1 °C for SSWFE, and 0.5 to 1.1 °C for SSWF overall (10th to 90th percentile), with only minor difference between the scenarios. The projected temperature range for 2090 shows larger differences between the scenarios. For the RCP4.5, the warming is 1.1 to 2.1 °C for SSWFW, 1.0 to 1.9 °C for SSWFE, and 1.2 to 2.0 °C for SSWF, while significantly higher warming is given for the RCP8.5 with a range of 2.6 to 4.2 °C for SSWFW, 2.4 to 3.9 °C for SSWFE and 2.6 to 4.0 °C for SSWF. In RCP2.6, further warming still occurs, but it is only slightly greater than for the 2030 projections (0.5 to 1.3 °C for SSWF).

Included in Fig 4.2.4 is an example of a model simulation. This is included to illustrate that individual simulations produce temporal variability similar to that of observed temperature, *i.e.* models do not simulate a sequentially steady increase in temperature from one year to another. Like in an observed time series, the projected model data shows individual years that are warmer or cooler than preceding years. When comparing the trajectory of warming to the spread of natural variability, the warming signal in regional temperature due to increased greenhouse emissions appears to emerge from the natural variability around the 2050s for most RCPs. This 'emergence' occurs when the range of temperatures in the future moves beyond the envelope of the current climate.

Overall, the warming rates of the SSWF cluster is consistent with the majority of other NRM clusters of Australia, with higher rates projected for inland western Australia and somewhat lower rates for the south-east and Tasmania.

Adding the projected change in annual mean temperature for the 2090 period (for a global warming case of 3.7 °C) onto the mapped observed climatology (here the 1986–2005 mean) illustrates the spatial pattern of warming across southern Australia, including the SSWF cluster (Figure 4.2.5). Where the climatology indicates mean temperatures for this period to range between 15 and 22 °C, with a strong south to north gradient, under a global warming of 3.7 °C, regional temperatures increase to range between about 18 and 27 °C. The pattern of annual mean temperature change produced by the statistical downscaling method is similar, with subtle, but potentially important, differences (Figure 4.2.5c). The warmer temperatures to the north of this cluster are shifted further south using this method, thus enhancing the gradient in temperature from the south coast inland.

Seasonal variability in the warming pattern is shown in Figure 4.2.6 and Table 1 in the Appendix for both SSWFW and SSWFE, displaying the range of warming simulated by the CMIP5 models for late in the 21st century. The range of expected warming is strongly dependent on the emission scenario. The models generally simulate a smaller range in winter and a greater increase in daily maximum temperature in spring in both SSWFW and SSWFE.

Looking at downscaling results for the cluster, there are no significantly different trends using either the dynamical or statistical downscaling method when compared with the direct model output shown in Figure 4.2.4.

Taking into consideration the strong agreement on direction and magnitude of change amongst GCMs and downscaling results, and the robust understanding of the driving mechanisms of warming and its seasonal variation, there is *very high confidence* in substantial increase in the SSWF cluster of annual and seasonal projections for mean, maximum and minimum temperature.

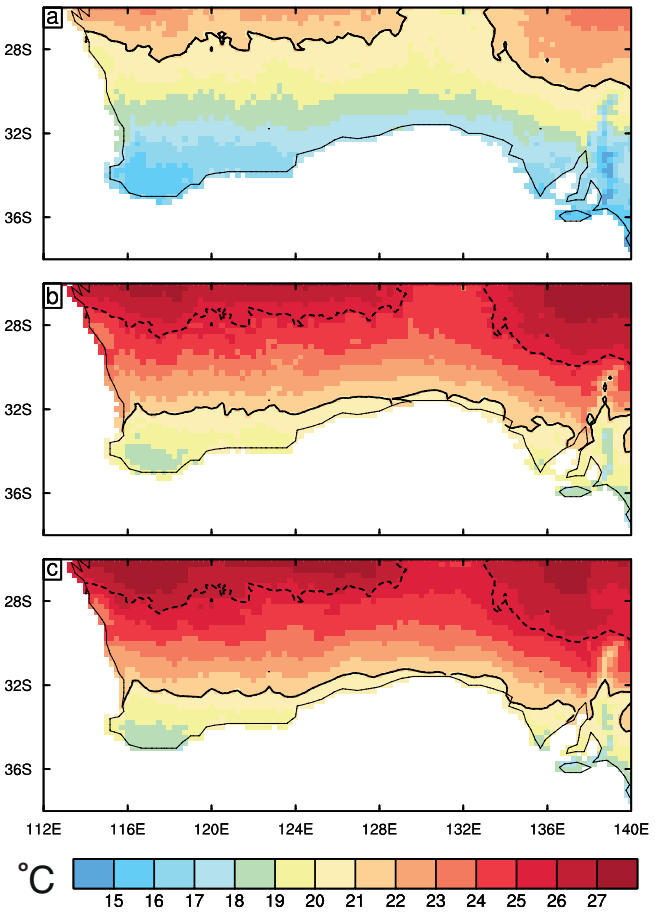

FIGURE 4.2.5: ANNUAL MEAN SURFACE AIR TEMPERATURE (°C) ACROSS SOUTHERN AUSTRALIA, FOR THE PRESENT CLIMATE (A), AND FOR 2090 USING TWO DOWNSCALING METHODS (B) AND (C). THE PRESENT IS USING AWAP FOR 1986–2005 (BASED ON A 0.25 DEGREE GRID). THE FUTURE CASE IS USING THE MEDIAN CHANGE AT 2090, UNDER THE HIGH EMISSION SCENARIO USING A SCALING METHOD (UNDER A GLOBAL WARMING OF 3.7 °C CASE) (B) AND THE ANALOGUE STATISTICAL DOWNSCALING METHOD (C). TO HIGHLIGHT THE SOUTHWARD MOVEMENT OF TEMPERATURE REGIMES, THE 21 °C CONTOUR IN EACH PANEL IS SHOWN WITH A SOLID BLACK LINE. IN (B) AND (C) THE CONTOUR FROM THE ORIGINAL CLIMATE IS PLOTTED AS A DOTTED LINE.

SSWFW

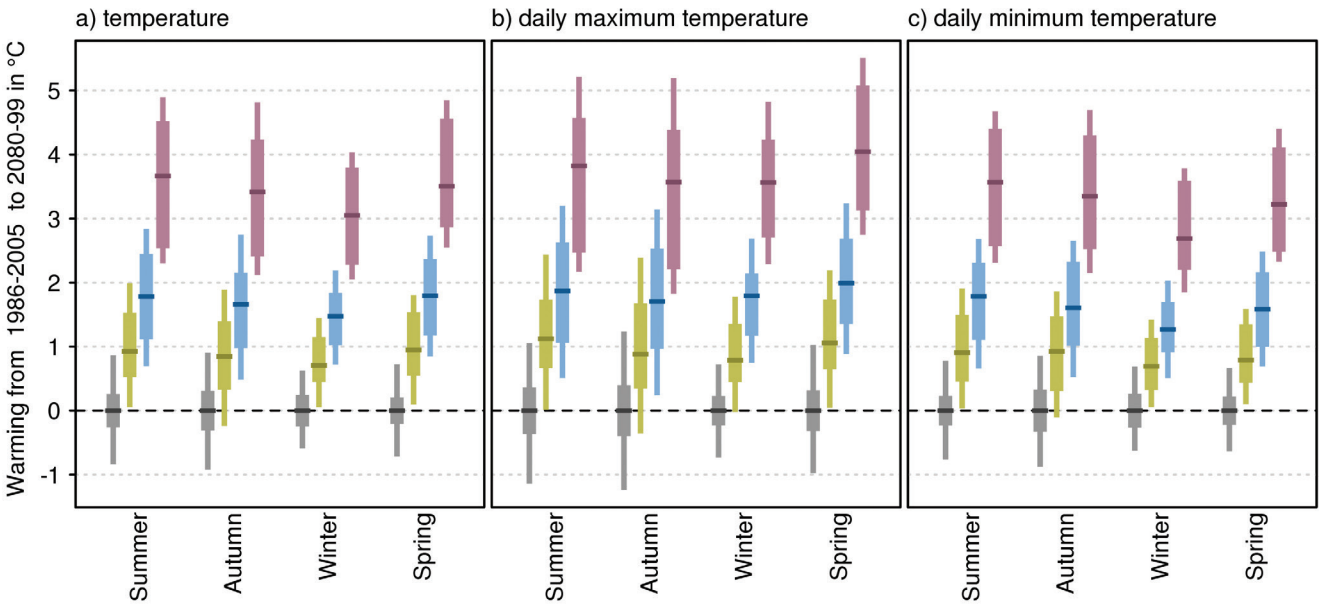

SSWFE

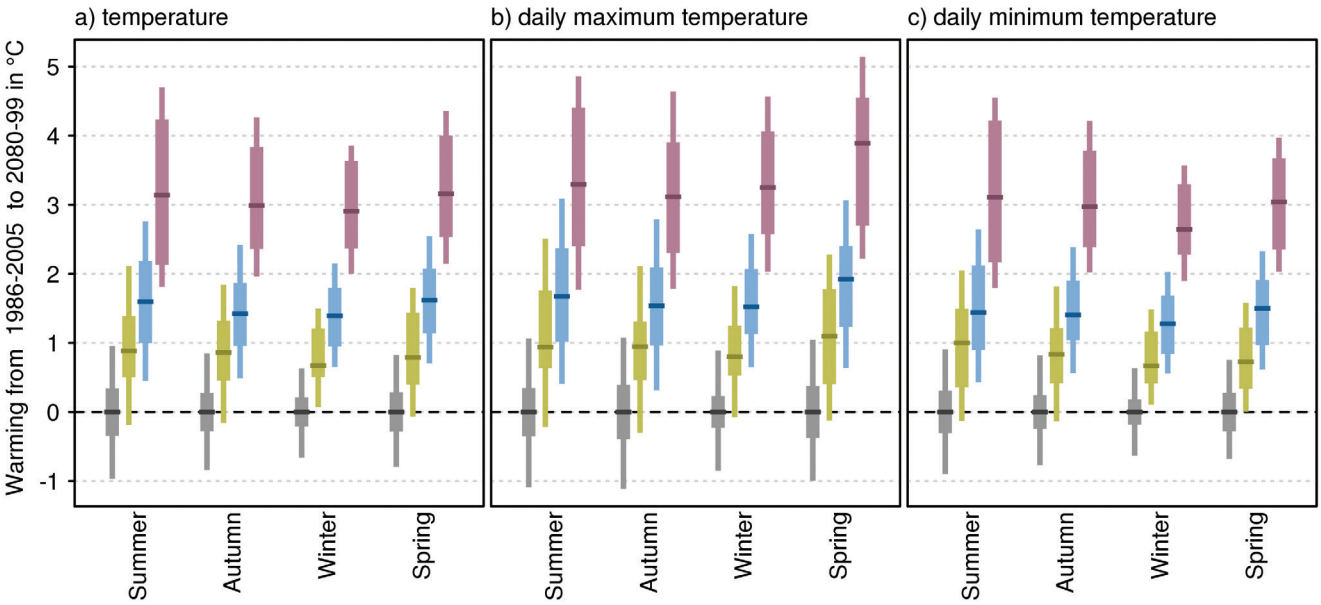

FIGURE 4.2.6: PROJECTED SEASONAL SURFACE AIR TEMPERATURE CHANGES FOR SSWFW (TOP PANEL) AND SSWFE (BOTTOM PANEL) FOR 2090. GRAPHS SHOW CHANGES TO THE: (A) MEAN, (B) DAILY MAXIMUM AND (C) DAILY MINIMUM TEMPERATURE. TEMPERATURE ANOMALIES ARE GIVEN IN °C RELATIVE TO THE 1986–2005 MEAN UNDER RCP2.6 (GREEN), RCP4.5 (BLUE) AND RCP8.5 (PURPLE). NATURAL CLIMATE VARIABILITY IS REPRESENTED BY THE GREY BAR. BAR PLOTS ARE EXPLAINED IN BOX 4.2.

4.2.1 EXTREMES

Changes to temperature extremes often lead to greater impacts than changes to the mean climate. To assess these, researchers examine CMIP5 projected changes to measures such as the warmest day in the year, warm spell duration and frost risk days (see definitions below).

Heat related extremes are projected to increase at a similar rate as projected mean temperature with a substantial increase in the number of warm spell days. Figure 4.2.7 (2090 case only) gives the CMIP5 model simulated warming on the hottest day of the year averaged across the cluster, and the corresponding warming for the hottest day in 20 years (20-year return level, equal to a 5 % chance of occurrence within any one year). The rate of warming for these hot days is similar to that for all days (*i.e.* the average warming reported in the previous Section). There is a marked increase in a warm spell index, which is defined as the annual count of events with at least six consecutive days with a cluster average temperature maximum above the 90th percentile (as an example, the 90th percentile for daily temperature maximum in Adelaide is 32.1 °C based on BOM historical data for January 1910 to June 2014).

Given the similarity in projected warming for the mean and hottest temperatures, an indication of the change in frequency of hot days locally can be obtained by applying the projected changes for maxima for selected time slices and RCPs to the historical daily record at selected sites. This is illustrated in Box 4.3, where it can be seen that the number of days above 35 °C in Perth or above 40 °C by late in the century (2090) is 150 % greater under the RCP4.5 and median model ensemble warming. The number of days above 35 °C in Adelaide also increases by about 150 %, but the number of days above 40 °C nearly doubles by late in the century (2090).

Strong model agreement and understanding of physical mechanisms of warming leads to *very high confidence* in a substantial increase in the heat related extremes discussed above and shown in Figure 4.2.7.

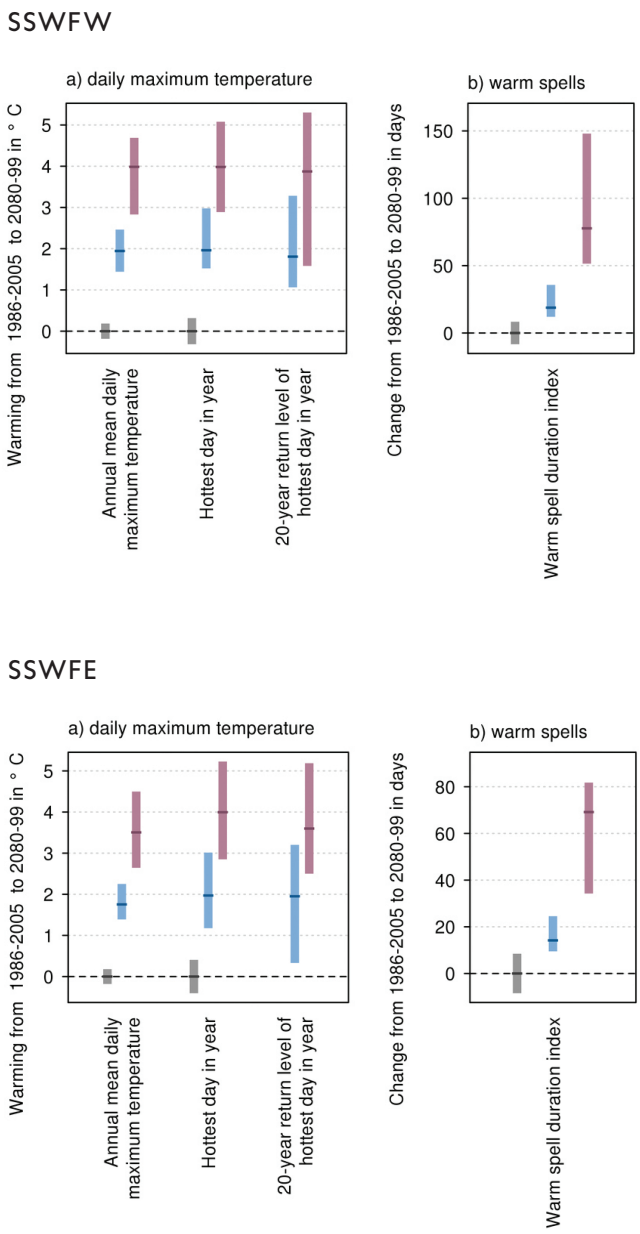

FIGURE 4.2.7: PROJECTED CHANGES IN SURFACE AIR TEMPERATURE EXTREMES BY 2090 IN A) MEAN DAILY MAXIMUM TEMPERATURE, HOTTEST DAY OF THE YEAR AND THE 20-YEAR RETURN VALUE OF THE HOTTEST DAY OF THE YEAR (°C); AND B) CHANGE IN THE NUMBER OF DAYS IN WARM SPELLS FOR FOR THE SSWFW (TOP) AND SSWFE (BOTTOM) SUB-CLUSTERS (SEE TEXT FOR DEFINITION OF VARIABLES). RESULTS ARE SHOWN FOR RCP4.5 (BLUE) AND RCP8.5 (PURPLE) RELATIVE TO THE 1986–2005 MEAN. NATURAL CLIMATE VARIABILITY IS REPRESENTED BY THE GREY BAR. BAR PLOTS ARE EXPLAINED IN BOX 4.2.

Changes in the frequency of surface frost (defined here as days when the 2 metre temperature is less than 2 °C) are also of importance to the environment, agriculture, energy and other sectors. Assessing frost occurrence directly from global model output is not reliable, in part because of varying biases in land surface temperatures. However, it is possible to evaluate what CMIP5 models say about changes to frost occurrences by superimposing the projected change in temperature onto the minimum daily temperature record. Statistical downscaling may also be used, with similar results (see Technical Report Section 7.1).

Box 4.3 illustrates the change in frost days using the simple approach (as was done for hot days) noting that actual occurrence of frost will depend on many local factors not represented by this method. Results show that for 2030 under RCP4.5 there is a projected reduction in the number of days with the potential for frost. By 2090 the number is further reduced, with zero days with the potential for frost in Adelaide under RCP8.5. These results, based upon the observed distribution of minimum temperatures provide some guidance.

Strong model agreement and understanding of physical mechanisms of warming lead to *high confidence* in a substantial decrease in the frequency of frost.

BOX 4.3: HOW WILL THE FREQUENCY OF HOT DAYS AND FROST RISK DAYS CHANGE IN PERTH AND ADELAIDE?

To illustrate what the CMIP5 projected warming implies for changes to the occurrence of hot days and frost days at Perth (WA) and Adelaide (SA), a simple downscaling example was conducted.

The type of downscaling used here is commonly referred to as 'Change Factor Approach' (see Section 6.3.1. in the Technical Report), whereby a change (calculated from the simulated model change) is applied to an observed time series. In doing so, it is possible to estimate the frequency of extreme days under different emission scenarios.

In Table B4.3, days with maximum temperatures above 35 and 40 °C, and frost risk days (minimum temperature less than 2 °C) are provided for a number of locations for a 30-year period (1981–2010), and for downscaled data using seasonal change factors for maximum or minimum temperature for 2030 and 2090 under different RCPs.

TABLE B4.3: CURRENT AVERAGE ANNUAL NUMBER OF DAYS (FOR THE 30-YEAR PERIOD 1981–2010) ABOVE 35 AND 40 °C AND BELOW 2 °C (FROSTS) FOR PERTH AIRPORT (WA) AND ADELAIDE CBD (SA) BASED ON ACORN-SAT. ESTIMATES FOR THE FUTURE ARE CALCULATED USING THE MEDIAN CMIP5 WARMING FOR 2030 AND 2090, AND WITHIN BRACKETS THE 10TH AND 90TH PERCENTILE CMIP5 WARMING FOR THESE PERIODS, APPLIED TO THE 30-YEAR ACORN-SAT STATION SERIES. NUMBERS ARE TAKEN FROM TABLE 7.1.2 AND TABLE 7.1.3 IN THE TECHNICAL REPORT.

THRESHOLD	PERTH (SSWFW)				ADELAIDE (SSWFE)			
	CURRENT	2030 RCP4.5	2090 RCP4.5	2090 RCP8.5	CURRENT	2030 RCP4.5	2090 RCP4.5	2090 RCP8.5
Over 35 °C	28	36 (33 to 39)	43 (37 to 52)	63 (50 to 72)	20	26 (24 to 29)	32 (29 to 38)	47 (38 to 57)
Over 40 °C	4	6.7 (5.4 to 7.5)	9.7 (6.9 to 13)	20 (12 to 25)	3.7	5.9 (4.7 to 7.2)	9.0 (6.8 to 12)	16 (12 to 22)
Below 2 °C	3.4	2.1 (2.5 to 1.4)	0.9 (1.3 to 0.7)	0.1 (0.4 to 0.0)	1.1	0.5 (0.8 to 0.4)	0.2 (0.4 to 0.1)	0.0 (0.0 to 0.0)

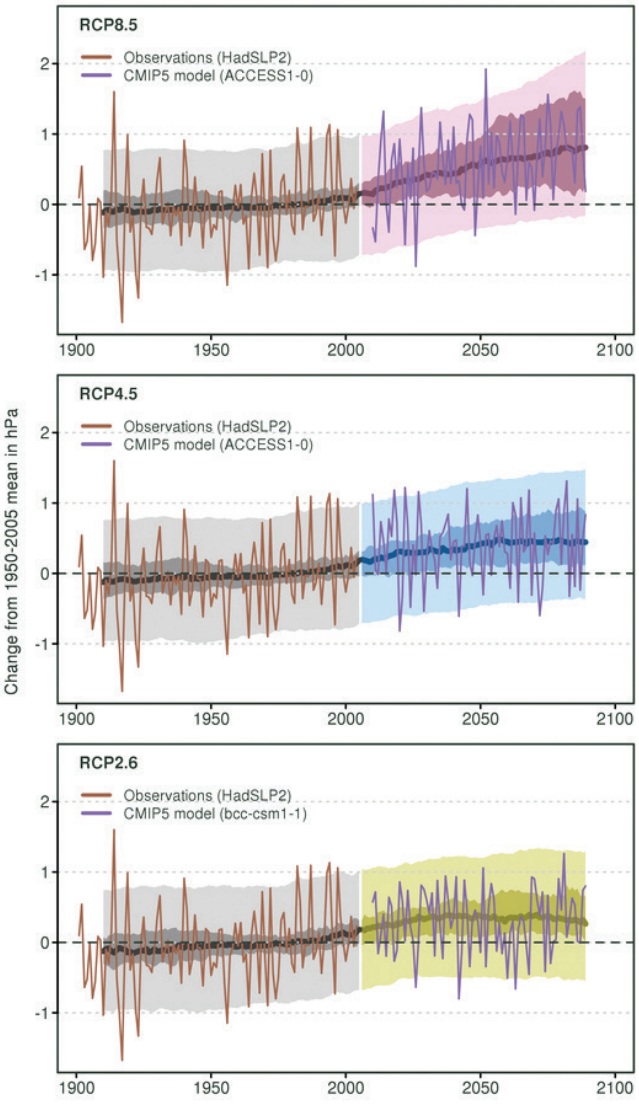

FIGURE 4.3.1: TIME SERIES FOR SSWF ANNUAL MEAN SEA LEVEL PRESSURE (HPA) FOR 1910–2090, AS SIMULATED IN CMIP5 RELATIVE TO THE 1950–2005 MEAN. THE CENTRAL LINE IS THE MEDIAN VALUE, AND THE SHADING IS THE 10TH AND 90TH PERCENTILE RANGE OF 20-YEAR MEANS (INNER) AND SINGLE YEAR VALUES (OUTER). THE GREY SHADING INDICATES THE PERIOD OF THE HISTORICAL SIMULATION, WHILE THREE FUTURE SCENARIOS ARE SHOWN WITH COLOUR-CODED SHADING: RCP8.5 (PURPLE), RCP4.5 (BLUE) AND RCP2.6 (GREEN). ACORN-SAT OBSERVATIONS AND PROJECTED VALUES FROM A TYPICAL MODEL ARE SHOWN. TIME SERIES PLOTS ARE EXPLAINED IN BOX 4.2.

4.3 MEAN SEA LEVEL PRESSURE

As discussed in Box 2.1, changes in mean sea level pressure are important as they relate to rainfall change in the Southern and South-Western Flatlands cluster, especially during the wetter months. Analysis of the CMIP5 projections confirms that most climate models are projecting an increase in the intensity of mean sea level pressure across southern Australia, depending on the magnitude of the projected warming (Figures 4.3.1 and 4.3.2). The intensification of mean sea level pressure is consistent with the observed broadening of the Hadley Cell or mean meridional (north-south) circulation (Box 2.1) and a shift of the Southern Annular Mode to its higher mode (contraction of storms around Antarctica). Future projections indicate a consensus amongst models toward a further broadening of the mean meridional circulation (IPCC, 2013, see Chapter 12).

Under all emission scenarios, annual mean sea level pressure is projected with *high confidence* to rise through the century over Southern and South-Western Flatlands (Figure 4.3.1). This is particularly driven by increased pressure in winter, with high consensus among the models under RCP4.5 and RCP8.5. Spring pressures also show an increase, but by a smaller magnitude than winter (Figure 4.3.2).

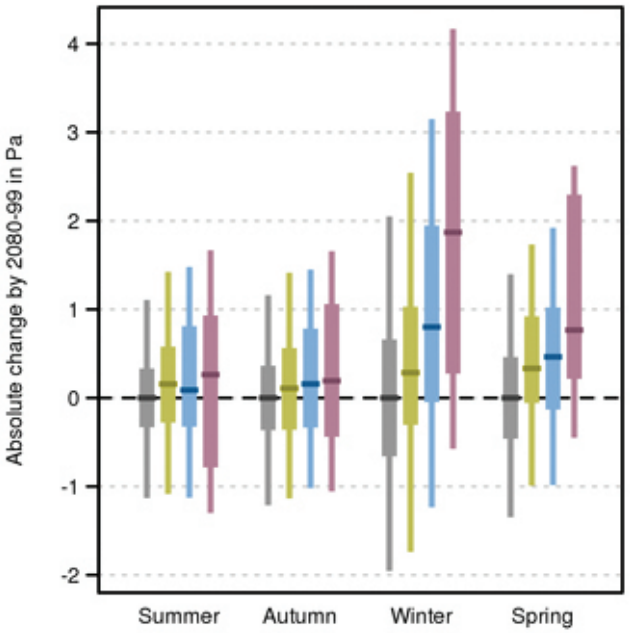

FIGURE 4.3.2: PROJECTED CHANGE IN SEASONAL SEA LEVEL PRESSURE (HPA) ACROSS SSWF FOR 2080–2099 WITH RESPECT TO 1986–2005 ACCORDING TO DIFFERENT SCENARIOS. THE BARS SHOW THE 10TH TO 90TH PERCENTILE RANGE OF THE CMIP5 RESULTS, THE HORIZONTAL LINE INDICATES THE MEDIAN. THE SCENARIOS FROM LEFT TO RIGHT ARE: NATURAL CLIMATE VARIABILITY ONLY (GREY), RCP2.6 (GREEN), RCP4.5 (BLUE), AND RCP8.5 (PURPLE). BAR PLOTS ARE EXPLAINED IN BOX 4.2.

4.4 RAINFALL

Early cool season (May, June and July) rainfall in both SSWFW and SSWFE has declined since 1960 with clear impacts on annual rainfall totals (Figure 4.4.1 and 4.4.2). In the first half of the 20th century, rainfall in SSWFW was very reliable and some years had totals of more than 150 mm above the mean. These very wet years are evident in Figure 4.4.1a. Since the 1970s the variability of SSWFW rainfall has dropped and there have been none of these very wet years (IOCI, 2002; Gallant *et al.,* 2007; Ryan and Hope, 2005; Ryan and Hope, 2006). A string of dry years since the late 1990s is visible in the data, suggesting a second step drop in the rainfall of SSWFW (Hope and Ganter, 2010). The trends and seasonal signature of rainfall change in SSWFE follow the shifts in SSWFW reasonably closely (slight increase in summer, decrease during the cooler seasons particularly in autumn), but the change is of a smaller magnitude (Figure 4.4.2).

SSWFE and SSWFW have not always experienced similar rainfall trends since 1910. For instance, SSWFE experienced very dry conditions in the years around 1930, which is aligned with what was happening in the eastern states later on with the World War II drought, although at that time, rainfall was close to average in SSWFW.

As outlined in Chapter 2, both sub-clusters are influenced by weather systems from the south through autumn, winter and spring, although SSWFE is also influenced by tropical weather systems in autumn and spring. An example is the string of very strong La Niña events that occured in the 1970s. The increased rainfall was sufficient to fill Lake Eyre and bring flooding to much of eastern Australia, but not to western Australia (Hope *et al.,* 2004). These different responses to the main drivers of rainfall mean that although there are associations between the two sub-clusters (Hope *et al.,* 2010), drivers can influence the sub-clusters in different ways and thus trends do not always align.

The rainfall reduction in the late 1960s brought extensive research to the study of climate in SSWFW. Large hemispheric changes (Frederiksen and Frederiksen, 2011) were found to be the major driver, resulting in fewer big winter storms (Hope *et al.*, 2006). It is likely that these changes impacted SSWFE as well (Hope *et al.*, 2010). June and July rainfall declines since 1999 in SSWFW have been attributed to the persistence of highs (Hope and Ganter, 2010) and is likely associated with the known growing intensity and expansion of the sub-tropical ridge in recent years that is associated with rainfall declines across south-east Australia (Timbal and Drosdowsky, 2013; Whan *et al.,* 2014).

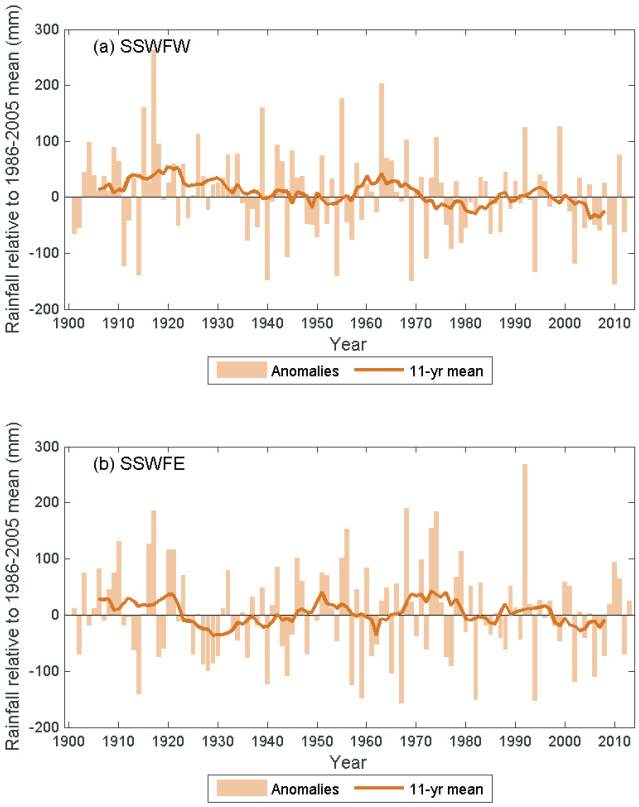

FIGURE 4.4.1: OBSERVED ANNUAL RAINFALL ANOMALIES (MM) FOR 1901–2013 COMPARED TO THE BASELINE1986–2005 FOR (A) SSWFW AND (B) SSWFE. DATA ARE FROM AWAP.

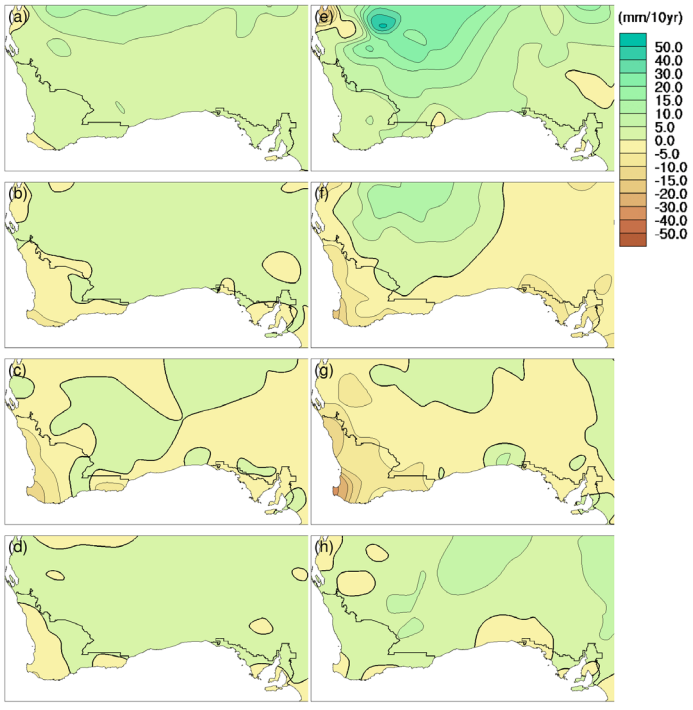

FIGURE 4.4.2: MAPS OF SEASONAL RAINFALL TRENDS (MM/DECADE). THE LEFT COLUMN OF MAPS SHOWS TRENDS FOR (A) SUMMER, (B) AUTUMN, (C) WINTER AND (D) SPRING FOR 1901–2013. THE RIGHT COLUMN SHOWS TRENDS FOR (E) SUMMER, (F) AUTUMN, (G) WINTER AND (H) SPRING FOR 1960–2013.

Future annual rainfall is projected to decline under all scenarios, including RCP2.6 (Figure 4.4.3). The annual averages from the single model show that even when the 20-year average median value is always below zero, wet years are possible.

Rainfall declines are strongest in winter and spring (Figure 4.4.4). In SSWFW, by 2090 under RCP8.5, every year's winter rainfall is projected to be lower than the current average. Projections for SSWFE winter rainfall are similar, although the projections allow for some years above average under RCP8.5. The projected change in winter in 2030 is around -15 to +5 % in both sub-clusters. For 2090 the winter change is around -30 to -5 % under RCP4.5 for SSWFW, and -45 to -15 % under RCP8.5. For SSWFE in winter, under RCP4.5 by 2090 the changes are around -25 to 0 % while under RCP8.5 the range is about -45 to -5 %. In spring under RCP8.5, some models project a rainfall decline by 2090 of more than 50 %. There is little change projected for autumn in both sub-clusters. These changes in spring and autumn are the reverse of that seen in observations in recent decades, where autumn declines were more significant than spring changes). This 'seasonal paradox' between past trends and projected changes is an area of ongoing research.

Projected summer rainfall shows a wide range with possible totals either above or below the observed mean. The natural variability in summer shown by the grey bar is also large. This may be due to the change being expressed in percentage relative to a small summer baseline value. Spatially, there is a common bias among climate models to simulate tropical rainfall extending further south than observed (see Figure 7.2.10 of Technical Report). This pattern of summer rainfall is projected to extend further south in many models and is physically plausible (see Technical Report for further discussion).

Downscaled results from the statistical method are very similar to the GCM results (Figure 4.4.5), although there is a tendency for an autumn decrease. The dynamical downscaled results, using only six simulations, are similar in winter and spring, but have a positive tendency when compared to the GCMs in autumn and summer. This projected increase in summer and autumn rainfall is likely due to the dynamical model's response to warm sea-surface temperatures. This is a plausible response and should not be discounted, although the autumn signal goes against recent observed trends. Spatially, downscaling can provide fine-scale data across the range of models, as shown by the statistical downscaling model for the 10th, 50th and 90th percentile models in the range of projected annual rainfall in Figure 4.4.6.

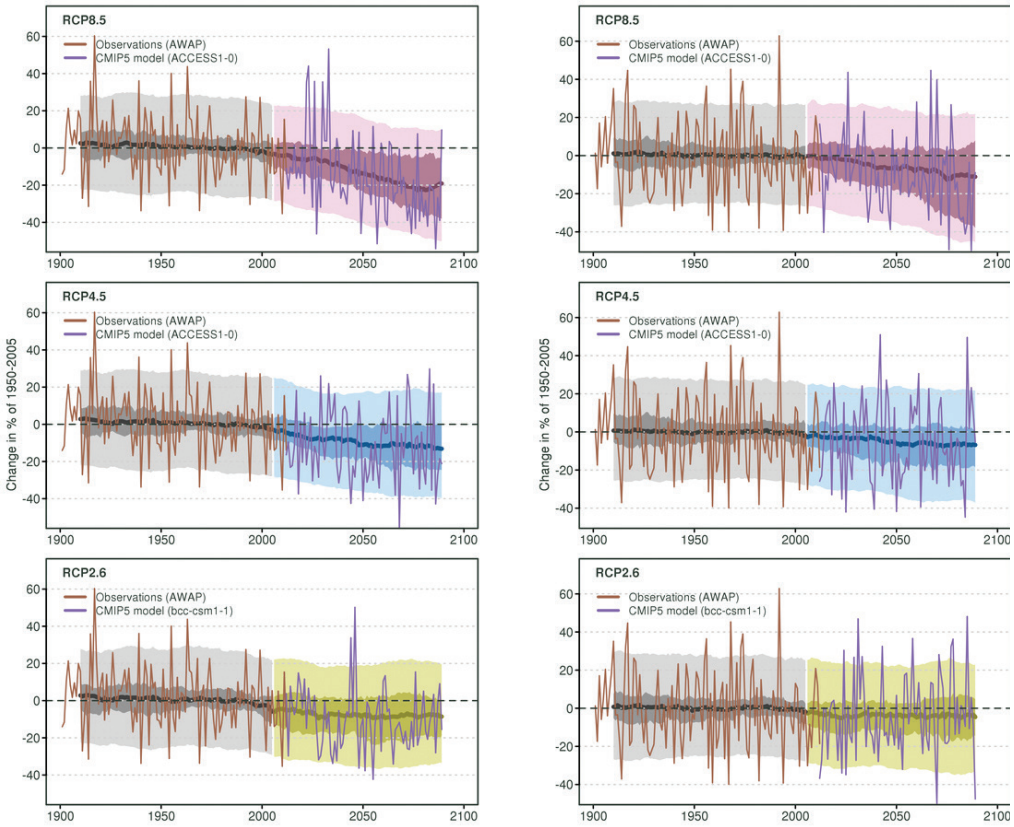

FIGURE 4.4.3: TIME SERIES FOR SSWFW (LEFT) AND SSWFE (RIGHT) ANNUAL RAINFALL FOR 1910–2090, AS SIMULATED IN CMIP5 EXPRESSED AS A PERCENTAGE RELATIVE TO THE 1950–2005 MEAN. THE CENTRAL LINE IS THE MEDIAN VALUE, AND THE SHADING IS THE 10TH AND 90TH PERCENTILE RANGE OF 20-YEAR MEANS (INNER) AND SINGLE YEAR VALUES (OUTER). THE GREY SHADING INDICATES THE PERIOD OF THE HISTORICAL SIMULATION, WHILE THREE FUTURE SCENARIOS ARE SHOWN WITH COLOUR-CODED SHADING: RCP8.5 (PURPLE), RCP4.5 (BLUE) AND RCP2.6 (GREEN). AWAP OBSERVATIONS (BEGINNING 1901) AND PROJECTED VALUES FROM A TYPICAL MODEL ARE SHOWN. TIME SERIES PLOTS ARE EXPLAINED IN BOX 4.2.

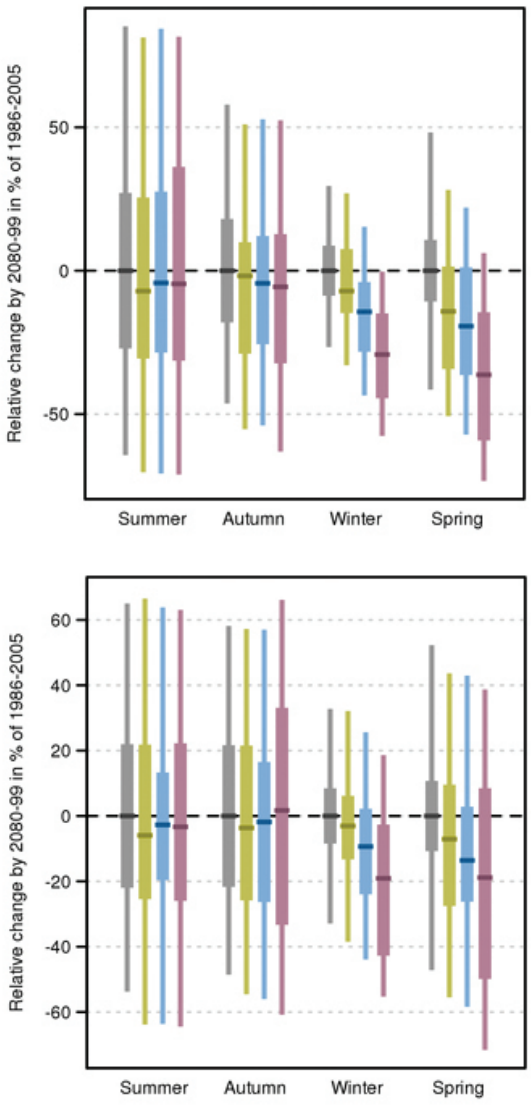

FIGURE 4.4.4: PROJECTED SEASONAL RAINFALL CHANGES FOR THE SSWFW SUB-CLUSTER (TOP) AND SSWFE SUB-CLUSTER (BOTTOM) FOR 2090. RAINFALL ANOMALIES ARE GIVEN IN PER CENT WITH RESPECT TO THE 1986–2005 MEAN UNDER RCP2.6 (GREEN), RCP4.5 (BLUE) AND RCP8.5 (PURPLE). NATURAL VARIABILITY IS REPRESENTED BY THE GREY BAR. BAR PLOTS ARE EXPLAINED IN BOX 4.2.

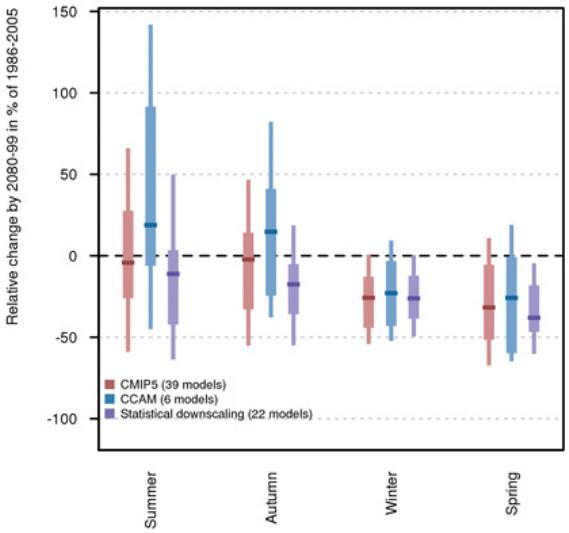

FIGURE 4.4.5: PROJECTED CHANGE IN SSWF SEASONAL RAINFALL FOR 2090 USING CMIP5 GCMS AND TWO DOWNSCALING METHODS (CCAM AND SDM). RAINFALL ANOMALIES ARE GIVEN IN PERCENT WITH RESPECT TO 1986–2005 UNDER RCP8.5. BAR PLOTS ARE EXPLAINED IN BOX 4.2.

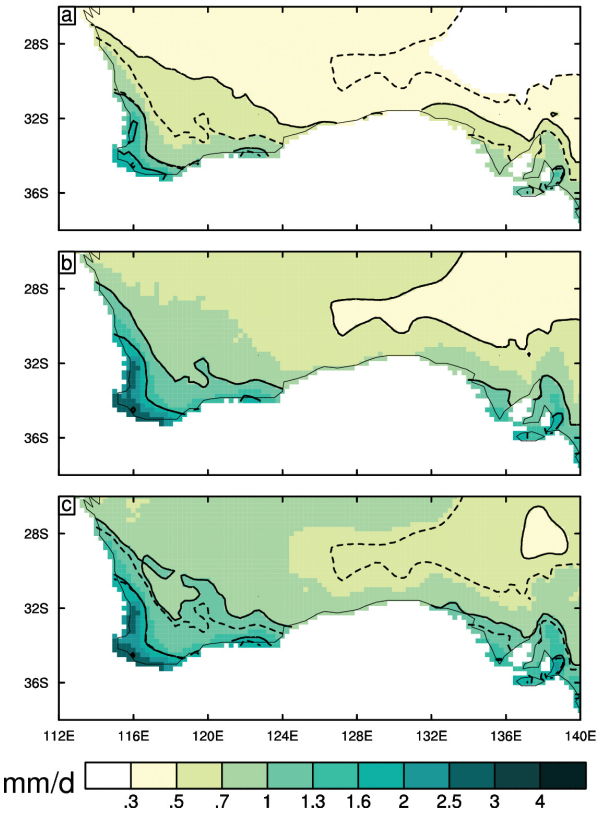

FIG. 4.4.6: ANNUAL MEAN RAINFALL (MM/DAY), FOR THE FUTURE CLIMATE IN 2090 UNDER RCP8.5, DERIVED BY THE STATISTICAL DOWNSCALING MODEL (SDM), FOR THREE PERCENTILES ACROSS THE MODEL RANGE: (A) 10TH PERCENTILE (DRIER END OF THE PROJECTED MODEL RANGE), (B) MEDIAN AND (C) 90TH PERCENTILE (WETTER END OF THE PROJECTED MODEL RANGE). IN EACH PANEL THE 0.5, 1, 1.6, AND 3 MM/DAY CONTOURS ARE PLOTTED WITH SOLID BLACK LINES. THE DASHED LINES SHOW THE SAME CONTOURS FOR THE MEDIAN SDM FIELD FOR 1986–2005. DATA VOIDS WITHIN THE CONTINENT ARE SHOWN AS WHITE.

In summary, decreases in winter (and annual) rainfall are projected by 2090 with *high confidence*. There is strong model agreement and good understanding of the contributing underlying physical mechanisms driving this change (southward shift of winter storm systems and greater prevalence of highs) and agreement with observed trends. Rainfall decreases are also projected for spring with *high confidence*.

The simulated change in autumn is not clear in the GCMs, but statistical downscaling suggests a further decline in this season, and there are physical climate mechanisms, such as the increasing intensity of the sub-tropical ridge, that support this. However, the dynamical downscaling results suggest more rainfall in autumn. This contradiction brings *low confidence* to projections of change in this season.

In summer, the GCMs project a wide range of possible climate futures from wetter to drier. As there is uncertainty over the shifts in rainfall over tropical Australia (see the cluster report for the Monsoonal North cluster) and in the tropical drivers such as ENSO (see Technical Report), the direction of change in summer rainfall over SSWF cannot be reliably projected.

4.4.1 HEAVY RAINFALL EVENTS

In a warming climate, the total rainfall from heavy rainfall events is expected to increase, mainly due to a warmer atmosphere being able to hold more moisture (Sherwood *et al.,* 2010).

The CMIP5 models simulate an increase in the 1-day annual maximum value and the 20-year return value for the period 2080– 2099 relative to the baseline period 1986–2005 (see Figure 4.4.7 for RCP8.5), where a 20-year return value is equivalent to a 5 %chance of occurrence within any one year. Comparing the trend in the two extreme indices with that of the annual mean rainfall shows that while mean rainfall is projected to strongly decrease in the cluster, the extremes are projected to increase in most models. This pattern is found in all other NRM clusters, and is also supported by results from other studies (see Technical Report, Section 7.2.2). However, the tendency for increased extremes is weaker in SSWFW than in other clusters. This is probably due to the southward shift in rain-bearing weather systems associated with the reduction in mean rainfall.

The magnitudes of the simulated changes in extreme rainfall indices are strongly dependent on the emission scenario and point of time in the future. Furthermore, the way changes simulated by GCMs manifest in terms of magnitude is uncertain because many smaller scale systems that generate extreme rainfall are not well resolved by GCMs (Fowler and Ekstroem, 2009). In summary, there is *high confidence* that the intensity of heavy rainfall events will increase in the cluster (*medium confidence* in SSWFW), but there is *low confidence* in the magnitude of change, and thus the time when any change may be evident against natural fluctuations cannot be reliably projected.

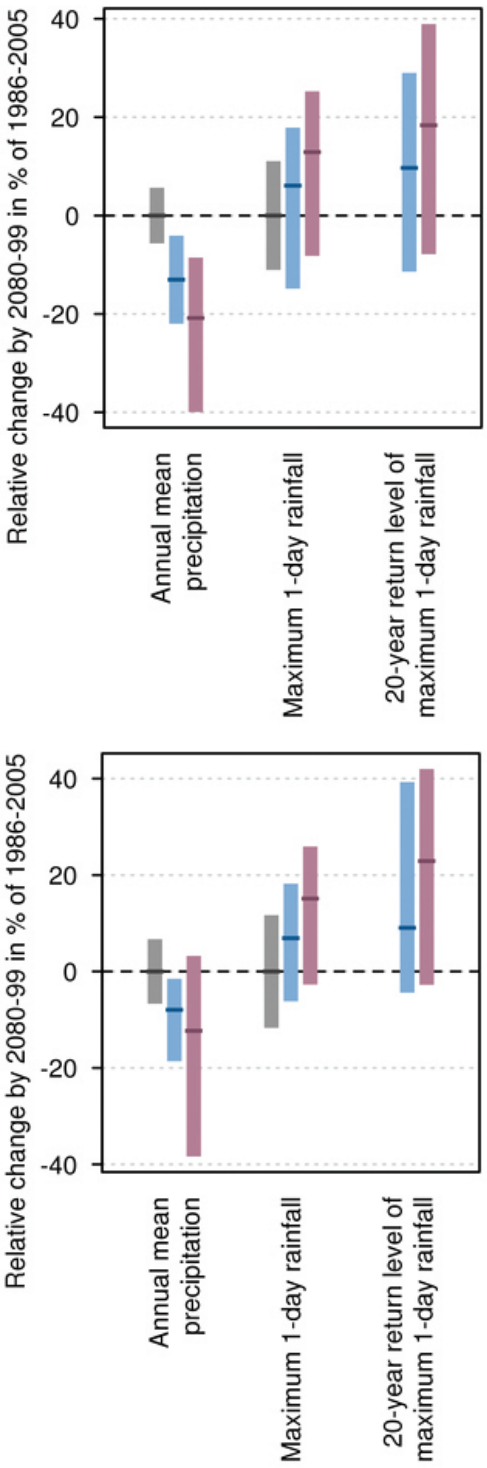

FIGURE 4.4.7: PROJECTED CHANGES IN MEAN RAINFALL, MAGNITUDE OF ANNUAL MAXIMUM 1-DAY RAINFALL AND MAGNITUDE OF THE 20-YEAR RETURN VALUE FOR THE 1-DAY RAINFALL FOR 2090 FOR SSWFW (LEFT) AND SSWFE (RIGHT) (SEE TEXT FOR DEFINITION OF VARIABLES). CHANGES ARE GIVEN IN PERCENTAGE WITH RESPECT TO THE 1986–2005 MEAN FOR RCP4.5 (BLUE) AND RCP8.5 (PURPLE). NATURAL CLIMATE VARIABILITY IS REPRESENTED BY THE GREY BAR. BAR PLOTS ARE EXPLAINED IN BOX 4.2.

4.4.2 DROUGHT

There are different definitions of drought and the choice depends on the intended application and the context of the study. For these projections a measure of meteorological drought, the Standardised Precipitation Index (SPI), was used to identify drought events. Droughts under this definition last for longer than one year. Estimates were also made of their severity and frequency in projected time series. For details on how to calculate the SPI and general information on drought, please see Section 7.2.3 in the Technical Report. Duration of time spent in drought and changes to the duration and frequency of droughts were calculated for different levels of severity (mild, moderate, severe and extreme).

Under all emission levels and at all time periods into the future, the time spent in drought is projected to increase compared to the present climate for both SSWFW and SSWFE, with these increases becoming large by late in the 21st century under RCP8.5 (Figure 4.4.8). The duration and frequency of droughts in the extreme category are also projected to increase. These projected changes are driven by the projected decline in annual rainfall and are of *high confidence*.

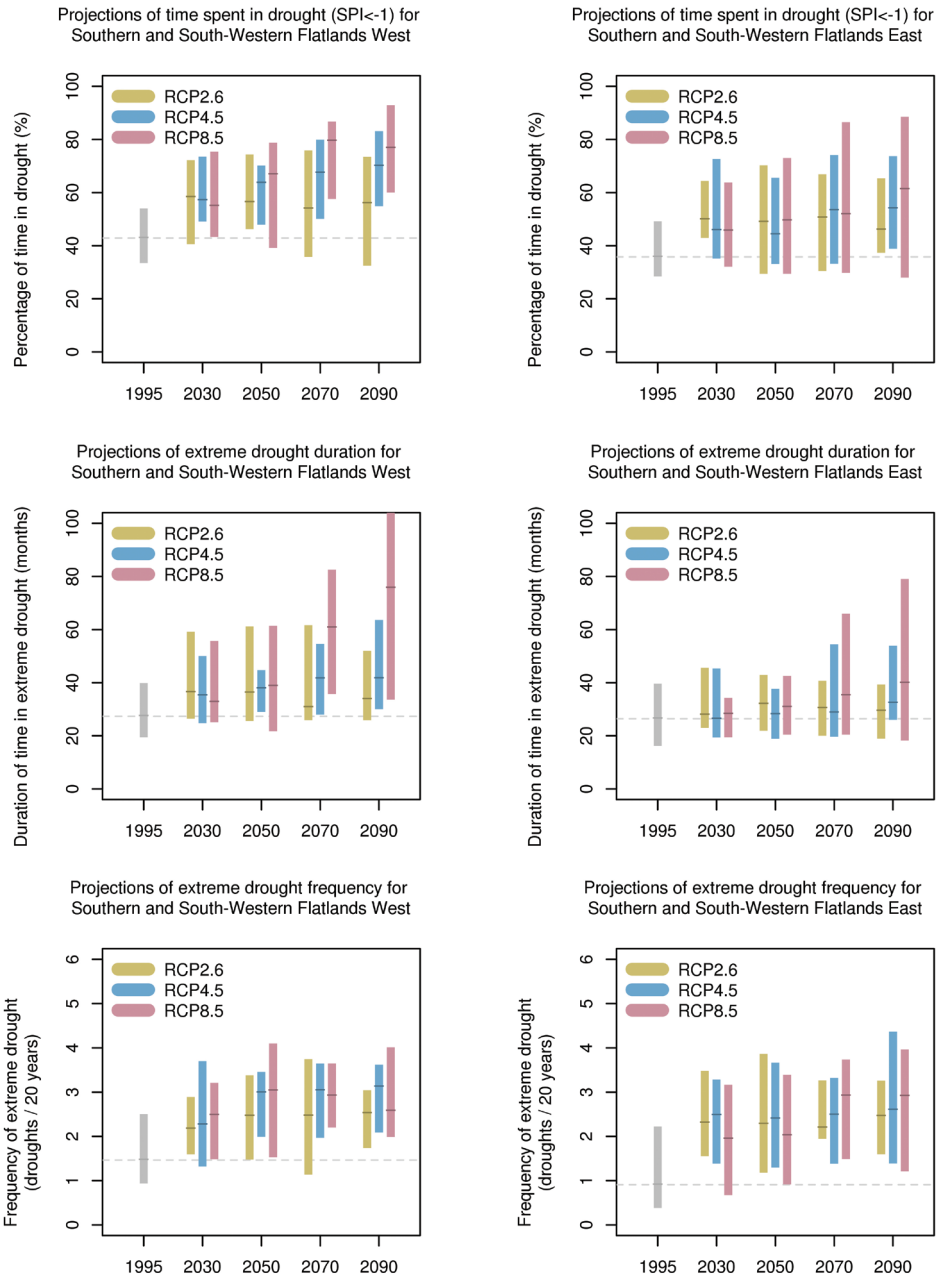

FIGURE 4.4.8: SIMULATED CHANGES IN DROUGHT BASED ON THE STANDARDISED PRECIPITATION INDEX (SPI). THE MULTI-MODEL ENSEMBLE RESULTS FOR SSWFW (LEFT) AND SSWFE (RIGHT) SHOW THE PERCENTAGE OF TIME IN DROUGHT (SPI LESS THAN -1) (TOP), DURATION OF EXTREME DROUGHT (MIDDLE) AND FREQUENCY OF EXTREME DROUGHT (BOTTOM) FOR EACH 20-YEAR PERIOD CENTRED ON 1995, 2030, 2050, 2070 AND 2090 UNDER RCP2.6 (GREEN), RCP4.5 (BLUE) AND RCP8.5 (PURPLE). NATURAL CLIMATE VARIABILITY IS REPRESENTED BY THE GREY BAR. SEE TECHNICAL REPORT CHAPTER 7.2.3 FOR DEFINITION OF DROUGHT INDICES. BAR PLOTS ARE EXPLAINED IN BOX 4.2.

4.5 WINDS, STORMS AND WEATHER SYSTEMS

4.5.1 MEAN WINDS

The surface wind climate is driven by the large-scale circulation pattern of the atmosphere although local and regional effects such as topography or strong heating can also be important. Trends in observed winds are difficult to establish due to sparse coverage of wind observations, difficulties with instruments and the changing circumstances of anemometer sites (*e.g.* sheltering effects due to increases in proximate vegetation or structures, which slow the winds). McVicar *et al.* (2012) and Troccoli *et al.* (2012) have reported weak and conflicting trends across Australia (although they considered winds at different altitudes). Projected changes in wind speed for the SSWF cluster are relatively small (Table 1 in the Appendix).

For 2030, the projected annual mean changes in wind speed are less than ±2 % under all RCPs (Table 1 in the Appendix). However, some models are showing a 5 % weakening in winter. By 2090 under RCP8.5, there is a clear decrease in simulated wind speed in both sub-clusters in winter, although the values remain less than -10 % (Figure 4.5.1). This is to be expected given the simulated increases in pressure in this season and related decline in storminess. Changes in other seasons are small compared to natural variability, except for a tendency for an increase in summer in SSWFW, which is significant in some models. The reason for this change is not understood but it may relate to a stronger sea breeze circulation or a systematic shift in synoptic weather systems. Given the strong projected reduction in spring rainfall, the lack of a wind change in spring suggests different processes behind the responses at the height of winter and during autumn and spring, which requires further analysis.

In summary, small changes are projected with *high confidence* for mean surface wind speeds by 2030. Decreases in wind speed in winter are projected for 2090 under RCP4.5 and RCP8.5 with *high confidence* based on model results and the projection of a reduction in storminess. In summer, most models project increases in mean wind speed in the SSWFW sub-cluster, although this is poorly understood and is of *low confidence*. Changes in other seasons are small compared to natural variability.

SSWFW

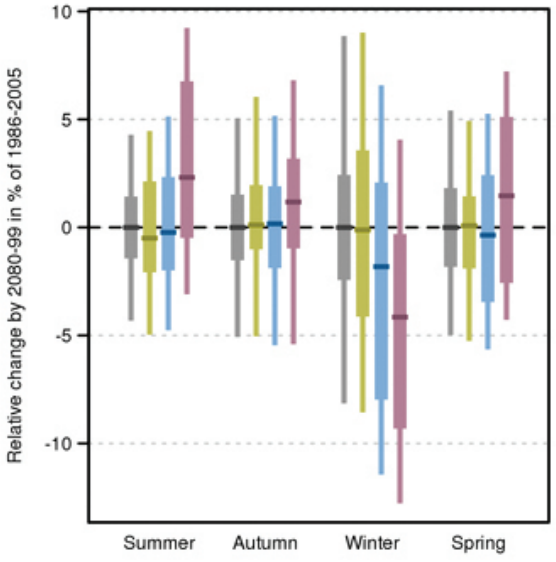

SSWFE

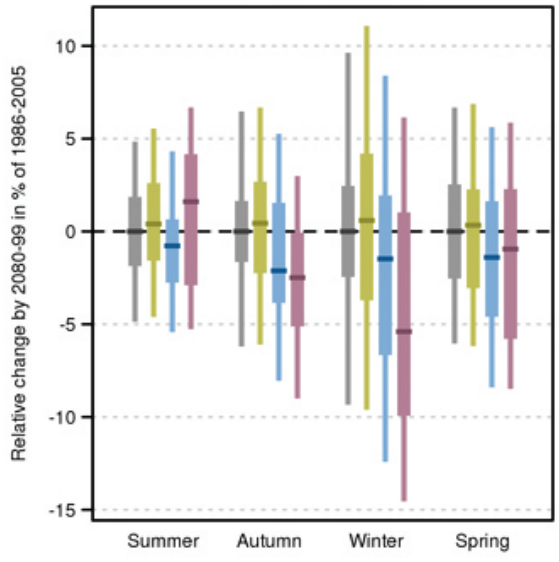

FIGURE 4.5.1: PROJECTED NEAR-SURFACE WIND SPEED CHANGES FOR 2090 FOR SSWFW (TOP) AND SSWFE (BOTTOM). ANOMALIES ARE GIVEN IN PERCENT WITH RESPECT TO 1986–2005 MEAN FOR RCP2.6 (GREEN), RCP4.5 (BLUE) AND RCP8.5 (PURPLE), WITH GRAY BARS SHOWING THE EXTENT OF NATURAL CLIMATE VARIABILITY. BAR PLOTS ARE EXPLAINED IN BOX 4.2.

4.5.2 EXTREME WINDS

The projections of extreme wind (annual maximum 1-day speed) presented here need to be considered in light of several limitations imposed on this variable. These include the limited number of GCMs that provide wind data and the need to estimate wind speed from daily vector component data. Furthermore, the intensity of observed extreme wind speeds across land is strongly modified by obstacles in the surrounding terrain that are not resolved at the relevant scale in GCMs. Many meteorological systems that generate extreme winds are not resolved either. For these reasons, confidence in model estimated changes for the SSWF cluster are reduced and their value lies foremost in the direction of change rather than the projected changes in magnitude. See further details in the Technical Report Section 7.3.

In light of the limitations mentioned above, projections of extreme winds indicate that reductions are more likely than increases, based on the model ensemble median. This is the case for the annual maximum daily wind speed and the 20-year return level of the maximum daily wind speed, under the RCP4.5 and RCP8.5 emission scenarios (Fig. 4.5.2), where a 20-year return value is equivalent to a 5 % chance occurrence within any one year. There is *medium confidence* in this projected decrease since it resonates with the projected changes in broad scale circulation and mean wind speed at these latitudes.

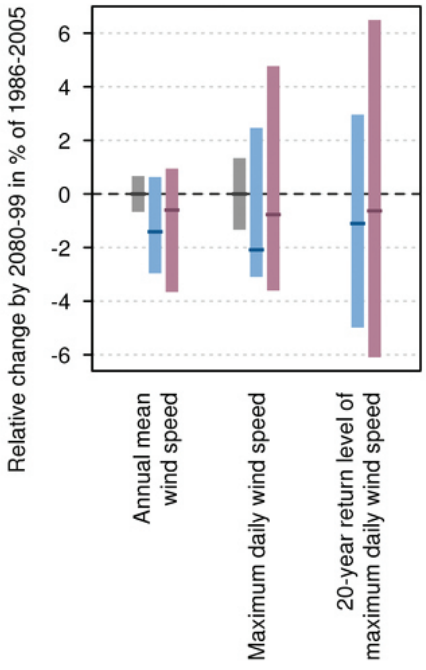

FIGURE 4.5.2: PROJECTED NEAR-SURFACE ANNUAL MEAN WIND SPEED, ANNUAL MAXIMUM DAILY WIND SPEED AND THE 20-YEAR RETURN VALUE FOR THE ANNUAL MAXIMUM DAILY WIND SPEED FOR 2090 FOR SSWF. ANOMALIES ARE GIVEN IN PER CENT WITH RESPECT TO THE 1986–2005 MEAN FOR RCP2.6 (GREEN), RCP4.5 (BLUE) AND RCP8.5 (PURPLE) WITH GREY BARS SHOWING THE EXTENT OF NATURAL CLIMATE VARIABILITY. BAR PLOTS ARE EXPLAINED IN BOX 4.2. THE CHANGES IN EXTREME WINDS ARE VERY SIMILAR ACROSS THE TWO SUB-CLUSTERS.

4.5.3 TROPICAL AND EXTRA-TROPICAL CYCLONES

The SSWF cluster is seldom directly affected by tropical cyclones in the present climate as it is too far south of the zone in which tropical cyclones typically occur. However, extra-tropical cyclones and tropical lows do move south into this cluster and are capable of causing heavy rainfall, while tropical cyclones or lows to the north can also interact with upper level troughs to spread significant rainfall much further south than their geographical location. The highest rainfall totals in summer at the eastern edge of SSWFW and the northern extent of SSWFE are mostly associated with tropical lows that have moved down from the north in the preceding days (Ganter, pers. comm., 2012).

Tropical cyclones can also feed rivers that are important to southern Australia and interact with frontal systems to bring heavy rainfall to the region in summer (Hope *et al.,* 2004). Projected changes of tropical cyclone frequency have been assessed in the current generation of GCMs over the north-east and north-west Australian region, from both the large-scale environmental conditions that promote cyclones and from direct simulation of cyclone-like synoptic features (see Section 7.3.3 of the Technical Report). Results in this region generally indicate a decrease in the formation of tropical cyclones, particularly for the north-west. These results are broadly consistent with current projections of cyclones over the globe (IPCC 2013, Section 14.6.1) which indicate little change through to substantial decrease in frequency. It is also anticipated that the proportion of the most intense storms will increase over the century while the intensity of associated rainfall may increase further, as can be anticipated from Section 4.3.1 here.

A larger proportion of storms decaying south of 25 °S in the late 21st century is likely to impact the SSWF although this projection is made with *low confidence*. In summary, based on global and regional studies, tropical cyclones are projected to become less frequent. The projection indicates an increase in the proportion of the most intense storms with *medium confidence*.

With regard to extra-tropical cyclones that influence SSWF, the observed trends suggest that cut-off lows might be decreasing in their number and contributing to rainfall less in recent years (Pook *et al.,* 2012) while the occurrence of fronts has not altered significantly (Hope *et al.,* 2014) since a large decline in their numbers in the late 1960s. These results align with an intensification and contraction of the storm track around Antarctica in the late 1960s (*e.g.* Yin, 2005). The recent reduction in the number of cut-off lows is consistent with a reduction in the potential for storm growth associated with the sub-tropical jet in winter (Frederiksen and Frederiksen, 2011; Frederiksen and Frederiksen, 2007) and an enhancement of the sub-tropical ridge (Timbal and Drosdowsky, 2013). Projections for south-east Australia suggest that the structure of the upper-atmosphere winter jets may change into the future making conditions less conducive to cut-off low formation (Grose *et al.,* 2012). The effect on SSWF will likely be similar.

4.6 SOLAR RADIATION

For 2030, the CMIP5 models overall simulate little change in solar radiation (less than 5 %) for both RCP4.5 and RCP8.5. For 2090, there is high model agreement for a substantial increase of up to 5 and 10 % respectively for RCP4.5 and RCP8.5 in winter, and about half of that in spring, as a result of a decrease in cloudiness and rainfall. Projected changes in summer and autumn are smaller, with models showing both increases and decreases (Figure 4.8.1). An Australian model evaluation suggested that some models are not able to adequately reproduce the climatology of solar radiation (Watterson *et al.,* 2013). Globally, CMIP3 and CMIP5 models appear to underestimate the observed trends in some regions due to underestimation of aerosol direct radiative forcing and/or deficient aerosol emission inventories (Allen *et al.,* 2013).

Taking this into account, we have *high confidence* in little change by 2030. For 2090, there is *high confidence* in increased winter radiation, and *medium confidence* in an increase in spring and in little change in summer and autumn.

4.7 RELATIVE HUMIDITY

CMIP5 projections of relative humidity indicate an overall tendency for decrease in all seasons (Figure 4.8.1b and Table 1 in the Appendix). Projected changes for 2030 are generally smaller than 2 % in all seasons for both RCP4.5 and 8.5. There are marked reductions projected for 2090, particularly in winter (up to -6 % under RCP8.5 in SSWFW) and spring (up to -5 % under RCP8.5 in the western sub-cluster), and smaller decreases in summer and autumn. A decrease in relative humidity away from the coasts is anticipated because an increase in the moisture holding capacity of a warming atmosphere and the greater warming of land compared to sea will produce increases in relative humidity over ocean and decreases over continents.

In summary, little change in relative humidity is projected for 2030 with *high confidence*. By 2090, for winter and spring across both sub-clusters, there is *high confidence* for substantial decrease of up to 5 % under RCP8.5, with smaller decreases in autumn and summer.

4.8 POTENTIAL EVAPOTRANSPIRATION

Projected changes for potential evapotranspiration using Morton's wet-environmental potential evapotranspiration (McMahon *et al*., 2013 and Technical Report Section 7.5.3) suggest increases for all seasons in SSWF (Figure 4.8.1 and Table 1 in the Appendix). For 2030, increases are less than 10 % in all scenarios. Increases by 2090 are larger. In relative terms, the largest increases are found in winter (10 to 30 % under RCP8.5 and approximately half that for RCP4.5) and autumn (about 10 to 20 % under RCP8.5 and approximately half that for RCP4.5), with lesser increases (about 5 to 15 % following RCP8.5) in summer and spring (Table 1 in the Appendix). In absolute terms, the largest projected increase is found in summer.

Overall, models show high agreement by 2030 and very high agreement by 2090 on a substantial increase in evapotranspiration. Despite having *high confidence* in increased evapotranspiration, there is only *medium confidence* in the projected magnitude of the increase. The method is able to reproduce the spatial pattern and the annual cycle of the observed climatology and there is theoretical understanding around increases as a response to increasing temperatures and an intensified hydrological cycle (Huntington, 2006), which adds to confidence. However, there has been no clear increase in observed Pan Evaporation across Australia in data available since 1970 (see Technical Report, Chapter 4). Also, earlier GCMs were not able to reproduce the historical linear trends found in Morton's potential evapotranspiration (Kirono and Kent 2011).

SSWFW

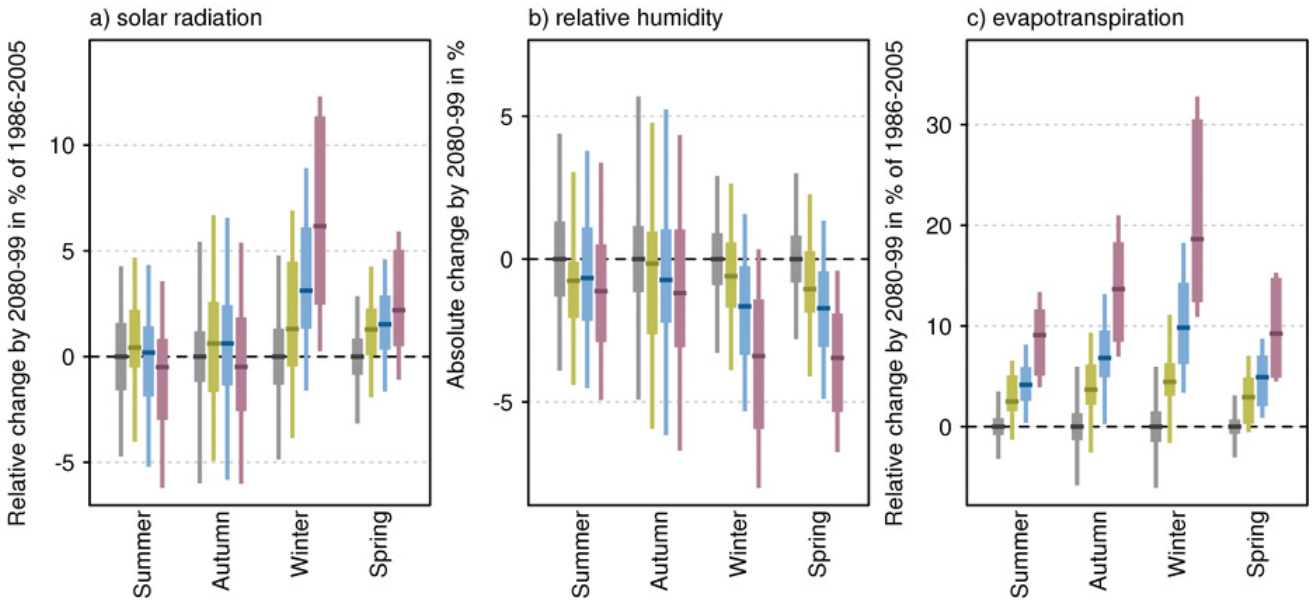

SSWFE

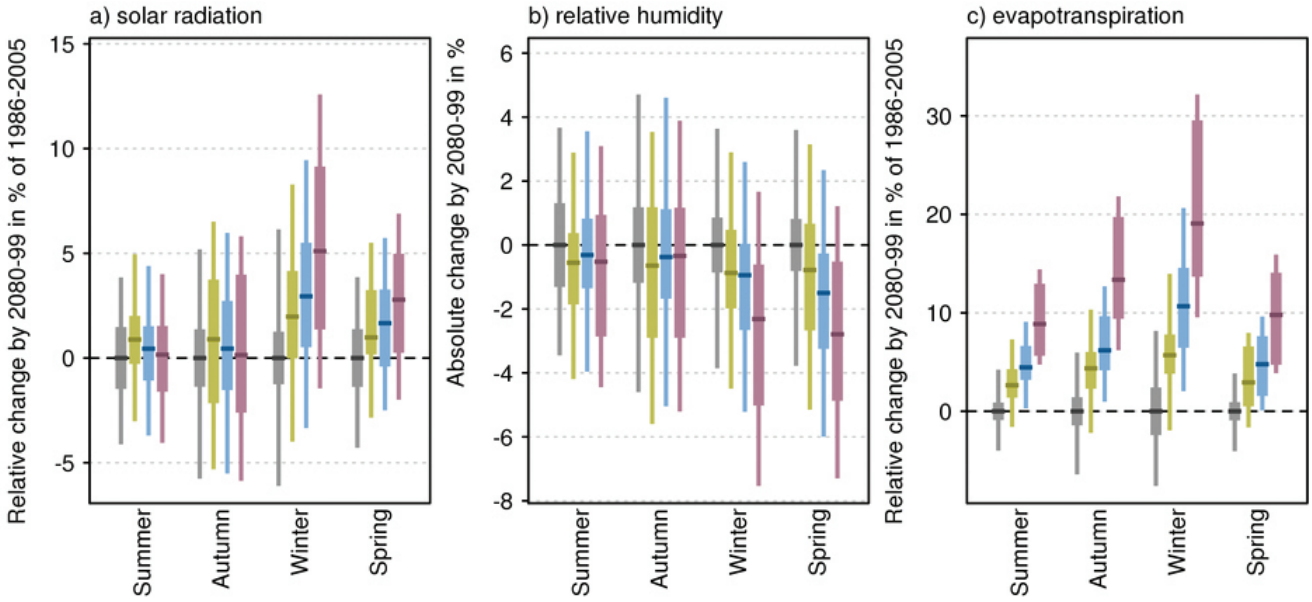

FIGURE 4.8.1: PROJECTED CHANGES IN (A) SOLAR RADIATION (%), (B) RELATIVE HUMIDITY (%, ABSOLUTE CHANGE) AND (C) WET-ENVIRONMENTAL POTENTIAL EVAPOTRANSPIRATION (%) FOR SSWFW (TOP) AND SSWFE (BOTTOM) IN 2090. THE BAR PLOTS SHOW SEASONAL PROJECTIONS WITH RESPECT TO THE 1986–2005 MEAN FOR RCP2.6 (GREEN), RCP4.5 (BLUE) AND RCP8.5 (PURPLE), AND THE EXTENT OF NATURAL CLIMATE VARIABILITY IS SHOWN IN GREY. BAR CHARTS ARE EXPLAINED IN BOX 4.2.

4.9 SOIL MOISTURE AND RUNOFF

Increases in potential evapotranspiration rates (Figure 4.8.1) combined with a decrease in rainfall in most seasons (Figure 4.3.1) have implications for soil moisture and runoff. However, soil moisture and runoff are difficult to simulate. This is particularly true in GCMs where, due to their relatively coarse resolution, the models cannot simulate much of the rainfall detail that is important to many hydrological processes, such as the intensity of rainfall. For these reasons, and in line with many previous studies, we do not present runoff and soil moisture as directly-simulated by the GCMs. Instead, the results of hydrological models forced by CMIP5 simulated rainfall and potential evapotranspiration are presented. Soil moisture is estimated using a dynamic hydrological model based on an extension of the Budyko framework (Zhang *et al.,* 2008), and runoff is estimated by the long-term annual water and energy balance using Budyko framework (Teng *et al.,* 2012). Runoff is presented as the change in 20-year averages, derived from output of a water balance model. The latter uses input from CMIP5 models as smoothed time series (30-year running means), the reason being that 30 years is the minimum required for dynamic water balance to attain equilibrium using the Budyko framework. For further details on methods (including limitations) see Section 7.7 of the Technical Report.

Decreases in soil moisture are projected, particularly in winter and spring (Figure 4.9.1), as are decreases in runoff (Figure 4.9.2). The annual changes in soil moisture for RCP8.5 by 2090 are about -10 to 0 % with high model agreement on a substantial decrease (Table 1 in the Appendix). Given that reduced rainfall and increased evapotranspiration both contribute to a decrease in soil moisture and runoff, and that there is *high confidence* in the projected direction of change for rainfall and evapotranspiration, the projected decrease in soil moisture is also given *high confidence*. However, due to the potential limitations of this method, there is only *low confidence* in the magnitude of change indicated here.

Further hydrological modelling with appropriate climate scenarios (*e.g.* Chiew *et al.,* 2009) could provide further insights into impacts on future runoff and soil moisture characteristics that may be needed for detailed climate change impact assessment studies.

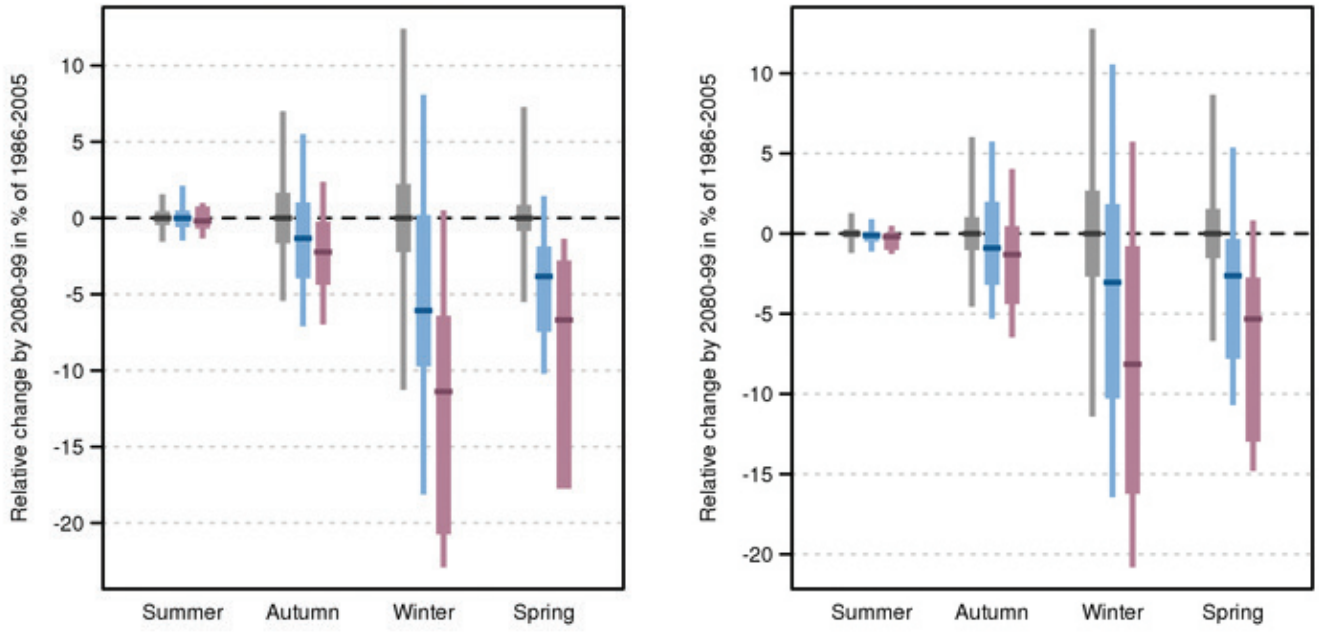

FIGURE 4.9.1: PROJECTED CHANGE IN SEASONAL SOIL MOISTURE (BUDYKO METHOD – SEE TEXT) IN SSWFW (LEFT) AND SSWFE (RIGHT) FOR 2090. ANOMALIES ARE GIVEN IN PER CENT WITH RESPECT TO THE 1986–2005 MEAN ACCORDING TO DIFFERENT SCENARIOS. THE SCENARIOS FROM LEFT TO RIGHT ARE: NATURAL CLIMATE VARIABILITY ONLY (GREY),FOR RCP4.5 (BLUE) AND RCP8.5 (PURPLE) WITH GREY BARS SHOWING THE EXTENT OF NATURAL VARIABILITY. BAR CHARTS ARE EXPLAINED IN BOX 4.2.

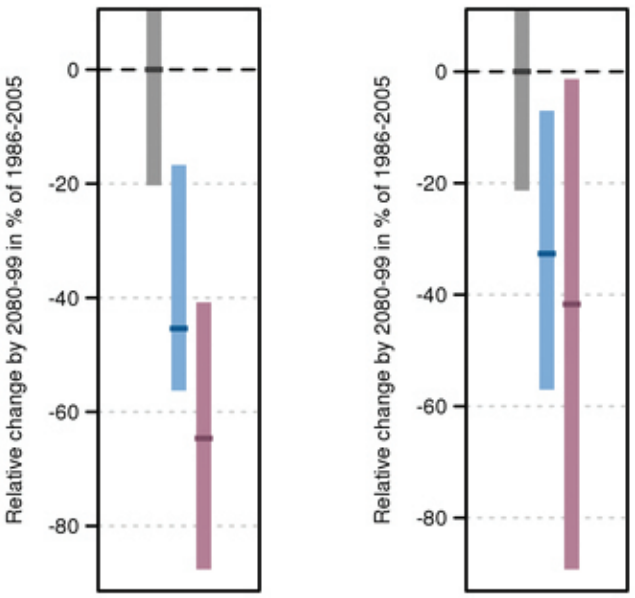

FIGURE 4.9.2: PROJECTED CHANGE IN RUNOFF (BUDYKO METHOD – SEE TEXT) IN SSWFW (LEFT) AND SSWFE (RIGHT) FOR 2090. ANOMALIES ARE GIVEN IN PER CENT WITH RESPECT TO THE 1986–2005 MEAN FOR RCP4.5 (BLUE) AND RCP8.5 (PURPLE) WITH GREY BARS SHOWING THE EXTENT OF NATURAL VARIABILITY. BAR CHARTS ARE EXPLAINED IN BOX 4.2.

4.10 FIRE WEATHER

Bushfire occurrence depends on four 'switches': 1) ignition, either human-caused or from natural sources such as lightning; 2) fuel abundance or load (a sufficient amount of fuel must be present; 3) fuel dryness, where lower moisture contents are required for fire, and; 4) suitable weather conditions for fire spread, generally hot, dry and windy (Bradstock, 2010). The settings of the switches depend on meteorological conditions across a variety of time scales, particularly the fuel conditions. Given this strong dependency on the weather, climate change will have a significant impact on future fire weather (*e.g.* Hennessy *et al.,* 2005; Lucas *et al.,* 2007; Williams *et al.,* 2009; Clarke *et al.,* 2011; Grose *et al*., 2014). In the Southern and South-Western Flatlands cluster, the study of Clarke *et al* (2013) shows significant increasing trends over 1973-2010 in observed fire weather in the eastern sub-cluster.

Fire weather is estimated here using the McArthur Forest Fire Danger Index (FFDI; McArthur, 1967), which captures two of the four switches (note that it excludes ignition). The fuel dryness is summarised by the drought factor (DF) component of FFDI, which depends on both long-term and short-term rainfall. The FFDI also estimates the ability of a fire to spread, as the temperature, relative humidity and wind speed are direct inputs into the calculation. Fuel abundance is not measured by FFDI, but does depend largely on rainfall, with higher rainfall generally resulting in a larger fuel load, particularly in regions dominated by grasslands. However, the relationship between fuel abundance and climate change in Australia is complex and only poorly understood. Fire weather is considered 'severe' when FFDI exceeds 50; bushfires have potentially greater human impacts at this level (Blanchi *et al.*, 2010).

Here, estimates of future fire weather using FFDI are derived from three CMIP5 models (GFDL-ESM2M, MIROC5 and CESM-CAM5), chosen to provide a spread of results across all clusters. Using a method similar to that of Hennessy *et al.* (2005), monthly mean changes to maximum temperature, rainfall, relative humidity and wind speed from these models are applied to observation based high quality historical fire weather records (Lucas, 2010). A period centred on 1995 (*i.e.* 1981–2010) serves as the baseline. These records are modified using the changes from the three models for four 30-year time slices (centred on 2030, 2050, 2070 and 2090) and the RCP4.5 and RCP8.5 emission scenarios. In the Southern and South-Western Flatlands cluster, significant fire activity occurs primarily in areas characterised by forests and woodlands. Fuel is abundant and the 'weather switch', well-characterised by FFDI, is key to fire occurrence. Six stations are used in the analysis for this cluster: Adelaide, Ceduna, Perth Airport (AP), Geraldton, Albany AP and Esperance.

Focusing on the 2030 and 2090 time slices, the results indicate a tendency towards increased fire weather risk in the future (Table 4.10.1). Increased temperature combined with lower rainfall results in a higher drought factor (DF). Across the cluster, the sum of all daily FFDI values over a year (∑FFDI from July to June) is broadly indicative of general fire weather danger, and increases by roughly 10 % by 2030, 12 % under RCP4.5 by 2090 and 30 % under RCP8.5 by 2090. The number of days with a 'severe' fire danger rating increases from 12 % (RCP8.5) to 20 % (RCP4.5) by 2030, and from 25 % (RCP4.5) to 65 % (RCP8.5) by 2090.

If considering indices on an individual station and model basis, there is considerable variability from the cluster mean (Tables 4.10.1 compared to Table 2 in Appendix). The baseline fire climate varies, with Ceduna and Geraldton having a harsher fire climate that is more similar to that of the nearby Rangelands cluster, with generally cooler stations (*e.g.* Adelaide, Esperance and Albany) having a fire weather climate more typical of southern Australia. At these cooler stations, the relative change is larger in both the number of severe days and ∑FFDI than the warmer stations. For example, the relative change in the number of severe days (2090, RCP8.5) is over 200 % at Adelaide compared to 41 % or 93 % for Ceduna and Geraldton, respectively.

Most models project similar warming. Two of the three models indicate small changes in annual rainfall, either a modest decline or a slight increase, while the GFDL-ESM2M model generally simulates a strong decline in rainfall. In the models with little change in rainfall, changes in fire weather are smaller. This reflects the interplay between the variables influencing fire danger. Increased temperatures by themselves result in some level of increased fire weather risk, but this is modulated by rainfall, as significant reductions in rainfall leads to more severe fire weather. A smaller relative temperature change may result in a greater

fire weather change if the rainfall decline is large enough (*e.g.* Perth AP for 2090 RCP8.5 in Table 2 of Appendix). Mean changes to relative humidity and wind speed are small in all models and do not appear to play a significant role in affecting the mean changes for fire weather.

There is *high confidence* that climate change will result in harsher fire weather in the future. This is visible in the mean changes (Table 4.10.1) and when examining individual models and scenarios (Table 2 of Appendix). However, there is *low confidence* in the magnitude of the change as this is strongly dependent on the rainfall projection.

TABLE 4.10.1: CLUSTER MEAN ANNUAL VALUES OF MAXIMUM TEMPERATURE (T; °C), RAINFALL (R; MM), DROUGHT FACTOR (DF; NO UNITS), THE NUMBER OF SEVERE FIRE DANGER DAYS (SEV; FFDI GREATER THAN 50) AND CUMULATIVE FFDI (∑FFDI; NO UNITS) FOR THE 1995 BASELINE AND PROJECTIONS FOR 2030 AND 2090 UNDER RCP4.5 AND RCP8.5 SCENARIOS. AVERAGES ARE COMPUTED ACROSS ALL STATIONS AND MODELS IN EACH SCENARIO. SIX STATIONS ARE USED IN THE AVERAGING: ADELAIDE, CEDUNA, PERTH, ESPERANCE ALBANY AND GERALDTON. SEE TABLE 2 IN APPENDIX FOR RESULTS AT INDIVIDUAL STATIONS AND FROM INDIVIDUAL MODELS.

VARIABLE	1995 BASELINE	2030, RCP4.5	2030, RCP8.5	2090, RCP4.5	2090, RCP8.5
T	23.0	24.1	24.1	25.0	26.6
R	581	483	499	475	401
DF	6.8	7.2	7.0	7.3	7.8
SEV	4.2	5.0	4.7	5.3	6.9
∑FFDI	3211	3562	3434	3612	4186

4.11 MARINE PROJECTIONS

Changes in mean sea levels and their extremes, as well as sea surface temperatures (SSTs) and ocean pH (acidity) have the potential to affect both the coastal terrestrial and marine environments. This is discussed at length in Section 8 of the Technical Report. Of particular significance for the terrestrial environment is the impact of sea level rise and changes to the frequency of extreme sea levels. Impacts will be felt through coastal flooding and erosion. For the adjacent marine environment, increases in ocean temperatures and acidity may alter the distribution of marine vegetation (*e.g.* sea grass and kelp forests), increase coral bleaching and mortality, and impact coastal fisheries.

4.11.1 SEA LEVEL

Changes in sea level are caused primarily by changes in ocean density ('thermal expansion') and changes in ocean mass due to the exchange of water with the terrestrial environment, including from glaciers and ice sheets (*e.g.* Church *et al.,* 2014, also see Technical Report, Section 8.1 for details). Over 1966–2009, the average of the relative tide gauge trends around Australia is a rise of 1.4 ± 0.2 mm/yr. After the influence of the El Niño Southern Oscillation (ENSO) on sea level is removed, the average trend is 1.6 ± 0.2 mm/yr. After accounting for and removing the effects of vertical land movements due to glacial rebound and the effects of natural climate variability and changes in atmospheric pressure, sea levels have risen around the Australian coastline at an average rate of 2.1 mm/yr over 1966–2009 and 3.1 mm/yr over 1993–2009. These observed rates of rise for Australia are consistent with global average values (White *et al.,* 2014).

Projections of future sea level changes are shown for Fremantle. These changes are indicative of the coasts around the south-west from Geraldton to Esperance, and Port Adelaide, and also the surrounding coastal areas (Figure 4.11.1). Values for this and other locations are provided for the 2030 and 2090 periods relative to the 1986–2005 period in Table 3 in the Appendix.

Continued increase in sea level for the SSWF cluster is projected with *very high confidence*. The rate of sea level rise during the 21st century will be larger than the averaged rate during the 20th century as greenhouse gas emissions grow (Figure 4.11.1). For the first decades of the 21st century the projections are almost independent of the emission scenario, but they begin to separate significantly from about 2050. For higher greenhouse gas emissions, particularly for RCP 8.5, the rate of rise continues to increase through the 21st century and results in sea level rise about 30 % higher than the RCP 4.5 level by 2100. Significant inter-annual variability will continue through the 21st century. An indication of its expected magnitude is given by the dashed lines in Figure 4.11.1. In the near future (2030) at Fremantle and Port Adelaide the projected range of sea level rise is 0.07 to 0.17 m above the 1986–2005 level (see appendix for other locations) with only minor differences between RCPs. For late in the century (2090) the rise is in the range 0.28 to 0.65 m for RCP 4.5 and 0.39 to 0.85 m for RCP 8.5. These ranges of sea level rise are considered *likely* (at least 66 % probability), however, if a collapse in the marine based sectors of the Antarctic ice sheet were initiated, these projections could be several tenths of a metre higher by late in the century (Church *et al.*, 2014).

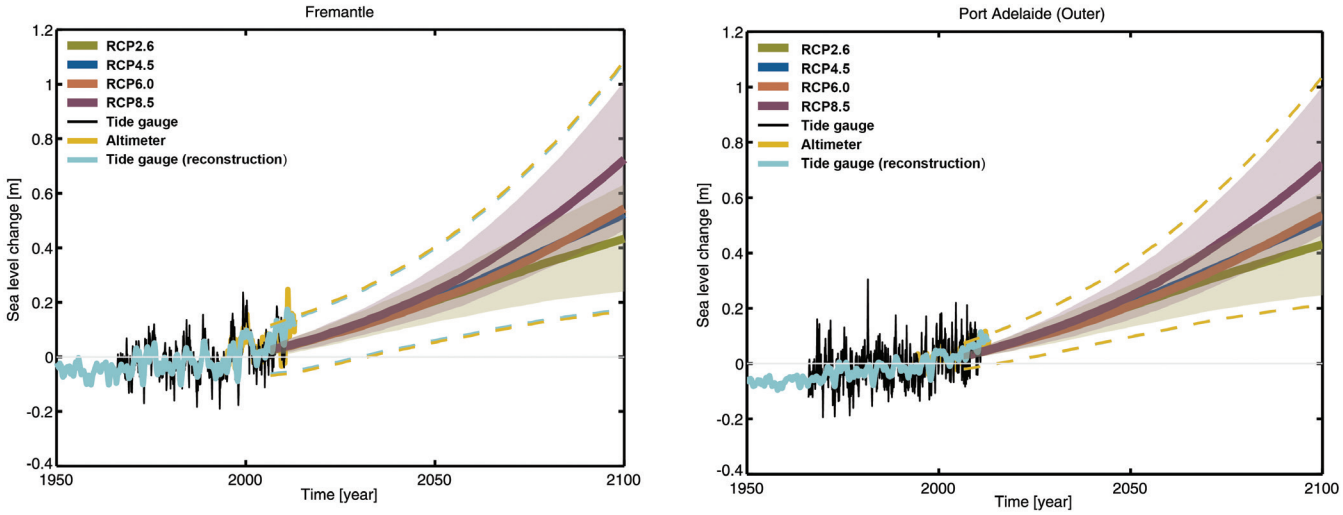

FIGURE 4.11.1: OBSERVED AND PROJECTED RELATIVE SEA LEVEL CHANGE (M) FOR FREMANTLE AND PORT ADELAIDE (WHICH HAVE CONTINUOUS RECORDS AVAILABLE FOR THE PERIOD 1966–2010). THE OBSERVED TIDE GAUGE RELATIVE SEA LEVEL RECORDS ARE INDICATED IN BLACK, WITH THE SATELLITE RECORD (SINCE 1993) IN MUSTARD AND TIDE GAUGE RECONSTRUCTION (WHICH HAS LOWER VARIABILITY) IN CYAN. MULTI-MODEL MEAN PROJECTIONS (THICK PURPLE AND OLIVE LINES) FOR THE RCP8.5 AND RCP2.6 SCENARIOS WITH UNCERTAINTY RANGES SHOWN BY THE PURPLE AND OLIVE SHADED REGIONS FROM 2006–2100. THE MUSTARD AND CYAN DASHED LINES ARE ESTIMATES OF INTER-ANNUAL VARIABILITY IN SEA LEVEL (UNCERTAINTY RANGE ABOUT THE PROJECTIONS) AND INDICATE THAT INDIVIDUAL MONTHLY AVERAGES OF SEA LEVEL CAN BE ABOVE OR BELOW LONGER TERM AVERAGES. NOTE THAT THE RANGES OF SEA LEVEL RISE SHOULD BE CONSIDERED *LIKELY* (AT LEAST 66 % PROBABILITY) AND THAT IF A COLLAPSE IN THE MARINE BASED SECTORS OF THE ANTARCTIC ICE SHEET WERE INITIATED, THESE PROJECTIONS COULD BE SEVERAL TENTHS OF A METRE HIGHER BY LATE IN THE CENTURY.

Extreme coastal sea levels are caused by a combination of factors including astronomical tides, storm surges and wind-waves, exacerbated by rising sea levels. Along the south coast of Australia, the majority of storm surges occur in conjunction with the passage of cold fronts during the winter months (McInnes and Hubbert, 2003).

Using the method of Hunter (2012), an allowance has been calculated based on the mean sea level rise, the uncertainty around the rise, and taking into account the nature of extreme sea levels along the SSWF coastline (Haigh *et al.,* 2014). The allowance is the minimum distance required to raise an asset to maintain current frequency of breaches under projected sea level rise. When uncertainty in mean sea level rise is high (*e.g.* in 2090), this allowance approaches the upper end of the range of projected mean sea level rise. For the SSWF in 2030 the vertical allowances along the cluster coastline are in the range of 0.11 to 0.13 m for all RCPs; and 0.48 to 0.56 for RCP4.5 by 2090; and 0.66 to 0.76 m for RCP8.5 by 2090 (see Table 3 in the Appendix).

4.11.2 SEA SURFACE TEMPERATURE, SALINITY AND ACIDIFICATION

Sea surface temperature (SST) has increased significantly across the globe over recent decades (IPCC, 2013). Increases in SST pose a significant threat to the marine environment through biological changes in marine species, including in local abundance, community structure, and enhanced coral bleaching risk. For 2030, the range of projected SST increase for Fremantle and Port Adelaide is 0.3 to 0.8 °C under RCP2.6 and 0.4 to 0.9 °C for RCP8.5 (see Table 3 in the Appendix). For 2090, there is a much larger range of warming between the different emission scenarios and different sites. For Fremantle the range of increase is projected to be 0.3 to 1.1 °C for RCP2.6 and 1.8 to 3.3 °C for RCP8.5 and for Port Adelaide it is 0.4 to 1.0 °C for RCP2.6 and 1.5 to 3.5 °C for RCP8.5. Across all four sites the ranges are 0.3 to 1.1 °C for RCP2.6 and 1.5 to 3.9 °C for RCP8.5.

Ocean salinity in coastal waters will be affected by changes to rainfall and evaporation, and this in turn can affect stratification and mixing, and potentially nutrient supply. Changes to salinity across the coastal waters of the Southern and South-Western Flatlands cluster span a large range that includes possible increases and decreases, particularly over the longer term and for higher emission scenarios as indicated in Table 3 (in Appendix). Locally, salinity can also be affected by riverine input.

About 30 % of the anthropogenic carbon dioxide emitted into the atmosphere over the past 200 years has been absorbed by the oceans (Ciais *et al.*, 2013) and this has led to a 0.1 unit decrease in the ocean's surface water pH, which represents a 26 % increase in the concentration of hydrogen ions in seawater (Raven *et al.*, 2005). As the carbon dioxide enters the ocean it reacts with the seawater to cause a decrease in pH and carbonate concentration, collectively known as ocean acidification. Carbonate is used in conjunction with calcium as aragonite by many marine organisms such as corals, oysters, clams and some plankton such as foraminifera and pteropods, to form their hard skeletons or shells. A reduction in shell mass has already been detected in foraminifera and pteropods in the Southern Ocean (Moy *et al.,* 2009; Bednaršek *et al*., 2012). Ocean acidification lowers the temperature at which corals bleach, reducing resilience to natural variability. Ocean acidification can affect fin and shellfish fisheries, aquaculture, tourism and coastal protection. In the cluster by 2030, pH change is projected to be another 0.08 units lower. By 2090, under RCP4.5 it is projected to be up to 0.15 units lower and up to 0.33 units lower for RCP8.5. This represents additional increases in hydrogen ion concentration of 40 % and 110 % respectively. These changes are accompanied by reductions in aragonite saturation state (see Table 3 in the Appendix) and together with SST changes will affect all levels of the marine food web, and make it harder for calcifying marine organisms to build their hard shells, potentially affecting resilience and viability of marine ecosystems.

In summary, there is *very high confidence* that sea surface temperatures will continue to rise along the Southern and South-Western Flatlands coastline, with the magnitude of the warming dependent on emission scenarios. Changes in salinity are related to changes in the hydrological cycle and are of *low confidence*. There is *very high confidence* that the ocean around Australia will become more acidic, showing a nett reduction in pH. There is also *high confidence* that the rate of ocean acidification will be proportional to carbon dioxide emissions.

4.12 OTHER PROJECTION MATERIAL FOR THE CLUSTER

Previous projection data across this cluster include the nationwide Climate Change in Australia projections produced by the CSIRO and Bureau of Meteorology in 2007 (CSIRO and BOM, 2007) and a range of state funded projects. The Western Australia government funded the Indian Ocean Climate Initiative (IOCI) which provided extensive information about the weather and climate of south-west Australia and the changes observed. Some projections were produced which included data downscaled to stations (*e.g.* Hope, 2006; Indian Ocean Climate Initiative, 2012; Bates *et al.,* 2008). A number of studies have produced projections at catchment scale. The recent WA Department of Water report on future climate projections (Department of Water, 2014) lists a number of these past studies as well as providing new information.

In South Australia, The Goyder Institute (http://www.goyderinstitute.org) project on the 'Development of an agreed set of downscaled climate projections for South Australia' focuses on information relevant to water managers and includes downscaled data at a station scale across a number of catchments such as the Onkaparinga. Rainfall and a host of other variables relevant to water management have also been downscaled under The Goyder Institute project at stations across each of the South Australian NRM regions. The downscaling is from 15 CMIP5 GCMs for both RCP4.5 and RCP8.5. Outputs will include rainfall, maximum temperature, minimum temperature, solar radiation (incoming shortwave at surface), vapour pressure deficit and Morton's wet areal potential evapotranspiration (Steve Charles, CSIRO, pers. comm.).

Some of the projection products that are currently available made use of previous generation models (*e.g.* CMIP3). These projections are still relevant, particularly if placed in the context of the latest modelling results (see Appendix A in the Technical Report for a discussion on CMIP3 and CMIP5 model-based projections).

5 APPLYING THE REGIONAL PROJECTIONS IN ADAPTATION PLANNING

The fundamental role of adaptation is to reduce the adverse impacts of climate change on vulnerable systems, using a wide range of actions directed by the needs of the vulnerable system. Adaptation also identifies and incorporates new opportunities that become feasible under climate change. For adaptation actions to be effective, all stakeholders need to be engaged, resources must be available and planners must have information on 'what to adapt to' and 'how to adapt' (Füssel and Klein, 2006).

This report presents information about 'what to adapt to' by describing how future climates may respond to increasing greenhouse gas concentrations. This Section gives guidance on how climate projections can be framed in the context of climate scenarios (Section 5.1) using tools such as the Climate Futures web tool, available on the Climate Change in Australia website (Box 5.1). The examples of its use presented here are not exhaustive, but rather an illustration of what can be done.

5.1 IDENTIFYING FUTURE CLIMATE SCENARIOS

In Chapter 4 of this report, projected changes are expressed as a range of plausible change for individual variables as simulated by CMIP5 models or derived from their outputs. However, many practitioners are interested in information on how the climate may change, not just changes in one climate variable. To consider how several climate variables may change in the future, data from individual models should be considered because each model simulates changes that are internally consistent across many variables. For example, one should not combine the projected rainfall from one model with temperature from another, as these would represent the climate responses of unrelated simulations.

The challenge for practitioners lies in selecting which models to look at, since models can vary in their simulated response to increasing greenhouse gas emissions. Climate models can be organised according to their simulated climate response to assist with this selection. For example, sorting according to rainfall and temperature responses would give an immediate feel for how models fall into a set of discrete climate scenarios framed in terms such as: *much drier and slightly warmer, much wetter and slightly warmer, much drier and much hotter*, and *much wetter and much hotter*.

The Climate Futures web tool described in Box 9.1 of the Technical Report presents a scenario approach to investigating the range of climate model simulations for projected future periods. The following Section describes how this tool can be used to facilitate the use of model output in impact and adaptation assessment.

BOX 5.1: USER RESOURCES ON THE CLIMATE CHANGE IN AUSTRALIA WEBSITE

The Climate Change in Australia website provides information on the science of climate change in a global and Australian context with material supporting regional planning activities. For example, whilst this report focuses on a selected set of emission scenarios, time horizons and variables, the website enables generation of graphs tailored to specific needs, such as a different time period or emission scenario.

The website includes a decision tree yielding application-relevant information, report-ready projected change information and the web tool Climate Futures (Whetton *et al.,* 2012). The web tool facilitates the visualisation and categorisation of model results and selection of data sets that are representative of futures that are of interest to the user. These products are described in detail in Chapter 9 of the Technical Report.

www.climatechangeinaustralia.gov.au

5.2 DEVELOPING CLIMATE SCENARIOS USING THE CLIMATE FUTURES TOOL

The example presented in Figure 5.1 represents the changes, as simulated by CMIP5 models, in temperature and rainfall in the SSWF cluster for 2060 (years 2050–2069) under the RCP4.5 scenario. The table organises the models into groupings according to their simulated changes in rainfall (rows) and temperatures (columns). Regarding rainfall, models simulate increases and decreases from *much drier* (less than -15 %) to *much wetter* (greater than 15 %), with 21 of 27 models showing drying conditions (less than -5 %) compared to one model showing rainfall increases (greater than 5 %) and five models showing *little change* (-5 to 5 % change). With regard to temperature, most models show results ranging from *warmer* (0.5 to 1.5 °C warmer) to *hotter* (1.5 to 3 °C warmer), 14 and 13 models respectively, with no models falling into the lowest category *slightly warmer* (less than 0.5 °C warmer) or the highest category *much hotter* (greater than 3.0 °C warming). When considering the two variables together, it can be seen that the most commonly

simulated climate for 2060 under RCP4.5 is a *hotter and drier* climate (7 of 27 models).

In viewing the projection data in this way, the user can gain an overview of what responses are possible when considering the CMIP5 model archive for a given set of constraints. In a risk assessment context, a user may want to consider not only the maximum consensus climate (simulated by most models), but also the best case and worst case scenarios. Their nature will depend on the application. A water-supply manager, for example, is likely to determine from Figure 5.1 that the best case scenario would be a *much wetter and warmer* climate and the worst case the *hotter and much drier* scenario.

Assuming that the user has identified what futures are likely to be of most relevance to the system of interest, Climate Futures allows exploration of the numerical values for each of the models that populates the scenarios. Further, it provides a function for choosing a single model that most closely represents the particular future climate of interest, but also taking into account models that have been identified as sub-optimal for particular regions based on model evaluation information (described in Chapter 5 of the Technical Report). Through this approach users can select a small set of models to provide scenarios for their application, taking into consideration model spread and the sensitivity of their application to climate change.

Alternatively, the user may wish to consider a small set of scenarios defined irrespective of emission scenario or date (but with their likelihood of occurrence being time and emission scenario sensitive). This may be in circumstances where the focus is on critical climate change thresholds. This strategy is illustrated for the SSWF cluster in Box 5.2, where results are produced in Climate Futures by comparing model simulations from separate time slices and emission scenarios. This box also illustrates each of these scenarios with current climate analogues (comparable climates) for selected sites.

Another user case could be the desire to compare simulations from different climate model ensembles (such as the earlier CMIP3 ensemble, or ensembles of downscaled results such as the results from the Goyder Institute for South Australia). Comparing model spread simulated by different generations of GCMs in Climate Futures allows assessment of the on-going relevance of existing impact studies based on selected CMIP3 models, as well as to compare scenarios developed using downscaled and GCM results.

CONSENSUS	PROPORTION OF MODELS
Not projected	No models
Very low	< 10 %
Low	10 to 33 %
Moderate	33 to 66 %
High	66 - 90 %
Very high	> 90 %

		Annual surface temperature (°C)			
		Slightly warmer 0 to +0.5	Warmer +0.5 to 1.5	Hotter +1.5 to +3.0	Much hotter > +3.0
Annual rainfall (%)	Much wetter > +15.0				
	Wetter +5.0 to +15.0		1 of 27 models		
	Little change -5.0 to +5.0		4 of 27 models	1 of 27 models	
	Drier -15.0 to -5.0		6 of 27 models	7 of 27 models	
	Much drier < -15.0		3 of 27 models	5 of 27 models	

FIGURE 5.1: AN EXAMPLE TABLE BASED ON OUTPUT FROM THE CLIMATE FUTURES WEB TOOL SHOWING RESULTS FOR SSWF WHEN ASSESSING PLAUSIBLE CLIMATE FUTURES FOR 2060 UNDER RCP4.5, AS DEFINED BY GCM SIMULATED ANNUAL RAINFALL (%- CHANGE) AND TEMPERATURE (°C WARMING).

BOX 5.2: INDICATIVE CLIMATE SCENARIOS FOR SOUTHERN AND SOUTH-WESTERN FLATLANDS AND ANALOGUE FUTURE CLIMATES

Users may wish to consider the future climate of their region in terms of a small set of scenarios defined irrespective of emission scenario or date (but with their likelihood of occurrence being time and emission scenario sensitive). An example of using this strategy for the Southern and South-Western Flatlands is illustrated here. Combining the results in Climate Futures for 2030, 2050, and 2090, under RCP2.6, RCP4.5, and RCP8.5 gives a set of future climate scenarios (see Figure B5.2). From these, five highlighted scenarios are considered representative of the spread of results (with other potential scenarios excluded as less likely than the selected cases or lying within the range of climates specified by the selected cases). For each case, when available, the current climate analogue for the future climate of Perth or Adelaide is given as an example in most cases. These were generated using the method described in Chapter 9.3.5 of the Technical Report and are based on matching annual average rainfall (within +/- 5 %) and maximum temperature (within +/- 1 °C). Note that other potentially important aspects of local climate are not matched, such as rainfall seasonality, and thus the analogues should not be used directly in adaptation planning without considering more detailed information.

- *Warmer* (0.5 to 1.5 °C warmer) and *drier* (5 to 15 % reduction). This would occur by 2030 under any emission scenario, but may persist through to late in the century under RCP2.6. In this case, Perth's future climate would be more like the current climate of Jurien (WA). Adelaide's future climate would be more like the current climate of Ravensthorpe (WA).
- *Hotter* (1.5 to 3.0 °C warming), but *much drier* (greater than 15 % reduction). This is possible by 2050 under RCP4.5 or RCP8.5. In this case Perth's future climate would be more like the current climate of Jurien (WA). Adelaide's future climate would be more like the current climate of Griffith (NSW).
- *Much hotter* (greater than 3.0 °C warmer) and *much drier* (greater than 15 % reduction). This is possible by late in the 21st century under RCP8.5. In this case, Perth's future climate would be more like the current climate of Dongara (WA) and Adelaide's future climate would be more like the current climate of Northam (WA).
- *Warmer* (0.5 to 1.5 °C warmer) with *little change in rainfall* (-5 to +5 %). This would occur by 2030 under any emission scenario, but may persist through to late in the century under RCP2.6. In this case, Perth's future climate would be more like the current climate of Yanchep Beach (WA). Adelaide's future climate would be more like the current climate of Wagga Wagga (NSW).
- *Warmer* (0.5 to 1.5 °C warmer) and *much drier* (greater than 15 % reduction). This would occur by 2030 under any emission scenario, but may persist through to late in the century under RCP2.6. In this case, Perth's future climate would be more like the current climate of Geraldton (WA). Adelaide's future climate would be more like the current climate of Narrandera (NSW).

FIGURE B5.2: A TABLE BASED OUTPUT FROM CLIMATE FUTURES SHOWING CATEGORIES OF FUTURE CLIMATE PROJECTIONS FOR THE SOUTHERN AND SOUTH-WESTERN FLATLANDS CLUSTER, AS DEFINED BY CHANGE IN ANNUAL TEMPERATURE (COLUMN) AND CHANGE IN RAINFALL (ROWS). WITHIN EACH FUTURE CLIMATE CATEGORY, MODEL SIMULATIONS ARE SORTED ACCORDING TO TIME (2030, 2050, AND 2090) AND CONCENTRATION PATHWAY (RCP2.6, RCP4.5, AND RCP8.5); THE NUMBER INDICATING HOW MANY MODEL SIMULATIONS OF THAT PARTICULAR SUB-CATEGORY FALL INTO THE CLIMATE CATEGORY OF THE TABLE (THE NUMBER OF MODELS USED IN THIS EXAMPLE VARIES FOR DIFFERENT CONCENTRATION PATHWAYS). A COLOUR CODE INDICATES HOW OFTEN A PARTICULAR CLIMATE IS SIMULATED AMONGST THE CONSIDERED MODELS (PERCENT OCCURRENCE). THE SCENARIOS DESCRIBED IN THE TEXT ARE HIGHLIGHTED IN BOLD.

Future Realisations for the Southern and South Western Flatlands cluster

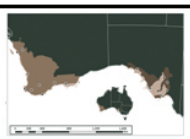

Annual Rainfall (%)	Annual Surface Temperature (°C)														
	Slightly Warmer 0 to +0.5				Warmer +0.5 to +1.5				Hotter +1.5 to +3.0				Much Hotter > +3.0		
	RCP	2030	2050	2090	2030	2050	2090		2030	2050	2090		2030	2050	2090
Much Wetter > +15.0	2.6														
	4.5														
	8.5														
Wetter +5.0 to +15.0	2.6					1	1								
	4.5										1				
	8.5				2					2					
Little Change −5.0 to +5.0	2.6				4	6	3				1				
	4.5				10	6	2				4				
	8.5				10	1				3	2				2
Drier −15.0 to −5.0	2.6				11	6	7			1					
	4.5				14	11	1			3	7				
	8.5				12	7				6	1				6
Much Drier < −15.0	2.6				3	4	6								
	4.5				3	4	3			3	9				
	8.5				5	2				8	3				15

By when and under what greenhouse gas pathway could this occur (colour code=% of models for that period/RCP)?

Not projected	<10%	10-33%	33-66%

RCP2.6-18 models
RCP4.5-27 models
RCP8.5-29 models

REFERENCES

ALLAN, R. & ANSELL, T. 2006. A new globally complete monthly historical gridded mean sea level pressure dataset (HadSLP2): 1850-2004. Journal of Climate, 19, 5816-5842.

ALLEN, R. J., NORRIS, J. R. & WILD, M. 2013. Evaluation of multidecadal variability in CMIP5 surface solar radiation and inferred underestimation of aerosol direct effects over Europe, China, Japan, and India. Journal of Geophysical Research-Atmospheres, 118, 6311-6336.

BEDNAršEK, N., TARLING, G., BAKKER, D., FIELDING, S., JONES, E., VENABLES, H., WARD, P., KUZIRIAN, A., LEZE, B. & FEELY, R. 2012. Extensive dissolution of live pteropods in the Southern Ocean. Nature Geoscience, 5, 881-885.

BLANCHI, R., LUCAS, C., LEONARD, J. & FINKELE, K. 2010. Meteorological conditions and wildfire-related house loss in Australia. International Journal of Wildland Fire, 19, 914-926.

BRADSTOCK, R. A. 2010. A biogeographic model of fire regimes in Australia: current and future implications. Global Ecology and Biogeography, 19, 145-158.

BROHAN, P., KENNEDY, J. J., HARRIS, I., TETT, S. F. & JONES, P. D. 2006. Uncertainty estimates in regional and global observed temperature changes: A new data set from 1850. Journal of Geophysical Research: Atmospheres (1984–2012), 111, D12, 1-21.

CHIEW, F., KIRONO, D., KENT, D. & VAZE, J. 2009. Assessment of rainfall simulations from global climate models and implications for climate change impact on runoff studies. *18th World Imacs Congress and Modsim09 International Congress on Modelling and Simulation: Interfacing Modelling and Simulation with Mathematical and Computational Sciences*. 3907-3913

CHURCH, J. A., CLARK, P. U., CAZENAVE, A., GREGORY, J. M., JEVREJEVA, S., LEVERMANN, A., MERRIFIELD, M. A., MILNE, G. A., NEREM, R. S., NUNN, P. D., PAYNE, A. J., PFEFFER, W. T., STAMMER, D. & UNNIKRISHNAN, A. S. 2014. Sea Level Change. In: STOCKER, T. F., D. QIN, G.-K. PLATTNER, M. TIGNOR, S. K. ALLEN, J. BOSCHUNG, A. NAUELS, Y. XIA, V. BEX AND P. M. MIDGLEY (ed.) *Climate Change 2013: The Physical Science Basis. Contribution of Working Group I to the Fifth Assessment Report of the Intergovernmental Panel on Climate Change*.

CIAIS, P., SABINE, C., BALA, G., BOPP, L., BROVKIN, V., CANADELL, J., CHHABRA, A., DEFRIES, R., GALLOWAY, J., HEIMANN, M., JONES, C., LE QUÉRÉ, C., MYNENI, R. B., PIAO, S. & THORNTON, P. 2013. Carbon and Other Biogeochemical Cycles. Contribution of Working Group I to the *Fifth Assessment Report* of the Intergovernmental Panel on Climate Change. In: STOCKER, T. F., D. QIN, G.-K. PLATTNER, M. TIGNOR, S.K. ALLEN, J. BOSCHUNG, A. NAUELS, Y. XIA, BEX, V. & MIDGLEY, P. M. (eds.) Climate Change 2013: The Physical Science Basis. Cambridge, United Kingdom and New York, NY, USA: Cambridge University Press.

CLARKE, H., LUCAS, C. & SMITH, P. 2013. Changes in Australian fire weather between 1973 and 2010. International Journal of Climatology, 33, 931-944.

CLARKE, H. G., SMITH, P. L. & PITMAN, A. J. 2011. Regional signatures of future fire weather over eastern Australia from global climate models. International Journal of Wildland Fire, 20, 550-562.

CSIRO AND BOM 2007. Climate change in Australia: Technical Report. Aspendale, Australia: CSIRO Marine and Atmospheric Research. URL http://www.climatechangeinaustralia.gov.au/technical_report.php Accessed 19/8/2014

DEPARTMENT OF WATER 2014. Selection of future climate projections for Western Australia. Western Australia Department of Water in press

FAWCETT, R., DAY, K. A., TREWIN, B., BRAGANZA, K., SMALLEY, R., JOVANOVIC, B. & JONES, D. 2012. On the sensitivity of Australian temperature trends and variability to analysis methods and observation networks, Centre for Australian Weather and Climate Research Technical Report No.050.

FOWLER, H. & EKSTRÖM, M. 2009. Multi-model ensemble estimates of climate change impacts on UK seasonal precipitation extremes. International Journal of Climatology, 29, 385-416.

FREDERIKSEN, J. S. & FREDERIKSEN, C. S. 2007. Interdecadal changes in southern hemisphere winter storm track modes. Tellus A, 59, 599-617.

FREDERIKSEN, J. S. & FREDERIKSEN, C. S. 2011. Twentieth century winter changes in Southern Hemisphere synoptic weather modes. Advances in Meteorology, 2011, Article ID 353829, 16 pages, doi:10.1155/2011/353829.

FÜSSEL, H.-M. & KLEIN, R. J. 2006. Climate change vulnerability assessments: an evolution of conceptual thinking. Climatic Change, 75, 301-329.

GALLANT, A. J., HENNESSY, K. J. & RISBEY, J. 2007. Trends in rainfall indices for six Australian regions: 1910-2005. Australian Meteorological Magazine, 56, 223-241.

GROSE, M. R., FOX-HUGHES, P., HARRIS, R. M. & BINDOFF, N. L. 2014. Changes to the drivers of fire weather with a warming climate–a case study of southeast Tasmania. Climatic Change, 124, 255-269.

GROSE, M. R., POOK, M. J., MCINTOSH, P. C., RISBEY, J. S. & BINDOFF, N. L. 2012. The simulation of cutoff lows in a regional climate model: reliability and future trends. Climate Dynamics, 39, 445-459.

HAIGH, I. D., WIJERATNE, E., MACPHERSON, L. R., PATTIARATCHI, C. B., MASON, M. S., CROMPTON, R. P. & GEORGE, S. 2014. Estimating present day extreme water level exceedance probabilities around the coastline of Australia: tides, extra-tropical storm surges and mean sea level. Climate Dynamics, 42, 121-138.

HENDON, H., THOMPSON, D. & WHEELER, M. 2007. Australian rainfall and surface temperature variations associated with the Southern Hemisphere annular mode. Journal of Climate, 20, 2452-2467.

HENNESSY, K., LUCAS, C., NICHOLLS, N., BATHOLS, J., SUPPIAH, R. & RICKETTS, J. 2005. Climate change impacts on fire weather in south-east Australia. Melbourne, Australia: Consultancy report for the New South Wales Greenhouse Office, Victorian Department of Sustainability and Environment, Tasmanian Department of Primary Industries, Water and Environment, and the Australian Greenhouse Office. CSIRO Atmospheric Research and Australian Government Bureau of Meteorology 78pp. URL http://laptop.deh.gov.au/soe/2006/publications/drs/pubs/334/lnd/ld_24_climate_change_impacts_on_fire_weather.pdf Accessed 18/8/2014

HOPE, P. K., DROSDOWSKY, W. & NICHOLLS, N. 2006. Shifts in synoptic systems influencing south west Western Australia. Climate Dynamics, 26, 751-764.

HOPE, P. & GANTER, C. 2010. Recent and projected rainfall trends in south-west Australia and the associated shifts in weather systems. *In*: JUBB, I., HOLPER, P. & CAI, W. (eds.) *Managing Climate Change*. Melbourne, Australia: CSIRO Publishing.

HOPE, P., KEAY, K., POOK, M., CATTO, J., SIMMONDS, I., MILLS, G., MCINTOSH, P., RISBEY, J. & BERRY, G. 2014. A Comparison of Automated Methods of Front Recognition for Climate Studies: A Case Study in Southwest Western Australia. Monthly Weather Review, 142, 343-363.

HOPE, P., TIMBAL, B. & FAWCETT, R. 2010. Associations between rainfall variability in the southwest and southeast of Australia and their evolution through time. International Journal of Climatology, 30, 1360-1371.

HOPE, P. K. 2006. Projected future changes in synoptic systems influencing southwest Western Australia. Climate Dynamics, 26, 765-780.

HOPE, P. K., NICHOLLS, N. & MCGREGOR, J. L. 2004. The rainfall response to permanent inland water in Australia. Australian Meteorological Magazine, 53, 251-262.

HUNTER, J. 2012. A simple technique for estimating an allowance for uncertain sea-level rise. Climatic Change, 113, 239-252.

HUNTINGTON, T. G. 2006. Evidence for intensification of the global water cycle: Review and synthesis. Journal of Hydrology, 319, 83-95.

INDIAN OCEAN CLIMATE INITIATIVE 2012. Western Australia's Weather and Climate. In: BATES, B., FREDERIKSEN, C. & WORMWORTH, J. (eds.) *A Synthesis of Indian Ocean Climate Initiative Stage 3 Research*. Australia: CSIRO and BOM. URL: http://www.ioci.org.au/publications/ioci-stage-3/cat_view/17-ioci-stage-3/23-reports.html Accessed 19/8/2014.

IOCI 2002. Climate variability and change in south-west Western Australia. Perth, Australia: Indian Ocean Climate Initiative Panel. URL: http://www.ioci.org.au/publications/ioci-stage-2/cat_view/16-ioci-stage-2/22-reports/32-general-reports.html Accessed 19/8/2014.

IPCC 2013. Climate Change 2013: The Physical Science Basis. In: STOCKER, T. F., D. QIN, G.-K. PLATTNER, M. TIGNOR, S. K. ALLEN, J. BOSCHUNG, A. NAUELS, Y. XIA, V. BEX & P. M. MIDGLEY (eds.) *Contribution of Working Group I to the Fifth Assessment Report of the Intergovernmental Panel on Climate Change*. Cambridge, UK, and New York, NY, USA: Cambridge University Press.

JONES, D. A., WANG, W. & FAWCETT, R. 2009. High-quality spatial climate data-sets for Australia. Australian Meteorological and Oceanographic Journal, 58, 233-248.

KIRONO, D. G. & KENT, D. M. 2011. Assessment of rainfall and potential evaporation from global climate models and its implications for Australian regional drought projection. International Journal of Climatology, 31, 1295-1308.

LEVITUS, S., ANTONOV, J. I., BOYER, T. P. & STEPHENS, C. 2000. Warming of the world ocean. Science, 287, 2225-2229.

LOVITT, C. 2011. Seasonal climate summary southern hemisphere (spring 2010): La Niña strengthens. Australian Meteorological Magazine, 61, 185-195.

LUCAS, C. 2010. On developing a historical fire weather data-set for Australia. Australian Meteorological Magazine, 60, 1-13.

LUCAS, C., HENNESSY, K., MILLS, G. & BATHOLS, J. 2007. Bushfire Weather in Southeast Australia: Recent Trends and Projected Climate Change Impacts. Consultancy Report prepared for The Climate Institute of Australia. Bushfire CRC and Australian Bureau of Meteorology CSIRO Marine and Atmospheric Research. URL http://www.royalcommission.vic.gov.au/getdoc/c71b6858-c387-41c0-8a89-b351460eba68/TEN.056.001.0001.pdf Accessed 18/8/2014

LUCAS, C., TIMBAL, B. & NGUYEN, H. 2014. The expanding tropics: a critical assessment of the observational and modeling studies. Wiley Interdisciplinary Reviews: Climate Change, 5, 89-112.

MASTRANDREA, M. D., FIELD, C. B., STOCKER, T. F., EDENHOFER, O., EBI, K. L., FRAME, D. J., HELD, H., KRIEGLER, E., MACH, K. J. & MATSCHOSS, P. R. 2010. Guidance note for lead authors of the IPCC *Fifth Assessment Report* on consistent treatment of uncertainties. *Intergovernmental Panel on Climate Change* (IPCC). URL http://www.ipcc.ch/pdf/supporting-material/uncertainty-guidance-note.pdf Accessed 18/8/2014

MCARTHUR, A. G. 1967. Fire behaviour in Eucalypt forests. Leaflet. Forestry Timber Bureau Australia, 35-35.

MCGREGOR, J. & DIX, M. 2008. An updated description of the conformal-cubic atmospheric model. In: HAMILTON, K. & OHFUCHI, W. (eds.) *High Resolution Numerical Modelling of the Atmosphere and Ocean*. Springer New York.

MCINNES, K. L. & HUBBERT, G. D. 2003. A numerical modeling study of storm surges in Bass Strait. Australian Meterological Magazine, 52, 143-156.

MCMAHON, T. A., PEEL, M. C., LOWE, L., SRIKANTHAN, R. & MCVICAR, T. R. 2013. Estimating actual, potential, reference crop and pan evaporation using standard meteorological data: a pragmatic synthesis. Hydrology and Earth System Sciences, 17, 1331-1363.

MCVICAR, T. R., RODERICK, M. L., DONOHUE, R. J., LI, L. T., VAN NIEL, T. G., THOMAS, A., GRIESER, J., JHAJHARIA, D., HIMRI, Y. & MAHOWALD, N. M. 2012. Global review and synthesis of trends in observed terrestrial near-surface wind speeds: Implications for evaporation. Journal of Hydrology, 416, 182-205.

MOSS, R. H., EDMONDS, J. A., HIBBARD, K. A., MANNING, M. R., ROSE, S. K., VAN VUUREN, D. P., CARTER, T. R., EMORI, S., KAINUMA, M., KRAM, T., MEEHL, G. A., MITCHELL, J. F. B., NAKICENOVIC, N., RIAHI, K., SMITH, S. J., STOUFFER, R. J., THOMSON, A. M., WEYANT, J. P. & WILBANKS, T. J. 2010. The next generation of scenarios for climate change research and assessment. Nature, 463, 747-756.

MOY, A. D., HOWARD, W. R., BRAY, S. G. & TRULL, T. W. 2009. Reduced calcification in modern Southern Ocean planktonic foraminifera. Nature Geoscience, 2, 276-280.

NAKIĆENOVIĆ, N. & SWART, R. (eds.) 2000. *Special Report on Emissions Scenarios. A Special Report of Working Group III of the Intergovernmental Panel on Climate Change*, Cambridge, United Kingdom and New York, NY, USA: Cambridge University Press.

NGUYEN, H., EVANS, A., LUCAS, C., SMITH, I. & TIMBAL, B. 2013. The Hadley Circulation in Reanalyses: Climatology, Variability, and Change. Journal of Climate, 26, 3357-3376.

POOK, M. J., RISBEY, J. S. & MCINTOSH, P. C. 2012. The synoptic climatology of cool-season rainfall in the Central Wheatbelt of Western Australia. Monthly Weather Review, 140, 28-43.

RAPHAEL, M. N. & HOLLAND, M. M. 2006. Twentieth century simulation of the Southern Hemisphere climate in coupled models. Part 1: Large scale circulation variability. Climate Dynamics, 26, 217-228.

RAUT, B. A., JAKOB, C. & REEDER, M. J. 2014. Linking rainfall changes over southwestern Australia and the Southern Annular Mode. Journal of Climate, submitted.

RAVEN, J., CALDEIRA, K., ELDERFIELD, H., HOEGH-GULDBERG, O., LISS, P., RIEBESELL, U., SHEPHERD, J., TURLEY, C. & WATSON, A. 2005. Ocean acidification due to increasing atmospheric carbon dioxide. The Royal Society 68pp.

RYAN, B. & HOPE, P. (eds.) 2005. Indian Ocean Climate Initiative Stage 2: Report of Phase 1 Activity, Perth, Australia: Indian Ocean Climate Initiative Panel.

RYAN, B. & HOPE, P. (eds.) 2006. Indian Ocean Climate Initiative Stage 2: Report of Phase 2 Activity, Perth, Australia: Indian Ocean Climate Initiative Panel.

SHERWOOD, S. C., ROCA, R., WECKWERTH, T. M. & ANDRONOVA, N. G. 2010. Tropospheric water vapor, convection, and climate. Reviews of Geophysics, 48, RG2001.

TAYLOR, K. E., STOUFFER, R. J. & MEEHL, G. A. 2012. An overview of CMIP5 and the experiment design. Bulletin of the American Meteorological Society, 93, 485-498.

TENG, J., CHIEW, F., VAZE, J., MARVANEK, S. & KIRONO, D. 2012. Estimation of climate change impact on mean annual runoff across continental Australia using Budyko and Fu equations and hydrological models. Journal of Hydrometeorology, 13, 1094-1106.

TIMBAL, B. & DROSDOWSKY, W. 2013. The relationship between the decline of South Eastern Australia rainfall and the strengthening of the sub-tropical ridge. International Journal of Climatology, 33, 1021-1034.

TIMBAL, B. & MCAVANEY, B. J. 2001. An analogue-based method to downscale surface air temperature: Application for Australia. Climate Dynamics, 17, 947-963.

TROCCOLI, A., MULLER, K., COPPIN, P., DAVY, R., RUSSELL, C. & HIRSCH, A. L. 2012. Long-term wind speed trends over Australia. Journal of Climate, 25, 170-183.

VAN VUUREN, D. P., EDMONDS, J., KAINUMA, M., RIAHI, K., THOMSON, A., HIBBARD, K., HURTT, G. C., KRAM, T., KREY, V. & LAMARQUE, J.-F. 2011. The representative concentration pathways: an overview. Climatic Change, 109, 5-31.

WATTERSON, I. G., HIRST, A. C. & ROTSTAYN, L. D. 2013. A skill score based evaluation of simulated Australian climate. Australian Meteorological and Oceanographic Journal, 63, 181-190.

WHAN, K., TIMBAL, B. & LINDESAY, J. 2014. Linear and nonlinear statistical analysis of the impact of sub-tropical ridge intensity and position on south-east Australian rainfall. International Journal of Climatology, 34, 326-342.

WHETTON, P., HENNESSY, K., CLARKE, J., MCINNES, K. & KENT, D. 2012. Use of Representative Climate Futures in impact and adaptation assessment. Climatic Change, 115, 433-442.

WHITE, N. J., HAIGH, I. D., CHURCH, J. A., KEON, T., WATSON, C. S., PRITCHARD, T., WATSON, P. J., BURGETTE, R. J., ELIOT, M., MCINNES, K. L., YOU, B., ZHANG, X. & TREGONING, P. 2014. Australian Sea Levels - Trends, regional variability and Influencing factors. Earth-Science Reviews, 136, 155-174.

WILLIAMS, R. J., BRADSTOCK, R. A., CARY, G. J., ENRIGHT, N., GILL, A., LIEDLOFF, A., LUCAS, C., WHELAN, R., ANDERSEN, A. & BOWMAN, D. 2009. Interactions between climate change, fire regimes and biodiversity in Australia- A preliminary assessment. Canberra: Department of Climate Change and Department of the Environment, Water, Heritage and the Arts. URL http://climatechange.gov.au/sites/climatechange/files/documents/04_2013/20100630-climate-fire-biodiversity-PDF.pdf Accessed 18/8/2014

YIN, J. H. 2005. A consistent poleward shift of the storm tracks in simulations of 21st century climate. Geophysical Research Letters, 32, 18701.

ZHANG, L., POTTER, N., HICKEL, K., ZHANG, Y. & SHAO, Q. 2008. Water balance modeling over variable time scales based on the Budyko framework – Model development and testing. Journal of Hydrology 360, 117-131.

APPENDIX

TABLE 1: GCM SIMULATED CHANGES IN A RANGE OF CLIMATE VARIABLES FOR THE 2020–2039 (2030) AND 2080–2099 (2090) PERIODS RELATIVE TO THE 1986–2005 PERIOD FOR SSWF, SSWF WEST AND SSWF EAST. THE TABLE GIVES THE MEDIAN (50TH PERCENTILE) CHANGE, AS PROJECTED BY THE CMIP5 MODEL ARCHIVE, WITH 10TH TO 90TH PERCENTILE RANGE GIVEN WITHIN BRACKETS. RESULTS ARE GIVEN FOR RCP2.6, RCP4.5, AND RCP8.5 FOR ANNUAL AND SEASONAL AVERAGES. 'DJF' REFERS TO SUMMER (DECEMBER TO FEBRUARY), 'MAM' TO AUTUMN (MARCH TO MAY), 'JJA' TO WINTER (JUNE TO AUGUST) AND 'SON' TO SPRING (SEPTEMBER TO NOVEMBER). THE PROJECTIONS ARE PRESENTED AS EITHER PERCENTAGE OR ABSOLUTE CHANGES. THE COLOURING (SEE LEGEND) INDICATES CMIP5 MODEL AGREEMENT, WITH 'MEDIUM' BEING MORE THAN 60 % OF MODELS, 'HIGH' MORE THAN 75 %, 'VERY HIGH' MORE THAN 90 %, AND 'SUBSTANTIAL' AGREEMENT ON A CHANGE OUTSIDE THE 10TH TO 90TH PERCENTILE RANGE OF MODEL NATURAL VARIABILITY. NOTE THAT 'VERY HIGH AGREEMENT' CATEGORIES ARE RARELY OCCUPIED EXCEPT FOR 'VERY HIGH AGREEMENT ON SUBSTANTIAL INCREASE', AND SO TO REDUCE COMPLEXITY THE OTHER CASES ARE INCLUDED WITHIN THE RELEVANT 'HIGH AGREEMENT' CATEGORY.

SSWF

VARIABLE	SEASON	2030, RCP2.6	2030, RCP4.5	2030, RCP8.5	2090, RCP2.6	2090, RCP4.5	2090, RCP8.5
Temperature mean (°C)	Annual	0.7 (0.5 to 0.9)	0.8 (0.5 to 0.9)	0.8 (0.5 to 1.1)	0.8 (0.5 to 1.3)	1.7 (1.2 to 2)	3.4 (2.6 to 4)
	DJF	0.8 (0.4 to 1.1)	0.8 (0.5 to 1)	0.9 (0.5 to 1.3)	1 (0.5 to 1.6)	1.8 (1.1 to 2.3)	3.5 (2.4 to 4.3)
	MAM	0.7 (0.4 to 1)	0.7 (0.4 to 1.1)	0.8 (0.4 to 1.2)	0.8 (0.4 to 1.3)	1.6 (1.1 to 2.1)	3.4 (2.5 to 4.1)
	JJA	0.6 (0.3 to 0.8)	0.7 (0.4 to 0.9)	0.7 (0.5 to 1)	0.7 (0.5 to 1.1)	1.5 (1 to 1.8)	3 (2.3 to 3.7)
	SON	0.7 (0.4 to 1)	0.8 (0.5 to 1)	0.9 (0.6 to 1.2)	0.9 (0.5 to 1.5)	1.8 (1.3 to 2.2)	3.5 (2.8 to 4.4)
Temperature maximum (°C)	Annual	0.8 (0.6 to 1.1)	0.8 (0.6 to 1.1)	0.9 (0.6 to 1.2)	1 (0.6 to 1.5)	1.8 (1.2 to 2.3)	3.8 (2.7 to 4.3)
	DJF	0.9 (0.6 to 1.3)	0.9 (0.5 to 1.2)	0.9 (0.6 to 1.3)	1.1 (0.7 to 1.8)	1.9 (1.1 to 2.5)	3.6 (2.5 to 4.4)
	MAM	0.7 (0.4 to 1)	0.8 (0.4 to 1.1)	0.8 (0.3 to 1.3)	0.9 (0.4 to 1.4)	1.6 (1 to 2.4)	3.5 (2.2 to 4.1)
	JJA	0.7 (0.4 to 1)	0.8 (0.4 to 1.1)	0.8 (0.6 to 1.2)	0.8 (0.5 to 1.3)	1.7 (1.1 to 2.1)	3.5 (2.7 to 4.2)
	SON	0.9 (0.5 to 1.2)	0.9 (0.6 to 1.2)	1 (0.7 to 1.5)	1.1 (0.6 to 1.7)	2 (1.3 to 2.6)	4 (3 to 5)
Temperature minimum (°C)	Annual	0.6 (0.4 to 0.9)	0.7 (0.4 to 0.8)	0.8 (0.4 to 1.1)	0.9 (0.4 to 1.3)	1.6 (1 to 2)	3.2 (2.5 to 3.8)
	DJF	0.8 (0.3 to 1.2)	0.7 (0.5 to 1)	0.8 (0.4 to 1.3)	0.9 (0.4 to 1.5)	1.7 (1.1 to 2.2)	3.5 (2.4 to 4.2)
	MAM	0.6 (0.3 to 1)	0.7 (0.4 to 1)	0.8 (0.4 to 1.2)	0.9 (0.4 to 1.4)	1.5 (1 to 2.2)	3.3 (2.5 to 4.1)
	JJA	0.5 (0.3 to 0.8)	0.6 (0.4 to 0.8)	0.6 (0.5 to 0.9)	0.7 (0.4 to 1.1)	1.3 (0.9 to 1.7)	2.7 (2.2 to 3.5)
	SON	0.6 (0.4 to 1)	0.7 (0.5 to 0.9)	0.8 (0.5 to 1.1)	0.8 (0.3 to 1.3)	1.6 (1 to 2)	3.2 (2.4 to 4)
Rainfall (%)	Annual	-7 (-15 to +3)	-6 (-13 to 0)	-4 (-14 to +2)	-5 (-20 to +2)	-10 (-22 to -1)	-15 (-36 to -2)
	DJF	-5 (-23 to +19)	-4 (-22 to +14)	+1 (-20 to +18)	-8 (-25 to +14)	-4 (-22 to +25)	-4 (-26 to +28)
	MAM	-7 (-19 to +7)	-3 (-18 to +9)	+0 (-22 to +12)	-2 (-21 to +10)	-3 (-22 to +10)	-2 (-33 to +14)
	JJA	-7 (-15 to +3)	-8 (-16 to +2)	-8 (-15 to +1)	-6 (-13 to +6)	-13 (-26 to -3)	-26 (-44 to -13)
	SON	-9 (-20 to +7)	-8 (-20 to +3)	-9 (-22 to +3)	-9 (-31 to -2)	-16 (-33 to +3)	-32 (-52 to -5)
Sea level pressure (hPa)	Annual	0.2 (0 to 0.5)	+0.2 (0 to +0.5)	0.3 (0 to 0.6)	+0.2 (-0.1 to +0.6)	+0.3 (0 to +0.9)	0.7 (0.2 to 1.6)
	DJF	+0.1 (-0.3 to +0.4)	+0.1 (-0.3 to +0.5)	+0.1 (-0.4 to +0.6)	+0.2 (-0.3 to +0.6)	+0.1 (-0.3 to +0.8)	+0.3 (-0.8 to +0.9)
	MAM	+0 (-0.3 to +0.5)	+0.1 (-0.2 to +0.6)	+0.2 (-0.3 to +0.7)	+0.1 (-0.4 to +0.6)	+0.2 (-0.3 to +0.8)	+0.2 (-0.4 to +1.1)
	JJA	+0.4 (-0.2 to +1.1)	+0.4 (-0.3 to +1.1)	+0.6 (-0.1 to +1.3)	+0.3 (-0.3 to +1)	+0.8 (0 to +1.9)	1.9 (0.3 to 3.2)
	SON	+0.3 (0 to +0.8)	+0.2 (-0.1 to +0.8)	+0.4 (-0.1 to +0.8)	+0.3 (-0.1 to +0.9)	+0.5 (-0.1 to +1)	0.8 (0.2 to 2.3)
Solar radiation (%)	Annual	0.7 (0 to 1.9)	+0.6 (-0.4 to +1.4)	+0.5 (-0.4 to +1.3)	+0.9 (-0.1 to +2.1)	1.1 (0.2 to 2)	+1.2 (-0.4 to +3.2)
	DJF	+0.4 (-0.6 to +2.3)	+0 (-1.3 to +1.5)	-0.2 (-1.3 to +1.2)	+0.5 (-0.4 to +2)	+0.3 (-1.7 to +1.1)	-0.3 (-2.5 to +1.2)
	MAM	+0.5 (-0.6 to +3)	+0.2 (-1.2 to +1.6)	-0.1 (-1.5 to +1.5)	+0.7 (-1.2 to +2.3)	+0.4 (-1.1 to +2.3)	-0.2 (-2.3 to +2.1)
	JJA	1.6 (0.3 to 2.9)	+1.6 (-0.1 to +3.4)	1.8 (0.4 to 4)	+1.3 (-0.3 to +4.4)	3.2 (1.5 to 5.4)	6 (2.3 to 10.2)
	SON	+0.8 (-0.1 to +2.6)	+0.9 (-0.1 to +2.3)	+1 (-0.4 to +2)	1.5 (0.1 to 2.4)	1.5 (0.3 to 3)	2.2 (0.8 to 5)

SSWF (CONTINUED)

VARIABLE	SEASON	2030, RCP2.6	2030, RCP4.5	2030, RCP8.5	2090, RCP2.6	2090, RCP4.5	2090, RCP8.5
Relative humidity (%, absolute)	Annual	-0.6 (-1.7 to +0.2)	-0.6 (-1.2 to +0.2)	-0.7 (-1.2 to +0.3)	-0.7 (-1.3 to +0)	-1 (-2.1 to -0.1)	-2 (-3.5 to -1)
	DJF	-0.5 (-1.9 to +0.4)	-0.5 (-1.6 to +0.6)	-0.4 (-1.8 to +0.5)	-0.9 (-1.7 to -0.1)	-0.7 (-1.8 to +0.9)	-0.9 (-2.7 to +0.8)
	MAM	-0.4 (-1.6 to +0.7)	-0.4 (-1.6 to +0.8)	-0.2 (-2 to +1.5)	-0.3 (-2.2 to +0.7)	-0.6 (-2 to +0.8)	-0.9 (-3 to +0.9)
	JJA	-0.6 (-2.1 to +0.3)	-0.5 (-2 to +0.3)	-0.8 (-1.9 to +0.5)	-0.6 (-1.8 to +0.5)	-1.5 (-3.3 to -0.2)	-2.9 (-5.4 to -1.6)
	SON	-0.5 (-2.1 to +0.5)	-0.7 (-2.1 to 0)	-0.9 (-2 to +0.3)	-1 (-2 to +0.3)	-1.5 (-3.1 to -0.5)	-3.4 (-4.8 to -1.9)
Evapo-transpiration (%)	Annual	2.6 (1.7 to 4.1)	2.3 (1.5 to 3.6)	2.9 (1.6 to 4.3)	3 (2 to 4.9)	5.3 (3.4 to 7.1)	10.6 (7 to 15.2)
	DJF	2.1 (1.4 to 3.3)	1.8 (0.9 to 3)	2.2 (1.2 to 3.4)	2.6 (1.5 to 4.9)	4.3 (2.8 to 5.8)	9.1 (5.1 to 12)
	MAM	3.6 (1.7 to 5.6)	3.2 (1.1 to 4.3)	3.3 (2.4 to 5.5)	3.9 (2.6 to 5.7)	6.1 (4.8 to 9.3)	13.9 (8.9 to 18.5)
	JJA	4.5 (2.2 to 6.9)	4.3 (1.9 to 7.4)	4.7 (2.8 to 7.8)	4.6 (3.4 to 6.7)	10.1 (6.5 to 13.8)	18.5 (12.6 to 29.9)
	SON	2.3 (0.8 to 4.5)	2.4 (0.5 to 3.6)	2.5 (0.7 to 4.7)	2.8 (0.2 to 5.1)	4.9 (1.9 to 7.2)	9.2 (4.5 to 14.5)
Soil moisture (Budyko) (%)	Annual	NA	-20.6 (-29.8 to -1)	-15.6 (-65.8 to -2.4)	NA	-39 (-53.1 to -12.9)	-5.6 (-10.9 to -2.9)
	DJF	NA	-0.3 (-1.1 to +0.1)	+0 (-1 to +0.2)	NA	-0.1 (-0.6 to +0.4)	-0.3 (-0.7 to +0.6)
	MAM	NA	-0.8 (-2.5 to +0)	-0.8 (-1.4 to +0.5)	NA	-1.3 (-3.4 to +1.5)	-1.8 (-4.3 to 0)
	JJA	NA	-3.5 (-7.5 to -0.3)	-3.8 (-6.8 to -1.2)	NA	-6.4 (-9.3 to +0.6)	-11.1 (-17.6 to -6.2)
	SON	NA	-2.5 (-5.9 to -0.8)	-2.8 (-4 to -1.4)	NA	-3.6 (-6.2 to -1.6)	-6.2 (-16.7 to -3.8)
Wind speed (%)	Annual	-0.2 (-1.5 to +1.8)	-0.4 (-1.8 to +1.1)	-0.1 (-2 to +1.4)	+0.3 (-2 to +1.3)	-0.8 (-2.8 to +0.9)	-0.3 (-3 to +1.8)
	DJF	+0.6 (-1.9 to +2.5)	+0 (-1.5 to +1.3)	+0.3 (-1.7 to +2.7)	-0.3 (-1.8 to +2.1)	-0.2 (-1.7 to +1.9)	+2.1 (-0.6 to +6.2)
	MAM	+0.2 (-1.2 to +1.6)	-0.3 (-1.7 to +1.3)	+0.4 (-3.1 to +2)	+0.4 (-0.8 to +2.3)	-0.5 (-2.4 to +1.6)	0 (-2.7 to +1.8)
	JJA	-0.9 (-3.1 to +2.6)	-0.5 (-5.3 to +2.3)	-1.2 (-4.2 to +1.6)	+0.3 (-4 to +3.1)	-2.1 (-6.9 to +2)	-4.7 (-8.9 to -0.3)
	SON	+0.3 (-1.3 to +1.7)	+0 (-2.2 to +1.4)	-0.5 (-2.6 to +1.9)	+0.1 (-2.1 to +1.7)	-0.8 (-3.3 to +1.8)	+1 (-3.3 to +3.9)

SSWF WEST

VARIABLE	SEASON	2030, RCP2.6	2030, RCP4.5	2030, RCP8.5	2090, RCP2.6	2090, RCP4.5	2090, RCP8.5
Temperature mean (°C)	Annual	0.7 (0.5 to 1)	0.8 (0.6 to 1)	0.8 (0.5 to 1.2)	0.8 (0.5 to 1.4)	1.7 (1.1 to 2.1)	3.5 (2.6 to 4.2)
	DJF	0.8 (0.5 to 1.1)	0.9 (0.5 to 1.1)	0.9 (0.5 to 1.3)	0.9 (0.5 to 1.5)	1.8 (1.1 to 2.4)	3.7 (2.5 to 4.5)
	MAM	0.7 (0.4 to 1.1)	0.7 (0.4 to 1.2)	0.8 (0.4 to 1.2)	0.8 (0.3 to 1.4)	1.7 (1 to 2.2)	3.4 (2.4 to 4.2)
	JJA	0.6 (0.3 to 0.9)	0.7 (0.4 to 0.9)	0.7 (0.5 to 0.9)	0.7 (0.4 to 1.2)	1.5 (1 to 1.8)	3.1 (2.3 to 3.8)
	SON	0.8 (0.5 to 1)	0.8 (0.5 to 1.1)	0.9 (0.6 to 1.4)	0.9 (0.5 to 1.5)	1.8 (1.2 to 2.4)	3.5 (2.9 to 4.6)
Temperature maximum (°C)	Annual	0.8 (0.5 to 1.1)	0.9 (0.6 to 1.1)	0.9 (0.6 to 1.2)	1 (0.6 to 1.6)	1.8 (1.3 to 2.4)	3.8 (2.7 to 4.5)
	DJF	0.9 (0.6 to 1.1)	1 (0.5 to 1.3)	0.9 (0.6 to 1.3)	1.1 (0.7 to 1.7)	1.9 (1.1 to 2.6)	3.8 (2.5 to 4.6)
	MAM	0.7 (0.4 to 1.1)	0.7 (0.3 to 1.3)	0.8 (0.4 to 1.3)	0.9 (0.3 to 1.7)	1.7 (1 to 2.5)	3.6 (2.2 to 4.4)
	JJA	0.7 (0.3 to 1.1)	0.8 (0.4 to 1.2)	0.8 (0.5 to 1.3)	0.8 (0.4 to 1.4)	1.8 (1.2 to 2.1)	3.6 (2.7 to 4.2)
	SON	0.9 (0.5 to 1.2)	0.9 (0.6 to 1.4)	1 (0.6 to 1.6)	1.1 (0.6 to 1.7)	2 (1.4 to 2.7)	4 (3.1 to 5.1)
Temperature minimum (°C)	Annual	0.6 (0.4 to 1)	0.7 (0.4 to 0.9)	0.8 (0.4 to 1.1)	0.9 (0.4 to 1.3)	1.6 (1 to 2)	3.2 (2.5 to 4)
	DJF	0.8 (0.4 to 1.2)	0.8 (0.5 to 1)	0.8 (0.4 to 1.3)	0.9 (0.5 to 1.5)	1.8 (1.1 to 2.3)	3.6 (2.6 to 4.4)
	MAM	0.6 (0.3 to 1.1)	0.7 (0.3 to 1.2)	0.8 (0.4 to 1.2)	0.9 (0.3 to 1.5)	1.6 (1 to 2.3)	3.3 (2.5 to 4.3)
	JJA	0.5 (0.2 to 0.8)	0.6 (0.3 to 0.8)	0.6 (0.4 to 1)	0.7 (0.3 to 1.1)	1.3 (0.9 to 1.7)	2.7 (2.2 to 3.6)
	SON	0.6 (0.4 to 1)	0.7 (0.4 to 0.9)	0.8 (0.4 to 1.2)	0.8 (0.4 to 1.3)	1.6 (1 to 2.2)	3.2 (2.5 to 4.1)

SSWF WEST (CONTINUED)

VARIABLE	SEASON	2030, RCP2.6	2030, RCP4.5	2030, RCP8.5	2090, RCP2.6	2090, RCP4.5	2090, RCP8.5
Rainfall (%)	Annual	-7 (-17 to 3)	-6 (-15 to -1)	-5 (-15 to 1)	-6 (-20 to 3)	-12 (-22 to -1)	-18 (-37 to -5)
	DJF	-4 (-29 to 36)	-8 (-31 to 17)	2 (-23 to 20)	-7 (-31 to 26)	-4 (-29 to 28)	-5 (-31 to 36)
	MAM	-4 (-21 to 6)	-4 (-20 to 10)	1 (-20 to 17)	-2 (-29 to 10)	-4 (-26 to 12)	-6 (-32 to 13)
	JJA	-7 (-14 to 3)	-7 (-18 to 4)	-9 (-18 to 2)	-7 (-15 to 8)	-14 (-28 to -4)	-29 (-44 to -15)
	SON	-14 (-25 to 5)	-11 (-23 to 4)	-11 (-28 to 4)	-14 (-34 to 1)	-19 (-36 to 1)	-36 (-59 to -14)
Sea level pressure (hPa)	Annual	0.2 (0 to 0.5)	0.2 (-0.1 to 0.5)	0.3 (0 to 0.6)	0.2 (-0.1 to 0.6)	0.3 (0 to 0.8)	0.6 (0.1 to 1.4)
	DJF	0.1 (-0.3 to 0.4)	0.1 (-0.3 to 0.5)	0.1 (-0.4 to 0.5)	0.1 (-0.3 to 0.6)	0 (-0.3 to 0.8)	0.3 (-0.7 to 0.9)
	MAM	0.1 (-0.3 to 0.6)	0.1 (-0.2 to 0.6)	0.2 (-0.2 to 0.7)	0.1 (-0.3 to 0.7)	0.2 (-0.3 to 0.8)	0.2 (-0.4 to 1)
	JJA	0.3 (-0.2 to 1)	0.4 (-0.3 to 1.1)	0.6 (-0.1 to 1.2)	0.3 (-0.3 to 0.9)	0.7 (0 to 1.8)	1.9 (0.3 to 3.1)
	SON	0.3 (-0.1 to 0.7)	0.1 (-0.2 to 0.7)	0.3 (-0.2 to 0.7)	0.3 (-0.1 to 0.8)	0.3 (-0.2 to 0.9)	0.6 (0.2 to 2)
Solar radiation (%)	Annual	0.8 (-0.1 to 2.1)	0.6 (-0.4 to 1.6)	0.4 (-0.6 to 1.6)	0.8 (-0.1 to 2.2)	1 (0 to 2.1)	1 (-0.6 to 3)
	DJF	0.2 (-1 to 2.5)	0.1 (-1.8 to 1.7)	-0.4 (-1.6 to 1.5)	0.4 (-0.5 to 2.2)	0.2 (-1.9 to 1.4)	-0.5 (-3 to 0.8)
	MAM	0.6 (-0.8 to 3.3)	0.2 (-1.5 to 2)	0.1 (-2.1 to 1.4)	0.6 (-1.7 to 2.6)	0.6 (-1.4 to 2.4)	-0.5 (-2.6 to 1.9)
	JJA	1.6 (0.2 to 3.2)	1.6 (-0.2 to 3.7)	1.5 (0.5 to 4.1)	1.3 (-0.5 to 4.5)	3.1 (1.3 to 6.1)	6.2 (2.5 to 11.4)
	SON	1 (-0.2 to 2.7)	0.8 (-0.2 to 2.1)	0.9 (-0.3 to 1.9)	1.3 (0.1 to 2.3)	1.5 (0.3 to 2.9)	2.2 (0.5 to 5.1)
Relative humidity (%, absolute)	Annual	-0.5 (-1.8 to 0.2)	-0.6 (-1.5 to 0.1)	-0.6 (-1.4 to 0.5)	-0.8 (-1.5 to 0.1)	-1.2 (-2.3 to 0)	-2.2 (-3.8 to -1)
	DJF	-0.5 (-2 to 1)	-0.6 (-2.3 to 0.3)	-0.5 (-1.9 to 0.8)	-0.8 (-2.1 to -0.1)	-0.7 (-2.2 to 1.1)	-1.1 (-2.9 to 0.5)
	MAM	-0.4 (-2.1 to 0.9)	-0.3 (-2.1 to 1)	-0.2 (-2.2 to 1.9)	-0.2 (-2.6 to 1)	-0.7 (-2.2 to 1)	-1.2 (-3.1 to 1)
	JJA	-0.7 (-2.5 to 0.2)	-0.6 (-2.1 to 0.5)	-0.9 (-1.9 to 0.4)	-0.6 (-1.7 to 0.6)	-1.7 (-3.4 to -0.2)	-3.4 (-6 to -1.4)
	SON	-0.7 (-2.1 to 0.1)	-0.8 (-2.3 to 0.1)	-0.9 (-2.1 to 0.3)	-1.1 (-1.9 to 0.3)	-1.7 (-3.1 to -0.4)	-3.5 (-5.4 to -1.9)
Evapo-transpiration (%)	Annual	2.6 (1.7 to 4)	2.5 (1.2 to 3.5)	2.8 (1.5 to 4.3)	2.9 (2 to 4.9)	5.4 (3.4 to 7.2)	10.3 (7.1 to 15.2)
	DJF	1.9 (1.1 to 3.4)	1.5 (0.5 to 3.1)	2.3 (0.7 to 3.6)	2.5 (1.5 to 5.1)	4.2 (2.5 to 5.9)	9.1 (5.1 to 11.7)
	MAM	3.6 (1.8 to 5.4)	3.2 (1.3 to 4.5)	3.3 (2.2 to 6.1)	3.7 (2.1 to 6.2)	6.8 (4.9 to 9.6)	13.7 (8.4 to 18.3)
	JJA	4.6 (1.8 to 6.8)	4.3 (1.3 to 7.3)	4.4 (2.5 to 7.7)	4.4 (3 to 6.3)	9.8 (6.2 to 14.3)	18.6 (12.4 to 30.5)
	SON	2.3 (0.7 to 4.3)	2.4 (0.4 to 3.3)	2.4 (0.5 to 4.5)	2.9 (0.3 to 4.9)	4.9 (2 to 7.1)	9.2 (4.8 to 14.8)
Soil moisture (Budyko) (%)	Annual	NA	-1.5 (-4.1 to -0.7)	-2 (-3.6 to -0.9)	NA	-3.1 (-6 to -0.3)	-5.9 (-12.4 to -3)
	DJF	NA	-0.3 (-1.3 to 0.1)	0.1 (-1.1 to 0.5)	NA	0 (-0.6 to 0.5)	-0.2 (-0.7 to 0.8)
	MAM	NA	-1.3 (-2.9 to 0.1)	-0.6 (-1.9 to 0.7)	NA	-1.3 (-4 to 1)	-2.2 (-4.4 to -0.2)
	JJA	NA	-3.1 (-7.8 to 0)	-4.2 (-7.4 to -1.4)	NA	-6.1 (-9.7 to 0.2)	-11.4 (-20.7 to -6.4)
	SON	NA	-2.6 (-5.6 to -0.7)	-2.9 (-4.8 to -1.1)	NA	-3.8 (-7.5 to -1.9)	-6.7 (-17.8 to -2.8)
Wind speed (%)	Annual	-0.1 (-1.5 to 2.1)	-0.1 (-1.7 to 1.1)	0 (-2 to 1.9)	0.2 (-2.1 to 1.1)	-0.3 (-2.6 to 1.4)	0.3 (-2.7 to 3.3)
	DJF	0.5 (-1.9 to 2.8)	0.3 (-1.8 to 1.8)	0.6 (-1.3 to 3.6)	-0.5 (-2.1 to 2.1)	-0.2 (-2 to 2.3)	2.3 (-0.5 to 6.8)
	MAM	0.3 (-1.3 to 1.6)	0 (-1.6 to 1.7)	1 (-2.2 to 2.2)	0.1 (-1 to 2)	0.2 (-1.9 to 1.9)	1.2 (-1 to 3.2)
	JJA	-1 (-3.4 to 2.2)	-1 (-4.9 to 1.9)	-1.5 (-4.2 to 1.4)	-0.1 (-4.1 to 3.6)	-1.8 (-8 to 2.1)	-4.2 (-9.3 to -0.3)
	SON	0.2 (-1.1 to 2)	0.1 (-1.7 to 1.6)	0 (-2.1 to 2.6)	0.1 (-1.9 to 1.4)	-0.4 (-3.5 to 2.4)	1.5 (-2.6 to 5.1)

SSWF EAST

VARIABLE	SEASON	2030, RCP2.6	2030, RCP4.5	2030, RCP8.5	2090, RCP2.6	2090, RCP4.5	2090, RCP8.5
Temperature mean (°C)	Annual	0.7 (0.4 to 0.9)	0.7 (0.5 to 0.9)	0.8 (0.5 to 1.1)	0.9 (0.5 to 1.2)	1.5 (1 to 1.9)	2.9 (2.4 to 3.9)
	DJF	0.7 (0.2 to 1)	0.7 (0.3 to 1.1)	0.9 (0.4 to 1.3)	0.9 (0.5 to 1.4)	1.6 (1 to 2.2)	3.1 (2.1 to 4.2)
	MAM	0.7 (0.3 to 1)	0.6 (0.3 to 1.1)	0.7 (0.4 to 1.2)	0.9 (0.5 to 1.3)	1.4 (1 to 1.9)	3 (2.4 to 3.8)
	JJA	0.6 (0.4 to 0.8)	0.6 (0.3 to 0.9)	0.7 (0.5 to 1)	0.7 (0.5 to 1.2)	1.4 (0.9 to 1.8)	2.9 (2.4 to 3.6)
	SON	0.7 (0.4 to 1)	0.7 (0.4 to 1)	0.8 (0.5 to 1.1)	0.8 (0.4 to 1.4)	1.6 (1.1 to 2.1)	3.2 (2.5 to 4)
Temperature maximum (°C)	Annual	0.8 (0.5 to 1.1)	0.7 (0.5 to 1)	0.8 (0.6 to 1.2)	1 (0.6 to 1.4)	1.6 (1.1 to 2.2)	3.3 (2.6 to 4.1)
	DJF	0.8 (0.4 to 1.5)	0.7 (0.4 to 1.3)	0.9 (0.6 to 1.3)	0.9 (0.6 to 1.8)	1.7 (1 to 2.4)	3.3 (2.4 to 4.4)
	MAM	0.7 (0.5 to 1.1)	0.7 (0.3 to 1.1)	0.7 (0.4 to 1.3)	0.9 (0.5 to 1.3)	1.5 (1 to 2.1)	3.1 (2.3 to 3.9)
	JJA	0.7 (0.5 to 1)	0.7 (0.4 to 1)	0.8 (0.6 to 1.2)	0.8 (0.5 to 1.2)	1.5 (1.1 to 2.1)	3.2 (2.6 to 4.1)
	SON	0.8 (0.5 to 1.2)	0.9 (0.5 to 1.1)	0.9 (0.6 to 1.3)	1.1 (0.4 to 1.8)	1.9 (1.2 to 2.4)	3.9 (2.7 to 4.6)
Temperature minimum (°C)	Annual	0.6 (0.3 to 0.9)	0.6 (0.5 to 0.8)	0.7 (0.5 to 1.1)	0.8 (0.5 to 1.2)	1.4 (1 to 1.9)	2.9 (2.3 to 3.7)
	DJF	0.7 (0.2 to 1.2)	0.7 (0.3 to 1.1)	0.8 (0.5 to 1.3)	1 (0.4 to 1.5)	1.4 (0.9 to 2.1)	3.1 (2.2 to 4.2)
	MAM	0.7 (0.4 to 0.9)	0.6 (0.4 to 0.9)	0.7 (0.3 to 1.1)	0.8 (0.4 to 1.2)	1.4 (1 to 1.9)	3 (2.4 to 3.8)
	JJA	0.5 (0.3 to 0.8)	0.6 (0.3 to 0.8)	0.6 (0.5 to 0.9)	0.7 (0.4 to 1.2)	1.3 (0.8 to 1.7)	2.6 (2.3 to 3.3)
	SON	0.6 (0.3 to 1)	0.6 (0.4 to 0.9)	0.8 (0.4 to 1)	0.7 (0.3 to 1.2)	1.5 (1 to 1.9)	3 (2.4 to 3.7)
Rainfall (%)	Annual	-4 (-12 to 5)	-4 (-13 to 4)	-2 (-13 to 5)	-4 (-16 to 5)	-7 (-18 to 3)	-9 (-37 to 6)
	DJF	-7 (-23 to 19)	0 (-24 to 30)	2 (-14 to 19)	-6 (-25 to 22)	-3 (-20 to 13)	-3 (-26 to 22)
	MAM	-2 (-18 to 13)	-1 (-22 to 18)	-3 (-22 to 23)	-4 (-26 to 22)	-2 (-26 to 17)	2 (-33 to 33)
	JJA	-3 (-17 to 7)	-6 (-16 to 6)	-5 (-16 to 5)	-3 (-13 to 6)	-9 (-24 to 2)	-19 (-43 to -3)
	SON	-4 (-20 to 13)	-5 (-20 to 10)	-7 (-23 to 10)	-7 (-28 to 10)	-14 (-26 to 3)	-19 (-50 to 9)
Sea level pressure (hPa)	Annual	0.3 (-0.1 to 0.6)	0.3 (0 to 0.6)	0.4 (0 to 0.8)	0.2 (-0.1 to 0.8)	0.4 (-0.1 to 1.1)	0.8 (0.2 to 2)
	DJF	0.2 (-0.2 to 0.5)	0.1 (-0.2 to 0.6)	0.1 (-0.4 to 0.7)	0.2 (-0.3 to 0.7)	0.2 (-0.5 to 0.8)	0.3 (-0.7 to 1.2)
	MAM	0.1 (-0.4 to 0.5)	0.1 (-0.4 to 0.7)	0.2 (-0.4 to 0.7)	0 (-0.5 to 0.7)	0.2 (-0.4 to 0.9)	0.2 (-0.6 to 1.3)
	JJA	0.4 (-0.3 to 1.5)	0.5 (-0.3 to 1.4)	0.6 (-0.2 to 1.6)	0.2 (-0.6 to 1.3)	0.8 (-0.2 to 2.3)	1.9 (0.1 to 3.8)
	SON	0.5 (-0.1 to 1.1)	0.3 (-0.1 to 1.1)	0.7 (0.1 to 1.1)	0.5 (-0.1 to 1.1)	0.7 (-0.1 to 1.4)	1.2 (0.3 to 3)
Solar radiation (%)	Annual	1.1 (0.2 to 1.9)	0.6 (-0.4 to 1.4)	0.5 (-0.5 to 1.4)	1.1 (0 to 2.3)	1.1 (-0.1 to 2.3)	1.5 (-0.1 to 3.6)
	DJF	1.2 (-0.5 to 2.4)	0.4 (-1.1 to 1.8)	0.2 (-1 to 1.3)	0.9 (-0.3 to 2)	0.4 (-1.1 to 1.5)	0.2 (-1.6 to 1.5)
	MAM	0.7 (-0.8 to 2.7)	0 (-1.6 to 2.3)	0.2 (-1.6 to 1.8)	0.9 (-2.2 to 3.7)	0.4 (-1.5 to 2.7)	0.1 (-2.6 to 4)
	JJA	1.6 (0.2 to 3.6)	1.5 (-0.5 to 3.7)	1.8 (0 to 3.9)	2 (0 to 4.2)	2.9 (0.5 to 5.5)	5.1 (1.4 to 9.1)
	SON	0.8 (-0.4 to 2.5)	0.9 (-0.3 to 2.4)	0.8 (-0.7 to 2.3)	1 (0.2 to 3.2)	1.7 (-0.4 to 3.3)	2.8 (0.2 to 5)
Relative humidity (%, absolute)	Annual	-0.4 (-1.8 to 0.2)	-0.3 (-1 to 0.4)	-0.5 (-1.1 to 0.3)	-0.7 (-1.9 to 0.2)	-0.8 (-2 to -0.1)	-1.6 (-3.2 to -0.3)
	DJF	-0.6 (-2.2 to 0.4)	0 (-1.6 to 1.3)	-0.4 (-1.8 to 1)	-0.6 (-1.9 to 0.4)	-0.3 (-1.4 to 0.8)	-0.5 (-2.9 to 0.9)
	MAM	-0.2 (-2.1 to 0.7)	0.2 (-1.6 to 1)	-0.4 (-1.3 to 1.5)	-0.6 (-2.9 to 1.2)	-0.4 (-1.7 to 1.1)	-0.3 (-2.9 to 1.2)
	JJA	-0.5 (-2 to 0.5)	-0.3 (-2.2 to 0.7)	-0.6 (-2.1 to 0.2)	-0.9 (-2 to 0.5)	-0.9 (-2.7 to 0)	-2.3 (-5 to -0.6)
	SON	-0.4 (-2.9 to 0.6)	-0.7 (-1.9 to 0.6)	-0.9 (-1.9 to 0.5)	-0.8 (-2.7 to 0.7)	-1.5 (-3.2 to -0.3)	-2.8 (-4.9 to -0.5)
Evapo-transpiration (%)	Annual	2.7 (1.6 to 4.3)	2.5 (1.4 to 3.5)	3 (2.1 to 4.5)	2.8 (2.1 to 4.8)	5.1 (3.4 to 7.3)	10.2 (7.4 to 15.7)
	DJF	2.6 (1.4 to 3.3)	2.6 (0.6 to 3.5)	2.4 (1.8 to 4.1)	2.6 (1.4 to 4.3)	4.5 (3.2 to 6.6)	8.9 (5.6 to 13)
	MAM	3.4 (2.3 to 6.1)	2.4 (0.5 to 5.6)	3.5 (1.9 to 5.9)	4.4 (2.3 to 6)	6.2 (4.2 to 9.7)	13.4 (9.4 to 19.7)
	JJA	4.4 (2.7 to 7.3)	4.5 (1.3 to 8.8)	5 (3.7 to 9.5)	5.7 (3.8 to 7.8)	10.7 (6.4 to 14.6)	19.1 (13.7 to 29.6)
	SON	2.5 (0.3 to 5.2)	2.2 (0.9 to 4.2)	2.3 (1 to 4.9)	2.9 (0.5 to 6.6)	4.8 (1.5 to 7.6)	9.8 (4.7 to 14.1)

SSWF EAST (CONTINUED)

VARIABLE	SEASON	2030, RCP2.6	2030, RCP4.5	2030, RCP8.5	2090, RCP2.6	2090, RCP4.5	2090, RCP8.5
Soil moisture (Budyko) (%)	**Annual**	**NA**	**-1.7 (-4.6 to 0.2)**	**-1.3 (-4.7 to 0)**	**NA**	**-1.8 (-5.6 to 1)**	**-4.4 (-8.7 to -0.9)**
	DJF	NA	-0.1 (-0.5 to 0.3)	-0.2 (-0.6 to 0.1)	NA	-0.1 (-0.5 to 0.1)	-0.2 (-1 to 0.1)
	MAM	NA	-0.7 (-3.2 to 1.3)	-0.3 (-2.1 to 1.4)	NA	-0.9 (-3.2 to 2)	-1.3 (-4.4 to 0.5)
	JJA	NA	-2.8 (-8 to 1.8)	-2.1 (-8.8 to 1)	NA	-3 (-10.3 to 1.9)	-8.1 (-16.2 to -0.8)
	SON	NA	-2.5 (-5.6 to -0.4)	-2.2 (-5.4 to -0.5)	NA	-2.6 (-7.8 to -0.3)	-5.3 (-13 to -2.7)
Wind speed (%)	**Annual**	**-0.3 (-1.8 to 1.4)**	**-0.9 (-2.3 to 1.1)**	**-0.5 (-3.1 to 0.7)**	**0.1 (-1.7 to 1.8)**	**-1.4 (-3.8 to 0.1)**	**-1.8 (-4.4 to 0)**
	DJF	-0.3 (-2.5 to 2.1)	-0.7 (-1.8 to 1)	0 (-2.2 to 1.6)	0.4 (-1.6 to 2.6)	-0.8 (-2.8 to 0.7)	1.6 (-2.9 to 4.2)
	MAM	0.1 (-3.2 to 1.9)	-0.9 (-3.2 to 1)	-0.9 (-4.4 to 2.5)	0.4 (-2.2 to 2.7)	-2.1 (-3.9 to 1.5)	-2.5 (-5.1 to -0.1)
	JJA	-0.9 (-4 to 2.9)	-0.4 (-6.2 to 3.5)	-0.7 (-4.4 to 2.7)	0.6 (-3.7 to 4.2)	-1.5 (-6.7 to 1.9)	-5.4 (-9.9 to 1)
	SON	-0.2 (-2.9 to 2.2)	-0.9 (-3.4 to 1.7)	-0.6 (-4.3 to 1.6)	0.3 (-3.1 to 2.3)	-1.4 (-4.6 to 1.6)	-1 (-5.8 to 2.3)

LEGEND TO TABLE 1

	Very high model agreement on substantial increase
	High model agreement on substantial increase
	Medium model agreement on substantial increase
	High model agreement on increase
	Medium model agreement on increase
	High model agreement on little change
	Medium model agreement on little change
	High model agreement on substantial decrease
	Medium model agreement on substantial decrease
	High model agreement on decrease
	Medium model agreement on decrease

TABLE 2: ANNUAL VALUES OF MAXIMUM TEMPERATURE (T; °C), RAINFALL (R; MM), DROUGHT FACTOR (DF; NO UNITS), THE NUMBER OF SEVERE FIRE DANGER DAYS (SEV: FFDI GREATER THAN 50 DAYS PER YEAR) AND CUMULATIVE FFDI (ΣFFDI; NO UNITS) FOR THE 1995 BASELINE AND PROJECTIONS FOR 2030 AND 2090 UNDER RCP4.5 AND RCP8.5. VALUES WERE CALCULATED FROM THREE CLIMATE MODELS AND FOR SIX STATIONS.

STATION	VARIABLE	1995 BASELINE	2030, RCP4.5			2030, RCP8.5			2090, RCP4.5			2090, RCP8.5		
			CESM	GFDL	MIROC	CESM	GFDL	MIROC	CESM	GFDL	MIROC	CESM	GFDL	MIROC
Adelaide (SSWFE)	T	22.1	23.2	23.3	23.2	23.4	23.1	23.0	24.7	23.7	23.7	26.4	25.4	24.6
	R	544	511	309	537	516	400	549	479	409	547.3	434	267	594
	DF	6.5	6.8	7.9	6.6	6.7	7.1	6.6	7.1	7.2	6.6	7.5	8.9	6.6
	SEV	1.7	2.3	3.5	1.9	2.1	2.3	1.9	2.9	2.6	2.2	4.3	5.4	2.3
	ΣFFDI	2942	3089	3885	3033	3067	3334	2985	3395	3373	3126	3835	4464	3085
Ceduna (SSWFE)	T	23.5	24.5	24.6	24.5	24.7	24.5	24.3	26.1	25.1	25.0	27.8	26.7	26.0
	R	292	253	147	265	261	202	270	238	204	269	215	135	294
	DF	8.7	8.9	9.6	8.7	8.8	9.2	8.6	9.0	9.2	8.7	9.2	9.7	8.6
	SEV	11.1	11.1	14.0	11.9	11.6	13.0	11.4	13.0	13.1	12.4	14.6	15.6	12.1
	ΣFFDI	4848	4932	5963	4925	4986	5452	4827	5370	5441	5042	5917	6453	4938
Perth AP (SSWFW)	T	24.6	25.8	25.9	25.8	25.9	25.6	25.7	27.4	26.2	26.4	29.2	28.0	27.9
	R	784	721	510	693	701	558	688	657	471	705	569	341	590
	DF	6.5	6.5	7.0	6.6	6.5	6.8	6.6	6.7	7.1	6.5	7.1	8.0	6.9
	SEV	2.5	2.6	3.8	2.9	3.0	2.9	2.9	4.3	2.9	3.4	6.8	6.3	4.7
	ΣFFDI	3647	3667	4458	3782	3836	4013	3776	4188	4107	3878	4664	5214	4246
Esperance (SSWFW)	T	21.7	22.9	23.0	22.9	23.0	22.6	22.8	24.5	23.3	23.5	26.3	25.1	25.0
	R	623	616	410	574	592	462	581	551	401	591	498	282	503
	DF	6.3	6.3	7.2	6.4	6.3	6.8	6.5	6.8	7.3	6.4	7.3	8.7	7.0
	SEV	1.4	1.6	2.3	1.7	1.8	1.8	1.8	2.3	2.1	1.9	2.9	3.7	2.3
	ΣFFDI	2087	2106	2847	2188	2232	2454	2183	2515	2603	2253	2932	3650	2568
Albany AP (SSWFW)	T	20.1	21.2	21.3	21.2	21.4	21.0	21.2	22.9	21.7	21.9	24.7	23.5	23.3
	R	795	787	517	742	765	591	738	702	507	762	631	355	646
	DF	5.6	5.6	6.4	5.7	5.7	6.0	5.8	6.0	6.3	5.7	6.5	7.7	6.1
	SEV	0.3	0.3	0.5	0.3	0.4	0.3	0.3	0.5	0.3	0.4	0.5	0.7	0.4
	ΣFFDI	1463	1474	2046	1540	1579	1705	1533	1774	1764	1585	2027	2552	1788
Geraldton (SSWFW)	T	25.9	27.0	27.1	27.0	27.2	26.8	27.0	28.7	27.5	27.7	30.5	29.3	29.2
	R	452	413	291	399	403	321	394	378	274	410	330	199	345
	DF	7.4	7.4	8.2	7.5	7.4	8.0	7.5	7.8	8.5	7.5	8.3	9.2	8.1
	SEV	8.1	8.3	12.2	8.8	9.0	9.0	8.5	11.1	10.1	9.1	13.7	15.6	11.5
	ΣFFDI	4276	4321	5421	4446	4547	4867	4434	4972	5061	4565	5636	6319	5061

TABLE 3: PROJECTED ANNUAL CHANGE IN SIMULATED MARINE CLIMATE VARIABLES FOR 2020–2039 (2030) AND 2080–2099 (2090) PERIODS RELATIVE TO 1986–2005 PERIOD FOR SSWF, WHERE SEA ALLOWANCE IS THE MINIMUM DISTANCE REQUIRED TO RAISE AN ASSET TO MAINTAIN CURRENT FREQUENCY OF BREACHES UNDER PROJECTED SEA LEVEL RISE. FOR SEA LEVEL RISE, THE RANGE WITHIN THE BRACKETS REPRESENTS THE 5TH AND 95TH PERCENTILE CHANGE, AS PROJECTED BY THE CMIP5 MODEL ARCHIVE WHEREAS FOR SEA SURFACE TEMPERATURE, SALINITY, OCEAN PH AND ARAGONITE CONCENTRATION THE RANGE REPRESENTS THE 10TH TO 90TH PERCENTILE RANGE. ANNUAL RESULTS ARE GIVEN FOR RCP2.6, RCP4.5, AND RCP8.5. NOTE THAT THE RANGES OF SEA LEVEL RISE SHOULD BE CONSIDERED *LIKELY* (AT LEAST 66 % PROBABILITY), AND THAT IF A COLLAPSE IN THE MARINE BASED SECTORS OF THE ANTARCTIC ICE SHEET WERE INITIATED, THESE PROJECTIONS COULD BE SEVERAL TENTHS OF A METRE HIGHER BY LATE IN THE CENTURY.

VARIABLE	LOCATION (°E, °S)	2030, RCP2.6	2030, RCP4.5	2030, RCP8.5	2090, RCP2.6	2090, RCP4.5	2090, RCP8.5
Sea level rise (m)	Fremantle (115.75, -32.07)	0.12 (0.07-0.16)	0.12 (0.07-0.16)	0.12 (0.08-0.17)	0.39 (0.22-0.56)	0.46 (0.28-0.65)	0.61 (0.39-0.84)
	Esperance (121.90, -33.87)	0.12 (0.07-0.17)	0.12 (0.08-0.17)	0.13 (0.08-0.18)	0.40 (0.24-0.56)	0.47 (0.30-0.65)	0.62 (0.42-0.85)
	Thevenard (133.64, -32.15)	0.11 (0.07-0.16)	0.12 (0.07-0.16)	0.12 (0.08-0.17)	0.38 (0.22-0.54)	0.45 (0.28-0.63)	0.59 (0.39-0.82)
	Port Adelaide (138.48, -34.78)	0.12 (0.07-0.16)	0.12 (0.08-0.16)	0.13 (0.08-0.17)	0.38 (0.23-0.55)	0.45 (0.28-0.63)	0.60 (0.39-0.83)
Sea allowance (m)	Fremantle (115.75, -32.07)	0.12	0.12	0.13	0.47	0.56	0.76
	Esperance (121.90, -33.87)	0.13	0.13	0.13	0.47	0.56	0.76
	Thevenard (133.64, -32.15)	0.11	0.11	0.12	0.42	0.49	0.66
	Port Adelaide (138.48, -34.78)	0.12	0.12	0.12	0.41	0.48	0.66
Sea surface temperature (°C)	Fremantle (115.75, -32.07)	0.5 (0.3 to 0.8)	0.6 (0.4 to 0.7)	0.6 (0.4 to 0.9)	0.8 (0.3 to 1.1)	1.2 (0.7 to 1.7)	2.6 (1.8 to 3.3)
	Esperance (121.90, -33.87)	0.5 (0.3 to 0.8)	0.6 (0.3 to 0.8)	0.6 (0.3 to 1.0)	0.7 (0.4 to 1.1)	1.3 (0.8 to 1.8)	2.4 (1.6 to 3.9)
	Thevenard (133.64, -32.15)	0.5 (0.3 to 0.7)	0.5 (0.3 to 0.7)	0.6 (0.3 to 0.9)	0.6 (0.5 to 1.0)	1.2 (0.9 to 1.8)	2.2 (1.7 to 3.4)
	Port Adelaide (138.48, -34.78)	0.5 (0.3 to 0.8)	0.5 (0.3 to 0.7)	0.5 (0.4 to 0.9)	0.7 (0.4 to 1.0)	1.2 (0.7 to 1.7)	2.2 (1.5 to 3.5)
Sea surface salinity	Fremantle (115.75, -32.07)	0.06 (-0.05 to 0.17)	-0.04 (-0.19 to 0.10)	0.02 (-0.12 to 0.11)	0.01 (-0.15 to 0.14)	-0.08 (-0.39 to 0.07)	-0.04 (-0.51 to 0.29)
	Esperance (121.90, -33.87)	0.04 (-0.06 to 0.11)	-0.02 (-0.09 to 0.13)	-0.02 (-0.07 to 0.13)	0.01 (-0.08 to 0.14)	-0.04 (-0.20 to 0.18)	0.09 (-0.26 to 0.38)
	Thevenard (133.64, -32.15)	-0.00 (-0.17 to 0.10)	0.01 (-0.18 to 0.09)	-0.02 (-0.23 to 0.11)	-0.00 (-0.11 to 0.13)	-0.03 (-0.22 to 0.23)	-0.13 (-0.46 to 0.43)
	Port Adelaide (138.48, -34.78)	-0.03 (-0.10 to 0.13)	-0.06 (-0.12 to 0.18)	-0.07 (-0.19 to 0.14)	0.01 (-0.10 to 0.14)	-0.00 (-0.14 to 0.22)	-0.09 (-0.71 to 0.39)

VARIABLE	LOCATION (°E, °S)	2030, RCP2.6	2030, RCP4.5	2030, RCP8.5	2090, RCP2.6	2090, RCP4.5	2090, RCP8.5
Ocean pH	Fremantle (115.75, -32.07)	-0.07 (-0.07 to -0.06)	-0.07 (-0.07 to -0.07)	-0.08 (-0.08 to -0.08)	-0.07 (-0.07 to -0.06)	-0.15 (-0.15 to -0.15)	-0.33 (-0.33 to -0.32)
	Esperance (121.90, -33.87)	-0.07 (-0.07 to -0.06)	-0.07 (-0.07 to -0.06)	-0.08 (-0.09 to -0.07)	-0.07 (-0.07 to -0.06)	-0.15 (-0.15 to -0.14)	-0.33 (-0.33 to -0.31)
	Thevenard (133.64, -32.15)	-0.06 (-0.07 to -0.06)	-0.07 (-0.07 to -0.06)	-0.08 (-0.08 to -0.07)	-0.07 (-0.07 to -0.06)	-0.15 (-0.15 to -0.14)	-0.32 (-0.32 to -0.31)
	Port Adelaide (138.48, -34.78)	-0.07 (-0.07 to -0.06)	-0.07 (-0.07 to -0.07)	-0.08 (-0.08 to -0.08)	-0.07 (-0.07 to -0.06)	-0.15 (-0.15 to -0.14)	-0.32 (-0.33 to -0.32)
Aragonite saturation	Fremantle (115.75, -32.07)	-0.32 (-0.36 to -0.25)	-0.33 (-0.38 to -0.31)	-0.40 (-0.45 to -0.35)	-0.32 (-0.33 to -0.27)	-0.72 (-0.79 to -0.65)	-1.45 (-1.55 to -1.27)
	Esperance (121.90, -33.87)	-0.30 (-0.35 to -0.26)	-0.30 (-0.38 to -0.29)	-0.35 (-0.44 to -0.32)	-0.27 (-0.32 to -0.24)	-0.62 (-0.72 to -0.59)	-1.24 (-1.41 to -1.18)
	Thevenard (133.64, -32.15)	-0.28 (-0.32 to -0.27)	-0.30 (-0.33 to -0.28)	-0.35 (-0.39 to -0.33)	-0.27 (-0.30 to -0.22)	-0.61 (-0.66 to -0.59)	-1.18 (-1.33 to -1.14)
	Port Adelaide (138.48, -34.78)	-0.28 (-0.30 to -0.27)	-0.31 (-0.32 to -0.28)	-0.34 (-0.38 to -0.32)	-0.28 (-0.29 to -0.24)	-0.60 (-0.65 to -0.57)	-1.15 (-1.28 to -1.12)

For sea level rise and sea allowance, the future averaging periods are 2020–2040 and 2080–2100. In the report, these are referred to as 2030 and 2090 respectively.

ABBREVIATIONS

ACORN-SAT	Australian Climate Observations Reference Network – Surface Air Temperature
AWAP	Australian Water Availability Project
BOM	Australian Bureau of Meteorology
CCAM	Conformal Cubic Atmospheric Model
CCIA	Climate Change in Australia
CMIP5	Coupled Model Intercomparison Project (Phase 5)
CSIRO	Commonwealth Scientific and Industrial Research Organisation
ENSO	El Niño Southern Oscillation
FFDI	Forest Fire Danger Index
GCMs	General Circulation Models or Global Climate Model
IOCI	Indian Ocean Climate Initiative
IOD	Indian Ocean Dipole
IPCC	Intergovernmental Panel on Climate Change
NRM	Natural Resource Management
RCP	Representative Concentration Pathway
SAM	Southern Annular Mode
SPI	Standardised Precipitation Index
SRES	Special Report on Emissions Scenarios
SST	Sea Surface Temperature
SSWF	Southern and South-Western Flatlands
SSWFE	Southern and South-Western Flatlands sub-cluster East
SSWFW	Southern and South-Western Flatlands sub-cluster West
STR	Sub-Tropical Ridge
SPI	Standardised Precipitation Index
SRES	Special Report on Emissions Scenarios
SST	Sea Surface Temperature
STR	Sub-tropical Ridge

NRM GLOSSARY OF TERMS

Adaptation	The process of adjustment to actual or expected climate and its effects. Adaptation can be autonomous or planned. *Incremental adaptation* Adaptation actions where the central aim is to maintain the essence and integrity of a system or process at a given scale. *Transformational adaptation* Adaptation that changes the fundamental attributes of a system in response to climate and its effects.
Aerosol	A suspension of very small solid or liquid particles in the air, residing in the atmosphere for at least several hours.
Aragonite saturation state	The saturation state of seawater with respect to aragonite (Ω) is the product of the concentrations of dissolved calcium and carbonate ions in seawater divided by their product at equilibrium: ($[Ca^{2+}] \times [CO^3_2]$) / $[CaCO^3] = \Omega$
Atmosphere	The gaseous envelope surrounding the Earth. The dry atmosphere consists almost entirely of nitrogen and oxygen, together with a number of trace gases (*e.g.* argon, helium) and greenhouse gases (*e.g.* carbon dioxide, methane, nitrous oxide). The atmosphere also contains aerosols and clouds.
Carbon dioxide	A naturally occurring gas, also a by-product of burning fossil fuels from fossil carbon deposits, such as oil, gas and coal, of burning biomass, of land use changes and of industrial processes (*e.g.* cement production). It is the principle anthropogenic greenhouse gas that affects the Earth's radiative balance.
Climate	The average weather experienced at a site or region over a period of many years, ranging from months to many thousands of years. The relevant measured quantities are most often surface variables such as temperature, rainfall and wind.
Climate change	A change in the state of the climate that can be identified (*e.g.* by statistical tests) by changes in the mean and/or variability of its properties, and that persists for an extended period of time, typically decades or longer.
Climate feedback	An interaction in which a perturbation in one climate quantity causes a change in a second, and that change ultimately leads to an additional (positive or negative) change in the first.
Climate projection	A climate projection is the simulated response of the climate system to a scenario of future emission or concentration of greenhouse gases and aerosols, generally derived using climate models. Climate projections are distinguished from climate predictions by their dependence on the emission/concentration/radiative forcing scenario used, which in turn is based on assumptions concerning, for example, future socioeconomic and technological developments that may or may not be realised.
Climate scenario	A plausible and often simplified representation of the future climate, based on an internally consistent set of climatological relationships that has been constructed for explicit use in investigating the potential consequences of anthropogenic climate change, often serving as input to impact models.
Climate sensitivity	The effective climate sensitivity (units; °C) is an estimate of the global mean surface temperature response to doubled carbon dioxide concentration that is evaluated from model output or observations for evolving non-equilibrium conditions.
Climate variability	Climate variability refers to variations in the mean state and other statistics (such as standard deviations, the occurrence of extremes, etc.) of the climate on all spatial and temporal scales beyond that of individual weather events. Variability may be due to natural internal processes within the climate system (internal variability), or to variations in natural or anthropogenic external forcing (external variability).
Cloud condensation nuclei	Airborne particles that serve as an initial site for the condensation of liquid water, which can lead to the formation of cloud droplets. A subset of aerosols that are of a particular size.

CMIP3 and CMIP5	Phases three and five of the Coupled Model Intercomparison Project (CMIP3 and CMIP5), which coordinated and archived climate model simulations based on shared model inputs by modelling groups from around the world. The CMIP3 multi-model dataset includes projections using SRES emission scenarios. The CMIP5 dataset includes projections using the Representative Concentration Pathways (RCPs).
Confidence	The validity of a finding based on the type, amount, quality, and consistency of evidence (*e.g.* mechanistic understanding, theory, data, models, expert judgment) and on the degree of agreement.
Decadal variability	Fluctuations, or ups-and-downs of a climate feature or variable at the scale of approximately a decade (typically taken as longer than a few years such as ENSO, but shorter than the 20–30 years of the IPO).
Detection and attribution	Detection of change is defined as the process of demonstrating that climate or a system affected by climate has changed in some defined statistical sense, without providing a reason for that change. An identified change is detected in observations if its likelihood of occurrence by chance due to internal variability alone is determined to be small, for example, less than 10 per cent. Attribution is defined as the process of evaluating the relative contributions of multiple causal factors to a change or event with an assignment of statistical confidence.
Downscaling	Downscaling is a method that derives local to regional-scale information from larger-scale models or data analyses. Different methods exist *e.g.* dynamical, statistical and empirical downscaling.
El Niño Southern Oscillation (ENSO)	A fluctuation in global scale tropical and subtropical surface pressure, wind, sea surface temperature, and rainfall, and an exchange of air between the south-east Pacific subtropical high and the Indonesian equatorial low. Often measured by the surface pressure anomaly difference between Tahiti and Darwin or the sea surface temperatures in the central and eastern equatorial Pacific. There are three phases: neutral, El Niño and La Niña. During an El Niño event the prevailing trade winds weaken, reducing upwelling and altering ocean currents such that the eastern tropical surface temperatures warm, further weakening the trade winds. The opposite occurs during a La Niña event.
Emissions scenario	A plausible representation of the future development of emissions of substances that are potentially radiatively active (*e.g.* greenhouse gases, aerosols) based on a coherent and internally consistent set of assumptions about driving forces (such as demographic and socioeconomic development, technological change) and their key relationships.
Extreme weather	An extreme weather event is an event that is rare at a particular place and time of year. Definitions of rare vary, but an extreme weather event would normally be as rare as or rarer than the 10th or 90th percentile of a probability density function estimated from observations.
Fire weather	Weather conditions conducive to triggering and sustaining wild fires, usually based on a set of indicators and combinations of indicators including temperature, soil moisture, humidity, and wind. Fire weather does not include the presence or absence of fuel load.
Global Climate Model or General Circulation Model (GCM)	A numerical representation of the climate system that is based on the physical, chemical and biological properties of its components, their interactions and feedback processes. The climate system can be represented by models of varying complexity and differ in such aspects as the spatial resolution (size of grid-cells), the extent to which physical, chemical, or biological processes are explicitly represented, or the level at which empirical parameterisations are involved.
Greenhouse gas	Greenhouse gases are those gaseous constituents of the atmosphere, both natural and anthropogenic, that absorb and emit radiation at specific wavelengths within the spectrum of terrestrial radiation emitted by the Earth's surface, the atmosphere itself, and by clouds. Water vapour (H_2O), carbon dioxide (CO_2), nitrous oxide (N_2O), methane (CH_4) and ozone (O_3) are the primary greenhouse gases in the Earth's atmosphere.
Hadley Cell/Circulation	A direct, thermally driven circulation in the atmosphere consisting of poleward flow in the upper troposphere, descending air into the subtropical high-pressure cells, return flow as part of the trade winds near the surface, and with rising air near the equator in the so-called Inter-Tropical Convergence zone.

Indian Ocean Dipole (IOD)	Large-scale mode of interannual variability of sea surface temperature in the Indian Ocean. This pattern manifests through a zonal gradient of tropical sea surface temperature, which in its positive phase in September to November shows cooling off Sumatra and warming off Somalia in the west, combined with anomalous easterlies along the equator.
Inter-decadal Pacific Oscillation	A fluctuation in the sea surface temperature (SST) and mean sea level pressure (MSLP) of both the north and south Pacific Ocean with a cycle of 15–30 years. Unlike ENSO, the IPO may not be a single physical 'mode' of variability, but be the result of a few processes with different origins. The IPO interacts with the ENSO to affect the climate variability over Australia. A related phenomena, the Pacific Decadal Oscillation (PDO), is also an oscillation of SST that primarily affects the northern Pacific.
Jet stream	A narrow and fast-moving westerly air current that circles the globe near the top of the troposphere. The jet streams are related to the global Hadley circulation. In the southern hemisphere the two main jet streams are the polar jet that circles Antarctica at around 60 °S and 7–12 km above sea level, and the subtropical jet that passes through the mid-latitudes at around 30 °S and 10–16 km above sea level.
Madden Julian Oscillation (MJO)	The largest single component of tropical atmospheric intra-seasonal variability (periods from 30 to 90 days). The MJO propagates eastwards at around 5 m s^{-1} in the form of a large-scale coupling between atmospheric circulation and deep convection. As it progresses, it is associated with large regions of both enhanced and suppressed rainfall, mainly over the Indian and western Pacific Oceans.
Monsoon	A monsoon is a tropical and subtropical seasonal reversal in both the surface winds and associated rainfall, caused by differential heating between a continental-scale land mass and the adjacent ocean. Monsoon rains occur mainly over land in summer.
Percentile	A percentile is a value on a scale of one hundred that indicates the percentage of the data set values that is equal to, or below it. The percentile is often used to estimate the extremes of a distribution. For example, the 90th (or 10th) percentile may be used to refer to the threshold for the upper (or lower) extremes.
Radiative forcing	Radiative forcing is the change in the net, downward minus upward, radiative flux (expressed in W m^{-2}) at the tropopause or top of atmosphere due to a change in an external driver of climate change, such as a change in the concentration of carbon dioxide or the output of the Sun.
Representative Concentration Pathways (RCPs)	Representative Concentration Pathways follow a set of greenhouse gas, air pollution (*e.g.* aerosols) and land-use scenarios that are consistent with certain socio-economic assumptions of how the future may evolve over time. The well mixed concentrations of greenhouse gases and aerosols in the atmosphere are affected by emissions as well as absorption through land and ocean sinks. There are four Representative Concentration Pathways (RCPs) that represent the range of plausible futures from the published literature.
Return period	An estimate of the average time interval between occurrences of an event (*e.g.* flood or extreme rainfall) of a defined size or intensity.
Risk	The potential for consequences where something of value is at stake and where the outcome is uncertain. Risk is often represented as a probability of occurrence of hazardous events or trends multiplied by the consequences if these events occur.
Risk assessment	The qualitative and/or quantitative scientific estimation of risks.
Risk management	The plans, actions, or policies implemented to reduce the likelihood and/or consequences of risks or to respond to consequences.
Sub-tropical ridge (STR)	The sub-tropical ridge runs across a belt of high pressure that encircles the globe in the middle latitudes. It is part of the global circulation of the atmosphere. The position of the sub-tropical ridge plays an important part in the way the weather in Australia varies from season to season.

Southern Annular Mode (SAM)	The leading mode of variability of Southern Hemisphere geopotential height, which is associated with shifts in the latitude of the mid-latitude jet.
SAM index	The SAM Index, otherwise known as the Antarctic Oscillation Index (AOI) is a measure of the strength of SAM. The index is based on mean sea level pressure (MSLP) around the whole hemisphere at 40 °S compared to 65 °S. A positive index means a positive or high phase of the SAM, while a negative index means a negative or low SAM. This index shows a relationship to rainfall variability in some parts of Australia in some seasons.
SRES scenarios	SRES scenarios are emissions scenarios developed by Nakićenović and Swart (2000) and used, among others, as a basis for some of the climate projections shown in Chapters 9 to 11 of IPCC (2001) and Chapters 10 and 11 of IPCC (2007).
Uncertainty	A state of incomplete knowledge that can result from a lack of information or from disagreement about what is known or even knowable. It may have many types of sources, from imprecision in the data to ambiguously defined concepts or terminology, or uncertain projections of human behaviour. Uncertainty can therefore be represented by quantitative measures (*e.g.* a probability density function) or by qualitative statements (*e.g.* reflecting the judgment of a team of experts).
Walker Circulation	An east-west circulation of the atmosphere above the tropical Pacific, with air rising above warmer ocean regions (normally in the west), and descending over the cooler ocean areas (normally in the east). Its strength fluctuates with that of the Southern Oscillation.

GLOSSARY REFERENCES

AUSTRALIAN BUREAU OF METEOROLOGY - http://www.bom.gov.au/watl/about-weather-and-climate/australian-climate-influences.shtml (cited August 2014)

INTERGOVERNMENTAL PANEL ON CLIMATE CHANGE - http://www.ipcc.ch/pdf/glossary/ar4-wg1.pdf (cited August 2014)

INTERGOVERNMENTAL PANEL ON CLIMATE CHANGE - http://ipcc-wg2.gov/AR5/images/uploads/WGIIAR5-Glossary_FGD.pdf (cited August 2014)

MUCCI, A. 1983. The solubility of calcite and aragonite in seawater at various salinities, temperatures, and one atmosphere total pressure *American Journal of Science*, 283 (7), 780-799.

NAKIĆENOVIĆ, N. & SWART, R. (eds.) 2000. *Special Report on Emissions Scenarios. A Special Report of Working Group III of the Intergovernmental Panel on Climate Change*, Cambridge, United Kingdom and New York, NY, USA: Cambridge University Press.

STURMAN, A.P. & TAPPER, N.J. 2006. *The Weather and Climate of Australia and New Zealand*, 2nd ed., Melbourne, Oxford University Press.


PHOTO: BARBARA COOK
−20°
−10°
0°
10°
20°
30°
40°
50°

WWW.CLIMATECHANGEINAUSTRALIA.GOV.AU

14-00140